Single-Grain Silicon TFTs on a Plastic Substrate by Doctor Blade Coating of Cyclopentasilane

Miki Trifunovic

MASTER OF SCIENCE THESIS

IN

ELECTRICAL ENGINEERING, MICROELECTRONICS

THESIS COMMITTEE MEMBERS:
PROF. R. ISHIHARA (SUPERVISOR)
PROF. C.I.M. BEENAKKER
PROF. A. BOSSCHE
IR. J. ZHANG

RESPONSIBLE PROFESSOR: PROF. P.M. SARRO

FACULTY OF ELECTRICAL ENGINEERING,
MATHEMATICS AND COMPUTER SCIENCE,

DELFT UNIVERSITY OF TECHNOLOGY,

THE NETHERLANDS

June 5, 2012

Preface

This thesis is written as a partial satisfaction for the requirements of the *Master of Science Degree* in *Microelectronics* at the faculty of *Electrical Engineering, Mathematics and Computer Science*, at *Delft University of Technology*.

The work is essentially combining the inexpensiveness of solution processing and the quality of crystalline silicon transistors. The contribution of this work will lead to the fabrication of quality transistors on flexible substrates using the new liquid silicon material that has only recently been discovered for electrical applications.

In this process, difficulties have arisen in some aspects and it was the help of many people that have brought this thesis to a success. I would therefore like to thank the following people:

- Prof. P.M. Sarro as the responsible professor for enabling my thesis work.

- Prof. R. Ishihara for his daily supervision and guidance during the course of my project. Also, for the many discussions during meetings and helping me publish some of my work.

- Prof. R. van Swaaij and Prof. A. Bossche for their support as Master Coordinators.

- Prof. C.I.M. Beenakker and Prof. A. Bossche for their participation in the thesis defense committee.

- Jin Zhang and Michiel van der Zwan for their processing support and discussions.

- To all members of the TFT group that have helped me enjoy my time in this research group including: Sten Vollebregt, Aslihan Arslan, Daniel Tajari Mofrad, Pengfei Sun.

- To my peers, fellow master students, that have experienced the same curriculum.

- My family for supporting me always.

- Finally, I would like to thank anyone that have helped me in any way during my *Masters*, including DIMES technicians, teachers, bachelor students, etc.

Miki Trifunovic
05/28/12

ii

Abstract

Liquid silicon is found as the material combining both the advantages of high quality silicon devices and the low cost solution processing method. Single-Grain Thin-Film Transistors can be produced by Excimer Laser Annealing of the resulting film and grain location control by the μ-Czochralski process. Other works have used spin-coating and inkjet printing for liquid silicon based devices, however both processes are not roll-to-roll process compatible. In addition a high thermal annealing step (650°C), incompatible to plastics, is required for the reduction of hydrogen content before laser crystallization.

In this work, both issues are focused on. A precursor of the gravure printing process, doctor blade coating, is used to imitate a roll-to-roll compatible solution process and is optimized to produce uniform films of liquid silicon. Excimer Laser Annealing is used as a low temperature pre-annealing method to decrease the hydrogen content for crystallization.

Pure cyclopentasilane has been used as the liquid silicon material. Silicon dioxide surface modification by 0.55%HF dip results in a better wetting of the liquid together with an elevated temperature of 70°C. Higher temperatures lead to even better wetting properties, but more liquid silicon will evaporate.

After UV polymerization of the CPS for 20 minutes and thermal annealing at 350°C for 1 hour, an a-Si layer has been formed. Excimer Laser pre-annealing of many low energy shots removes hydrogen without significant deterioration of the film. A maximum grain size of 5μm has been produced by using a long pulse configured laser recipe that decreases the number of shots linearly while increasing the laser energy density by 50mJ/cm².

SG-TFTs on polyimide have been manufactured at the maximum processing temperature of 350°C. The mobility of the NMOS was ..., and the mobility of the PMOS was .... [to be obtained by mid June].

Finally, a next step towards gravure printing has been taken, by advancing the doctor blade coating method to the removal of the excess layer while keeping the cavity patterns in the film filled. Blade elasticity is a dominant factor in manual blading. An elastic blade can remove more excess than a rigid blade since the flexibility allows adjustment on the surface, but will also remove the liquid from inside the patterns. A combination of a rigid blade and the careful excess removal by the elastic blade gives the best results.

This work shows the potential of liquid silicon, and brings us closer to the mass production on flexible substrates using this new material.

iv

Contents

List of Figures

List of Tables

Abbreviations

AMOLED	Active-Matrix Organic Lighte-Emitting-Diode
a-Si	amorphous silicon
a-Si:H	hydrogenated amorphous silicon
BJT	Bipolar Junction Transistor
CMOS	Complementary Metal-Oxide-Semiconductor
CPS	Cyclopentasilane
c-Si	single-crystalline silicon
ERD	Elastic Recoil Detection
FTIR	Fourier Transform Infrared Spectroscopy
GF	Grain Filter
GPC	Gel Permeation Chromatography
HF	Hydrofluoric acid
HOMO	Highest Occupied Molecular Orbital
IC	Integrated Circuit
ICP	Inductively Coupled Plasma
IPA	Isopropanol
LCD	Liquid-Crystal display
LUMO	Lowest Unoccupied Molecular Orbital
MOSFET	Metal-Oxide-Semiconductor Field-Effect Transistor
NIP	Non-impact Printers
OLED	Organic Light-Emitting-Diode
OPRA	Overlay Printing Registration Accuracy
OTFT	Organic Thin-Film Transistor
PCB	Printed Circuit Board
PECVD	Plasma-Enhanced Chemical Vapor Deposition
RBS	Rutherford Backscattering Spectroscopy
RFID	Radio-frequency Identification
RIE	Reactive-Ion Etching
RPM	Rounds per minute
SFE	Surface Free Energy
SG-TFT	Single-Grain Thin-Film Transistor
TEOS	Tetraethylorthosilicate ($Si\{OCH_2CH_3\}_4$)
TFT	Thin-Film Transistor
UV	Ultraviolet light
XPS	X-ray Photoelectron Spectroscopy

Chapter 1

Introduction

As electronic chips make up an increasing part of our daily lives, there is a big desire for the optimization in production methods. One interpretation of Moore's Law defines a period of 18 months in which chip performance doubles, and as the physical limitations in chips are being approached, other ways of improving chip fabrication is being investigated.

Conventional methods for the production of electronic integrated circuits are complex and require high material compatibility. Large area electronics for display applications are based on Thin-Film Transistors that can be deposited on top of a supporting substrate, which is conventionally glass. The fabrication processes require expensive machinery such as the photolithography stepper, a vacuum atmosphere that requires energy and limits the producible area, and are based on batch processing which leads to a low throughput. In addition, the process wastes a lot of its materials due to its subtractive processing nature. The methods are based on batch processing and mass production is because of all this not possible. Mass producing chips will bring the electronics fabrication industry to a whole new level, making common chips as inexpensive as printing on plain paper.

(a)   (b)
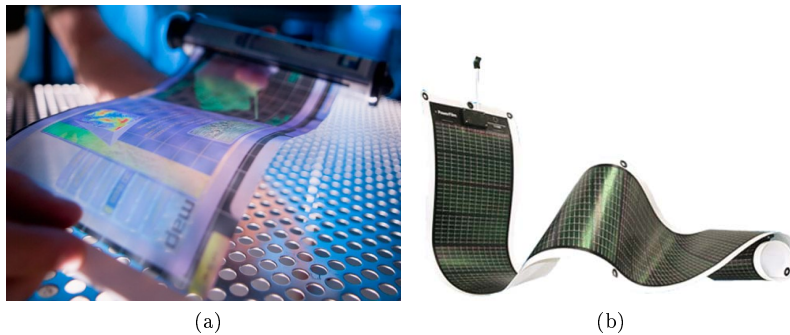
Figure 1.1: Flexible display (a) and flexible solar panel (b)

With the help of low-temperature processing, plastic substrates may be used for the production of flexible, light-weight, inexpensive displays as well as solar panels, as shown in Fig. 1.1. In addition, conventional vacuum processing limits the maximum obtainable sizes of these displays due to the limiting size of the vacuum chamber. Therefore, a process which does not require a vacuum ambient will not only lead to large scale manufacturing of displays, but allows roll-to-roll production.

Solution processing is an alternative way of processing electronics which has a potential to be used for mass production ends. Although still at its infancy, a lot of research is focusing on finding the right types of materials that can be incorporated as inks into mass producing printing machinery. Most of the research has focused on organic materials due to their ease in conversion to solutions that can be used as inks. However, these materials still experience poor material properties limiting their electrical performance at the level of hydrogenized amorphous silicon. This makes them only suitable for limited applications. In addition, the materials are quite unstable.

Problem

Solution processing at this point has the bottleneck of using the type of inks that have a low performance as well as stability. It is important to find a material that has electrical properties approaching the current high quality crystalline silicon level, yet still is solution processable as well as highly stable. This will have a huge impact in the chip manufacturing industry, as well as the display industry, driving the cost of electronic devices to a minimum while keeping the quality of these devices high. New application areas will emerge for which costs would be far too high when constructed by conventional processing methods such as flexible tablet devices as the super e-paper (displayed in Fig.1.2), or food packages RFID and sensors.
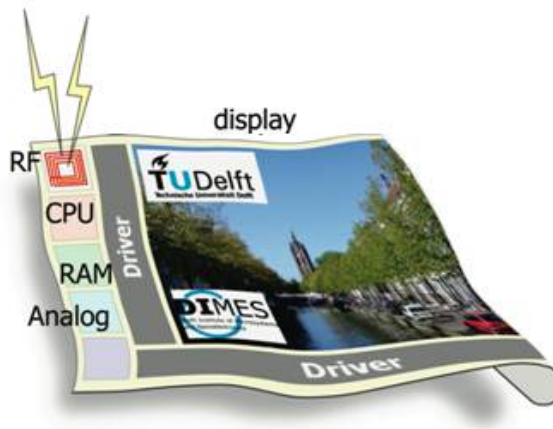
Figure 1.2: Super E-paper

Liquid silicon has been introduced in other works by Shimoda et al. [1] among others. They have shown the possibility of transforming a precursor into amorphous silicon by a combination of photopolymerization and thermal annealing. Also Zhang et al. [2] have reported the fabrication of Single-Grain Thin-Film transistors. Both use a thermal annealing temperature which is too high to be used on plastic substrates. They also used spin-coating and inkjet printing for the deposition of the material, however, neither can be used in roll-to-roll applications.

Approach

In this work, the following three approaches were taken to solve the problems:

1. A doctor blade coating method is introduced for depositing the liquid silicon material over a surface which is compatible to roll-to-roll processing. This method may in the future be extended into slot-die coating and finally gravure printing, a widely accepted printing method that is known for high-speed mass production.

2. The second issue of a thermal annealing temperature, incompatible to plastic substrates is dealt with by using Excimer Laser annealing that allows dehydrogenation and melting of thin layers without the penetration of the heat to more sensitive underlying layers such as flexible substrates.

3. A SG-TFT device will be fabricated on a polyimide substrate by the doctor blade coating of liquid silicon. For the first time, high quality silicon devices will be produced on a plastic substrate, bringing high electrical performance and solution processing together.

Working method

A general method of producing an amorphous silicon film from the liquid silicon has been adapted using many different variables aimed to optimize the method of fabricating a uniform film by doctor blade coating. Fig. 1.3 shows the flowchart from liquid silicon to the SG-TFT. The focus in this work was in the liquid and target preparation step, coating step, and the dehydrogenation step. The coating has been performed on substrates with grain filters that allow location controlled crystallization during the subsequent Excimer Laser irradiation. This irradiation process uses various recipes but is generally based on shooting at low energy densities to remove hydrogen content from the film that cause deterioration of the film when exposed to crystallizing energy levels, followed by shooting at increasing energy levels. Finally, the single crystals are used to fabricate the SG-TFTs. Substrates with a polyimide layer deposited on top of the single-crystalline substrate before oxide deposition are used. The substrate allows peeling off of the polyimide layer to obtain a fully flexible result.
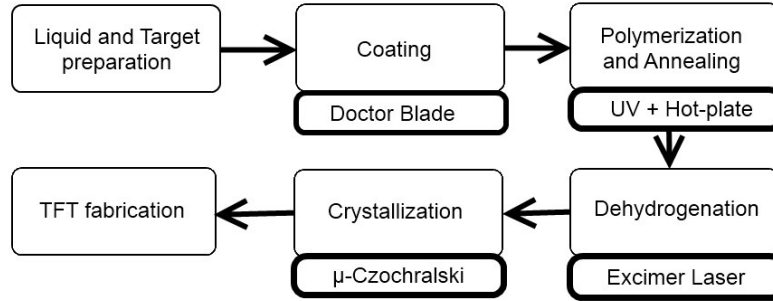
Figure 1.3: Flowchart of the SG-TFT fabrication process from the liquid silicon

Goal of this study

The focus of this study is aimed at achieving four specific goals:

1. Uniform layer formation of liquid silicon by doctor blade coating

2. Low temperature ($<350°$C) formation of a-Si

3. Low temperature single grain formation from the coated a-Si layer

4. SG-TFT production on a plastic substrate

Structure

This thesis starts by explaining some of the conventional processing methods and explain the benefits from the methods and materials used in this work in Chapter 2. This chapter is followed by the experiments that are conducted regarding: doctor blade coating of liquid silicon in Chapter 3, low temperature annealing by Excimer Laser in Chapter 4, and the measurement results of the subsequently produced liquid silicon SG-TFTs in Chapter 5. In addition, the next step towards gravure printing has been investigated in Chapter 6. Finally, conclusions and recommendations are presented regarding all experiments in Chapter 7

Chapter 2

Solution TFT process and liquid Silicon

Many of the electronic devices nowadays, are built using silicon, and the process has been optimized up to a certain extent for this material. Alternative materials are being researched now that physical limitations start to play a role. Yet an alternative way of processing may lead to inexpensive device fabrication formerly considered as impossible for silicon devices.

Solution processing has gained immense popularity, however pure silicon cannot be used in this process due to its high melting point of 1414°C incompatible with many other materials. Organic materials are attractive due to their ease in dissolving without losing their electrical properties. The organic electrical characteristics are quite poor as well as unstable, but they seem to be acceptable for some applications such as Organic Light-Emitting-Diodes (OLEDs) but cannot be integrated in more complex circuitry. Organic material properties are currently being optimized and have recently surpassed the level of hydrogenized amorphous silicon (a-Si:H), conventionally used for display applications.

The liquid silicon precursor used in this work can be solution processed similar to organic materials, however, they can be crystallized into polycrystalline silicon that already have two orders of magnitude higher mobility than the current best organic mobility. In addition, when the location of these crystals are controlled, the channel of the transistor can be positioned within a crystal grain, which is one of the great advantages of Single-Grain Thin-Film Transistor (SG-TFT).

In this chapter a description will be given on solution processing, which will be compared to conventional processing methods. This section is followed by the characteristics of organic semiconductors, silicon as it is used nowadays, and a full description of the liquid silicon material used in this work.

2.1   Solution Processing

A type of processing that uses solutions or liquids for the fabrication of electronic devices is called solution processing. This type of processing has attracted a lot of attention recently due to the many advantages over conventional processing. Two different types of conventional processing need to be discussed.

The first one is the use of Metal-Oxide-Semiconductor Field-Effect Transistors (MOSFETs) or Bipolar Junction Transistors (BJTs) that use the bulk of the silicon material as the channel and are produced by traditional processing methods that start with the wafers produced by the *Czochralski* and/or *Floating Zone* methods. These wafers are further processed by means of subtractive processing using photolithography and masking layers. High quality devices are produced in this way.

A second type of process focuses on the production of devices such as Thin-Film Transistors (TFTs) on top of a supporting substrate, such as the case for displays. In general this is done on top of glass, however, when sufficiently low temperatures are reached, deposition on flexible substrates may be possible as well. Current technologies use Plasma-Enhanced Chemical-Vapor Deposition (PECVD) for the deposition of the various layers and use a-Si:H as the semiconductor layer. For display applications, the quality of the devices do not have to be high.

In both cases, a highly controlled atmosphere is required and many different steps are necessary to produce various patterns on the substrate as well as doping of the layers within the bulk of the material. Material wastage and time consumption is a central issue in both cases. It is therefore necessary to find a way to produce high quality devices in a less stringent ambient with high throughput at low temperatures.

As an alternative to the conventional processing, solution processing gained popularity due to their ability to overcome most of the issues of current processes. Table 2.1 compares solution processing to conventional processing. In essence, the solution process itself, is the various uses of solutions or liquids to create electronic devices such as TFTs. Some of the most commonly used solution process, that is also used in conventional processing for instance, is spin-coating. Table 2.2 gives a list of all solution processing types currently used and researched [6, 11].

The effects of these different types of processes on the thin film quality of the deposited layer are mainly dependent on the concentration of semiconductor material in the solution and its solubility, evaporation rate of the solvent, and properties of the target surface[9].

Printing is the process of reproducing by means of applying ink to a substrate into a certain arrangement, and is an advanced solution processing technique. Today's wildly used applications include the printing of mass produced newspapers, magazines, books, packages, etc. Printers known for their mass production qualities would be a useful tool for constructing cheap electronic devices allowing to deposit already patterned layers onto various substrates. This makes the manufacturing process of electronic devices a lot simpler and less expensive.

Table 2.1: Comparing conventional and solution processing

	Conventional Processing		Solution Processing
+	High quality devices can be fabricated due to the high control of external factors [3], as well as the quality of silicon	-	Quality of the devices is low due to the usage of organic semiconductors. These materials are also quite unstable
+	Device density is high due to the high resolution of this type of process [3]	-	Device density is relatively low when considering printing only, due to the current resolution of printers
-	Process is quite complex [4, 5]	+	Simple and fast process [4, 7, 8]
-	Vacuum ambient is required and can be produced by chambers that limit the size of the substrates[2, 6]	+	No vacuum ambient is required, so no chambers that limit the maximum processable substrate size or pumping down time needed [4, 9, 10]
-	Difficult handling of the gaseous materials [6]	±	Easier handling of liquid materials, although solution issues such as bleed-out needs to be avoided in printing systems. [10]
-	Use of a lot of materials due to subtractive processing [2, 3, 4, 5, 6]	±	Subtractive processing in most coating methods since patterns are not directly transferred. Additive processing only for printer types
-	High cost [4, 5]	+	Lower cost per unit area[4, 7, 8, 9, 10]
-	Low throughput due to batch processing	+	High throughput when considering roll-to-roll processability
-	Substrates are limited to wafers or glass due to high temperature processing.	+	Flexible, plastic, substrates can be used due to the low temperature processing when using organic solutions. [10]

Special materials are used for inks that can be used in printers for solution processing of layers with electrical properties. Using silicon itself as ink would be unrealistic due to its high melting point of over 1400°C making it incompatible to printers as well as substrates. A lot of research has gone into organic semiconductors due to their ease in creating a solution from the material at room temperatures. In this way the material can be printed onto flexible substrates that are incapable of handling high temperatures. Furthermore, the size of these substrates is not limited to the limited size of the conventional machinery, and therefore large areas of electronics can be printed inexpensively. The price of these devices can be driven to the level of conventional printing, and many new applications of electronics can be made feasible. Some of the applications due to this cost minimizing process take the advantages of printing directly to the

Table 2.2: List solution processing types

Spin-coating	Process in which the solution is positioned at the center of a certain substrate after which the substrate is rotated at a certain speed. Due to centrifugal force the solution is spread across the surface. By varying the speed, a varying thickness of the resulting layer can be formed.
Drop-casting	Deposition of a drop of liquid on a specific surface after which it is spread due to external forces until solvent is dried.
Doctor blade coating	A liquid is spread across a surface by means of a doctor blade, pushing the liquid in desired areas.
Slot die coating	A liquid is forced out of a chamber through a slot by pressure onto a moving substrate.
Roll coating	Commonly referred to as roll-to-roll printing processes which are in most cases impact printer types. Cylinders are used to transport the solution from one surface to the other by adhesive forces after applying a certain pressure. Gravure printing, direct lithography, and letterpress/flexography printing fall into this category.
Offset printing	An intermediate carrier is used to transport a certain pattern arrangement of the solution from one roll to another. Generally used in offset lithography setup to decrease water transport to the target substrate.
Curtain coating	A constant stream of uninterrupted solution is dropped on a surface which is placed on a conveyer belt and is traveling in a direction with a certain speed. This constant motion will result in a uniform layer on top of the substrate.
Dip coating	The substrate as a whole is dipped into a solution. Upon raising the substrate out of the solution, adhesive forces will cause the solution to stay on the substrate.
Spray coating	A hose is used to spray a solution on a certain substrate.
Anodization	An anode and a cathode are placed within a solution and a certain electric field is applied. This field will cause some of the material within the solution to react with one of the electrodes on which a metallic target may be placed. Commonly used for anodic oxidation.
Screen printing	Solution patterns are pressed through a mask onto a certain substrate.
Inkjet printing	A solution is propelled toward a surface in the form of droplets by thermal, piezo-electric, or acoustic forces applied at the nozzle.

market [12] these are listed in Table 2.3 .

Table 2.3: Printing advantages in electronics

Printing advantage	Electronic application
Inexpensive as paper	Integration in any product (e. g. packages)
Large area production	Billboards, solar cells, displays
Flexible substrate usage	Clothing, anti-vandalism
High throughput[10]	Cheaper electronics overall
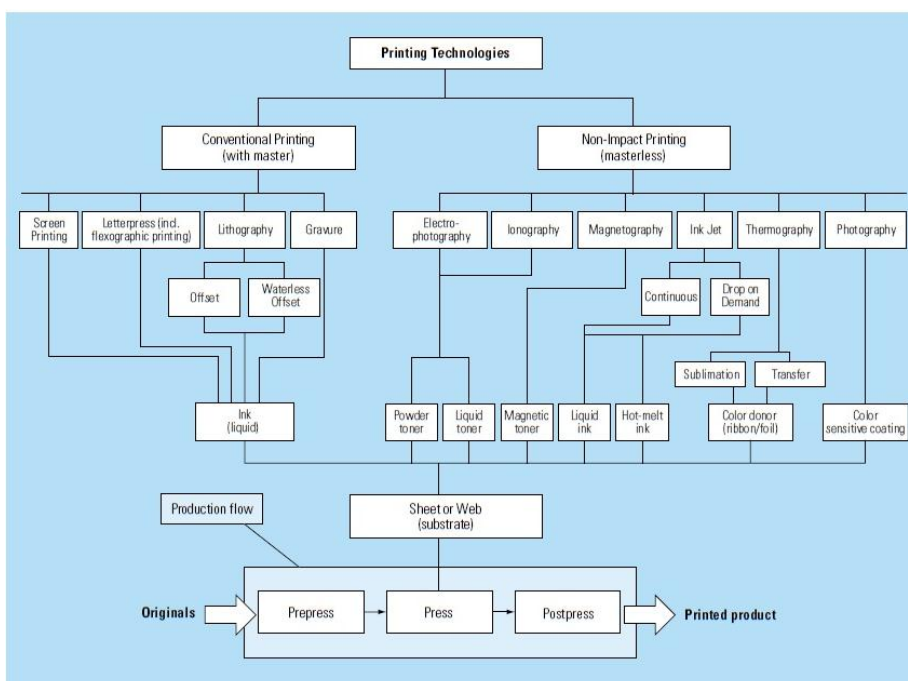
Figure 2.1: Overview of different types of impact and non-impact printers [13]

There are many different types of printers. Each printer has its own significant advantages and disadvantages and can be divided into two main groups: *Impact printers* and *Non-Impact Printers*. *Impact Printers* are also known as printers with masters that can be reused to produce highly reproducible inexpensive print runs, whereas the *Non-Impact Printers* do not use a fixed master but allow digital processing and highly variable print runs. Within these groups a further subdivision can be made. Fig. 2.1 shows an overview of the main types of printers that are currently in use. For an overview of the most popular printer types for the fabrication of electronics, the reader is referred to Appendix B, where the advantages, disadvantages, basic working and current research regarding the printer type is presented, after which a final conclusion

is given for best printer type for manufacturing electronics.

This thesis studies the doctor blade coating of liquids on a surface, which is by itself not a printing type. It is however a precursor of gravure printing as displayed in Fig. 2.2. Initial tests have to be run for doctor blade coating and accurate excess removal before delving into the gravure printing process.
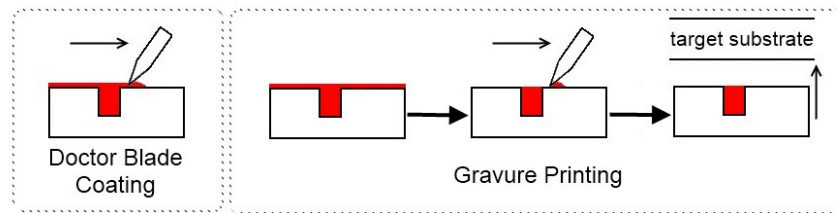
Figure 2.2: Schematic of the difference between doctor blade coating and gravure printing.

The reason why gravure printing is chosen is because of the great advantages of this type of printer when considering mass production. Highly uniform and quality print runs are realized which can potentially dominate the printing industry of electronics. Doctor blade coating used in this work itself can already be used in a roll-to-roll process, and is therefore a good first step towards mass production of liquid silicon.

2.2   Semiconductors

Many advantages exist in printing solution processable materials compared to conventional processing. However, compatibility is required for the conversion of the right types of materials into inks that can be used in the printing process. It has been shown that every part of the transistor can be constructed by printing techniques. Metal wiring by means of nanoparticles for contacts, and dielectric deposition are, among others, important aspects in the construction of the field-effect transistors. Table 2.4 and 2.5 lists the different solution processable types of materials used for dielectrics and conductors respectively [12, 14].

Table 2.4: Types of materials used as inks for printing dielectrics and their properties

	+	Easy solution process
	+	Good uniformity in thickness
Polymers (most frequently used)	+	Low surface roughness
	+	Flexible
	+	Compatible to organic semiconductors

The key ingredient in the transistor is the path between one contact to the other, the channel region, for which a semiconductor is required. The or-

Table 2.5: Types of materials used as inks for printing conductors and their properties

Conducting polymers	-	Difficult to dissolve
	-	Degrades easily
	+	Low temperature process
	+	Organic semiconductor compatible
Metal Flakes	+	Low cost
	-	Only as good as the smallest particle
Metal Nanoparticles	+	High conductivity
	+	Low temperature process
	+	Wide material variety and availability
	-	Colloidal stability
	-	Printability
	-	Film roughness
	-	Purity of the final film
	-	Electromigration
Metal-organic or metal-salt precursors	+	Low cost
	+	Easy to prepare
	+	Much better stability due to lack of discrete particles
	+	Solution processable, so no clogging of the inkjet nozzle
	-	Low mass loading that can lead to poor mechanical films
	-	Purity of final film

ganic semiconductor, commonly used as the semiconducting inks will first be discussed. Their basic working, application areas, but mainly the drawbacks of these semiconductors will be made apparent, after which the conventional silicon is explained, and finally the liquid silicon used in this work will be introduced.

2.2.1 Organic Semiconductors

Organic electronics, are electrical devices that make use of materials that are based on carbon molecules. In the past, one did not associate organic molecules to conducting electricity; it was rather found to be a good insulator. Although in nature it has been noticed that the firefly emits light through bio-luminescence caused by enzymes that excite organic molecules[15]. Inorganic semiconductors such as silicon or germanium have mainly governed the semiconductor industry and after the accidental discovery of the usefulness of organic semiconductors in electronics by Dr. Shirakawa in 1977[16], research of these materials have found their way in the market due to their[15, 16]:

- Significant fabrication cost reduction due to solution processability of the materials,

- Low temperature processing that allow these materials to be deposited on inexpensive flexible substrates,

- Molecular tunability, allowing the materials to change properties such as volatility, solubility, and wetting characteristics.

Unlike high quality single-crystalline silicon materials, these organics are built in TFT processes much like a-Si:H. Research today has advanced the mobility of organic semiconductors to surpass the level of a-Si:H (1 cm^2/Vs) [17, 18, 19]. Although these are still nowhere near the mobility of single-crystalline silicon, which is three orders of magnitude higher [16], they show their potential in rather inexpensive applications.

The basis for the conduction of organic materials are slightly different from their inorganic counterparts. Bonds play a major role in these devices, and this section will be devoted to the understanding of their operating principles.

Conduction in general

A discussion about charge transport is directly related to the bonding properties of various materials. In both inorganic and organic semiconductors, covalent bonds are the main bond type that keep the molecule together. This type of bond is based on the attraction of two atoms due to its desire to fill the electron shells around the atoms. Sharing of electrons among the two atoms realizes this desire. Both silicon as well as carbon for example can share four electrons with neighboring atoms. Within this type of bonding, the electrons become a pair and orbit around the pair of atoms; they cannot move around freely and therefore do not conduct electricity unlike metals that are bound by a cloud of valence electrons that move around freely. Covalent bonds in inorganic semiconductors are relatively weaker so that some of the electrons may be thermally activated. These materials can conduct to a certain extent and are hence called semiconductors [20].

The interaction of two atoms results in splitting of the quantized energy level into two discrete energies. When many atoms interact with each other, the energy will be split into a band of discrete energy levels. In some materials there are energy levels for which the electron can not occupy. These are called forbidden energies, or the bandgap [20]. Various models try to describe this band theory further through the use of Schrödinger's equation (e. g. The Kronig-Penny Model, the Ziman model, and the Feynman model). The reader is referred to [15] for a more thorough understanding of the band theory.

Out of the many energy bands that exist due to the interaction of multiple atoms, the two highest bands are of particular interest: the valence band and the conduction band. In insulators the valence band is filled with electrons, and the conduction band is completely empty. The bands are separated by a bandgap, and an application of an electric field will not cause the electrons to

change energy levels when the bandgap is sufficiently large for the electrons to cross. No current will flow through the material since no electrons are activated. A partially empty band results in the possibility of electrons increasing their energy level due to an applied electric field and move through the material. The net flow of these electrons will define the current. This situation happens for semiconductors in which thermally activated electrons can cross the bandgap and jump into the conduction band allowing the material to conduct current to a certain extent since the bands are not completely filled or empty. In metals, two situations may exist regarding the band filling. The first case is a fully occupied valence band, and a partially filled conduction band that allow these electrons to move freely when an electric field is applied. The second possibility is that valence and conduction bands overlap so that electrons do not have to bridge a bandgap and can easily occupy other energy states [20].

Organic conduction

Compared to inorganic semiconductors, organic semiconductors that use covalent bonding interaction have quite a large bandgap that prevents the material from conducting electrons. So the electrons inside this material need to be assisted in order for them to raise their energy and be able to move around. Two carbon atoms interacting with each other are joined by one covalent bond due to the pairing of one of the dangling bonds of each atom. This effect can be seen as the pairing of s orbitals and is therefore also known as σ-bonds. Each carbon atom has 4 dangling bonds and can form covalent bonds with four other atoms. It can also however form a pair with the already interacting carbon atom and create weaker bonds perpendicular to the σ-bond plane. This weaker bond is similar to the structure of two p-orbitals and is therefore known as π-bonds. The electron configuration of Carbon: $1s^2$, $2s^2$, $2p^2$, the sigma bonds lie closer to the atoms and are therefore stronger [15] The Fig. 2.3 shows this situation.

(a)   (b)
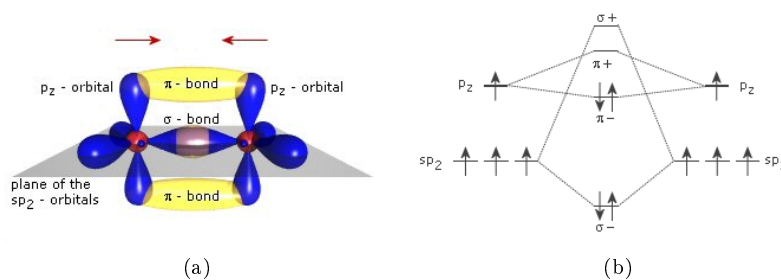
Figure 2.3: Bonding representation of two carbon molecules with σ-bonds and π-bonds (a), and its band representation (b).[21]
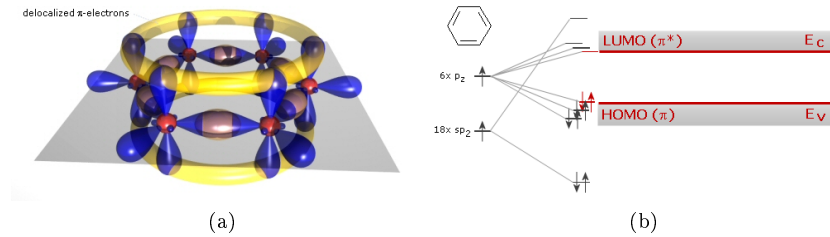
Figure 2.4: Bonding representation of benzene with σ-bonds and π-bonds (a), and its band representation (b).[21]

These π-bonds cause a further splitting of the energy level. A lower level is known as the bonding state, and the higher energy level is known as the anti-bonding state. Similar to insulators, under normal conditions the lower bonding states are occupied and the higher anti-bonding states are empty. When multiple double bonds are formed in an atom, such as the case for the benzene ring, multiple energy level splitting will occur for every π-bond as can be seen from Fig. 2.4 For large molecule systems such as polymers, this number of π-bonds can significantly increase to form whole bands of bonding and anti-bonding states. These states are separated by a bandgap. The energy state closest to the bandgap is called HOMO (highest occupied molecular orbital) for the bonding states, and LUMO (lowest unoccupied molecular orbital) for the anti-bonding states. This bandgap however is significantly smaller than when no π-bonds are present. This results in the possibility of charge transfer to the higher unoccupied energy states due to external excitation, much like a semiconductor. In this way the molecule will be able to transfer charge through the material, only by using the highly polarizable π-bonds. Fig. 2.5 shows the band diagram of conjugated polymers [15]. Doping in these materials will enable the production of n- or p-type TFTs. Impurity atoms replace some of the hydrogen atoms in this case and form the source of electrons or holes [15].

Although solution processable, significant disadvantages exist when using organic semiconductors:

- In many cases the organic semiconductors are p-type since stable n-type semiconductors are hard to find [16]. This makes the production of complementary circuitry such as CMOS hard to realize with organic materials only.

- These devices are known to give mobilities that are limited to the level of a-Si:H

- Organic materials are highly reactive to water and oxygen and are therefore prone to reliability issues
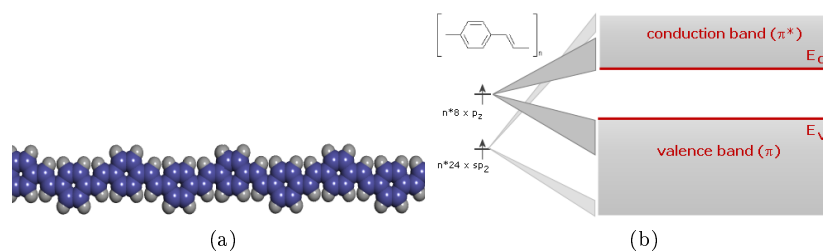
Figure 2.5: Bonding representation of an arbitrary polymer (a), and its band representation (b).[21]

Polymers and Small molecule organic systems

Long polymer chains with alternating double bonds or π-bonds are being used as organic semiconductors. Polymer materials generally are hard to purify since they have a large variation in molecular size. They may also have structural defects due to monomer mislinkage that can induce traps against charge carriers. Large polymer chains are however not the only way for organic materials to behave as semiconductors. Small-molecule organic semiconductors can behave in a similar fashion and form the alternative to polymer organics. Due to their small size they can assemble more easily into regular geometric arrangements. This tendency towards the formation of molecular crystals lead to larger carrier mobilities than compared to disordered chains of polymers. A few differences between the two types should however be noted [16, 17, 22]:

- Small-molecule organic semiconductors are commonly deposited from the vapor phase whilst polymeric semiconductors are deposited from the solution. Solution processability is an important factor for printed electronics. Polymeric solvents are however known to be quite toxic since they are either chlorinated or aromatic.

- Small-molecule systems, when deposited on low roughness surfaces can form a highly ordered crystalline region leading to efficient π-stacking and therefore higher mobilities than polymers.

- Small-molecules are more easily purified than polymers since their structure is well defined.

Research so far

A lot of research is being conducted in organic electronics. Organic devices are constructed with higher mobilities and with higher stability [17, 18, 22, 23], and have already come to the level of a-Si:H ($1cm^2/Vs$). However, it is still a long

way before reaching the high quality crystalline silicon level that have mobilities of a few orders of magnitudes higher.

The organic n-type counterpart of common p-type organic semiconductors are being researched to be able to make CMOS designs for high speed, energy efficient circuitry. Currently, many n-type materials are either too unstable or have a lot lower mobilities. Fig. 2.6 shows both a p-type and an n-type device characteristics, that have been designed for CMOS purposes.
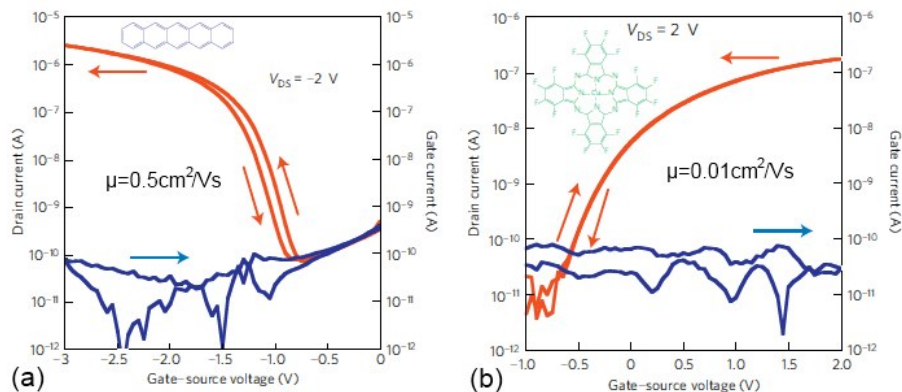
Figure 2.6: Performance of the p-type organic material pentacene (a), and n-type $F_{16}CuPc$ (b), both fabricated in a CMOS design on a plastic substrate. [24]

The organic devices in general have also gained popularity in the consumer market for displays based on OLED or AMOLED, since these applications do not require high quality devices. They can achieve a high brightness, high resolution, large viewing angle, and are thinner, light weight, and less expensive than conventional displays [25]. Organic solar cells are also increasingly popular for their inexpensive and flexible properties.

The advantage of inexpensive printing onto large area flexible substrates have not only found improved uses of current applications, but also new applications such as pressure sensors used for artificial skin [26, 27]

2.2.2   Solid Silicon

Organic materials are used for their solution processability. Their electrical quality, although close to the a-Si:H level, is still nowhere near polycrystalline silicon. Silicon as it is used conventionally, can obtain mobilities of three orders of magnitude higher in today's integrated circuits. An alternative to this is given by their production in large areas by using chemical vapor deposition technique that deposits a-Si:H over large areas at the cost of electrical performance.

Amorphous and polycrystalline silicon

Silicon is the most common known and widely used semiconductor in the electronics industry. Various types of semiconductors are defined by their crystal structure.

Amorphous silicon is a cluster of silicon atoms with random orientations throughout the material. It has relatively low electrical performance and is currently mainly used in its hydrogenated form as solar cells or display TFTs.

Polycrystalline silicon is a material formed as a combination of multiple crystals. It can be directly deposited on a substrate, or formed from an already deposited a-Si film. Excimer laser can be used on such a film to create a polysilicon layer that can achieve higher mobilities. These mobilities however are limited to approximately 50 to 100 cm²/Vs. This is due to crystal grain boundaries that are formed from randomly produced grains during laser crystallisation. Removal of these grain boundaries can lead to devices approaching the single-crystalline silicon level, however careful control of grain formation is important.

Single Grain Thin Film Transistor

The Thin-Film Transistor (TFT) is a device that is similar to the MOSFET, except that the device is produced on top of a supporting substrate rather than within the bulk of the substrate material. The reader is referred to Appendix C for a more detailed description about the characteristics of this type of device.

The main application for this type of device was the display industry where large area displays are produced by manufacturing TFTs on top of a glass substrate. This is usually done by PECVD of hydrogenated amorphous silicon (a-Si:H) as the semiconductor, although organic semiconductors have in some instances been used as well, such as Active-Matrix Organic Light-Emitting Diodes (AMOLEDs). Producing devices on a large area was the main aim of this type of device. The solution processable organic materials allowed even lower temperature processing, so that other substrates such as plastics could be used that are much thinner, cheaper and flexible.

Many of the TFT types such as organic semiconductor based ones or amorphous silicon based ones still suffer from low mobilities. High mobility TFTs are desirable to be able to integrate more complicated devices on plastic substrates. Currently many of the flexible displays require external drivers that prevent the final product from being fully flexible.

The quality of the a-Si semiconductor can be increased by Excimer Laser crystallization of the film into polycrystalline silicon. The random grain boundaries limit the electrical performance of the device. When the location of these grain boundaries and therefore single grains are controlled, high quality devices may be produced within a single grain.

Single-Grain TFTs are TFTs that are constructed within a single grain from a polysilicon film. The location of grains produced during laser crystallisation are carefully controlled by grain filter cavities. The μ-Czochralski method is

the process of creating the location controlled single grains. Fig. 5.1 shows step-by-step the fabrication process. In essence an amorphous silicon layer is deposited on a substrate with grain filter cavities. A subsequent Excimer laser crystallization step allows a single crystal seed at the bottom of the cavity, to grow into the molten layer on top. This single crystal grain can be used to produce a TFT from which the channel region contains this high quality semiconductor film.
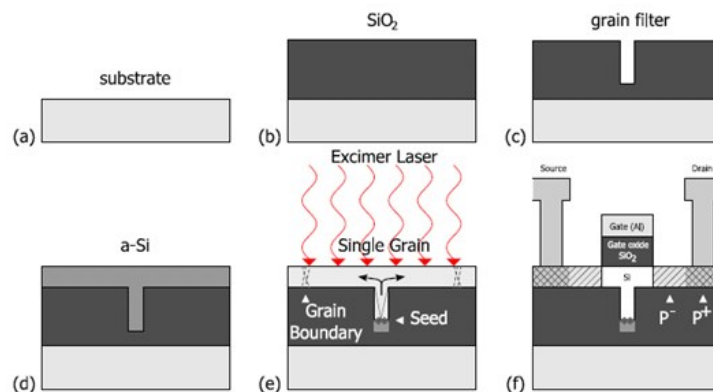
Figure 2.7: SG-TFT fabrication process using the μ-Czochralski method. The plastic substrate in (a), followed by deposition of a SiO2 layer (b). A grain filter is etched in this layer (c). Subsequent a-Si deposition fills the cavity (d). Excimer laser melts the top layer and leaves a seed of a-Si at the bottom of the cavity which grows to become a crystalline island on the surface (e). Within this island a TFT is created (f). [28]

Using the Excimer laser gives four important considerations. The first one requires a low hydrogen content of the silicon film. During Excimer-laser irradiation, any hydrogen atom left inside the silicon film may destroy the film while it is evaporated. Lowering the hydrogen content can either be done by thermal annealing or laser annealing. Both cases should take the fragility of the plastic substrate into account.

The second issue is the heat produced by the laser. The amorphous silicon layer may absorb the laser energy but heat could diffuse and destroy the underlying layers. Therefore a buffer layer of silicon dioxide is used. The thickness of this buffer layer should be at least 0.5μm since the heat will diffuse no more than 300nm.

Thirdly, an excess layer of amorphous silicon should be available on top of the cavity. This layer forms the main protection of underlying layers that are harmed by the laser irradiation itself.

The final challenge lies in the energy density that the Excimer laser should and can use. A too high energy density may melt all of the amorphous silicon and may damage underlying layers. It could also cause the limited amount of

hydrogen atoms to destroy the silicon film more easily. A high energy density leads however to larger grains. On the other hand, a lower energy density will result in smaller grain sizes. A bigger thickness of amorphous silicon layer could increase the possibility to enhance the energy density of the laser. A thicker layer may however have more hydrogen atoms that can result in ablation. [2, 29]

2.2.3   Liquid Silicon

Organic semiconductors suffer from poor stability, and relatively poor electrical performance and are therefore still not vastly implemented in today's more complex products, despite the fact that they are compatible to solution processing. Inorganic materials are more stable, can get higher mobilities but are difficult to use into solution processing. One example is the use of metal chalcogenide semiconductors achieving a mobility of $10cm^2/Vs$. Mobilities of solution processed devices approaching the crystalline silicon level are desired and would open up many possibilities.

Silicon in conventional fabrication techniques has a melting temperature of 1414°C [30]. This means that for printing the silicon as a liquid, not only is there a lot of energy needed, the printer itself as well as the substrate, need to be compatible to this high temperature. Flexible substrates such as plastics have no chance of surviving when processed in this way. Lowering the fabrication temperature is of essence when considering material compatibility and machine and energy costs. This is the area where organic devices have an advantage of low temperature solution processing, with the lack the quality and stability. Being able to process silicon at lower temperatures, and yet producing a high quality and stable device is essential. Using silicon in its purest form is out of the question.

A compound that can transform into high quality silicon at low temperatures may be the solution to this problem. This compound has been found in 1973 [31] but has only recently found to be useful for microelectronic applications. Dr. Shimoda et al. describe the compound used, and its transformation to silicon films [4, 5]. They have successfully fabricated poly-crystalline silicon devices with the formation of an a-Si layer at a maximum processing temperature of 430°C.

Cyclopentasilane for liquid silicon
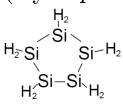
To create a high quality silicon layer, the required compound should be carbon- and oxygen free [1, 7, 8]. Dangling bonds should then be avoided by hydrogenation. The choice of the compound is then limited to a composition of silicon and hydrogen atoms as either a straight molecule (Si_nH_{2n+2}), a cyclic compound (Si_nH_{2n}), or a multicycled compound (Si_nH_{2n-2}) [6]. In order to transform from these compounds to a high quality silicon layer, the compound needs to polymerize. A cyclic structure is preferred due to its high reactivity with light so that photopolymerization can occur efficiently, these will undergo ring-opening

as they are exposed to UV light [6]. A single cyclic structure is preferred over the multicycled structure due to its ease of synthesis and purification.

The number of silicon elements in the single cyclic structure should be carefully chosen. According to [1, 8], when n is more than or equal to three, the compound is liquid at room temperature and will transform into a-Si when a temperature of 300°C is reached. For n smaller than ten, the boiling point of the compound will be less than 300°C, which would mean that the compound evaporates before it decomposes to amorphous silicon. This problem can however be solved by the photopolymerizing the compound before thermal annealing. The compound Cyclopentasilane, Si_5H_{10} has been chosen for its high photo reactivity on UV light and its relative stability[8]. In this work, the term liquid silicon is used for any compound used in solution processing that can be transformed into an amorphous silicon film. This includes: pure CPS, UV irradiated CPS, CPS mixed with an organic solution, and the combination of UV irradiation of the CPS mixture.

The compound is also highly reactive to oxygen and should therefore be processed in an inert gas ambient. When it is exposed to air, the material will inflammate. Adding oxygen however after the photopolymerization step and during thermal treatment can create silicon dioxide films instead of a-Si. Table 2.6 lists the general information of CPS. For more detailed information about the compound, the reader is referred to the datasheets [32].

Table 2.6: General information Cyclopentasilane

Appearance	Colorless liquid (at room temperature)
Shipping name	Pyrophoric liquid, organic, n. o. s. (Cyclopentasilan)
Molecular Structure	
Freezing point	-10.5°C
Boiling point	194 °C
Molecular weight	150.5 g/mol
Density	0.963 g/cm^3
CAS number	289-22-5
Other Information	Spontaneously Combustible Insoluble in Water

CPS synthesis

Synthesis of CPS is found to be quite complicated. This is one of the reasons why research in this field has been lacking. Although there are multiple ways to produce this compound, its quality is essential for the conversion to a high purity silicon film for good electrical performance of the final devices. One of the ways of synthesis will be described in this section.

Decaphenylcyclopentasilane is first prepared from a Wurtz-type coupling (formation of carbon-carbon bond by the reaction of an alkyl-halide with sodium) of dichlorodiphenylsilane and fused with lithium metal. All phenyl groups are then substituted with bromine by a cyclosilane reaction with HBr (anhydrous HBr has been used in a bomb tube at room temperature). This reaction will result in a benzene solution of decabromocyclopentasilane. It is a colorless crystal that is extremely sensitive to moisture and melts at 195°C. The active breathing vibration of this ring as well as the Si-Br bonds are at 510cm-1. By exposing this solution to very pure ethereal (LiAlH4), the material gets hydrogenated. Slowly it gets added to a benzene solution of bromocyclosilane. All Br groups are substituted with hydrogen. After removing the solvent and isolation from residue under reduced pressure, the final product of cyclopentasilane will result [7, 31]. Fig. 2.8 shows this process.
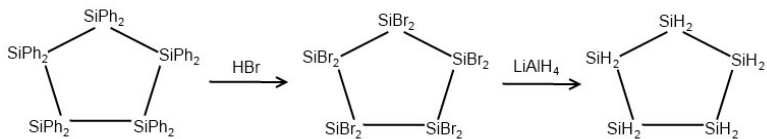
Figure 2.8: CPS synthesis

Structure of CPS

When considering the compound CPS, various structural formations need to be analyzed. In principle there are three main structures: Envelope (Cs), Twist (C2), and Planar (D5h) [4, 5, 33]. Fig. 2.9a shows the differences between these three structures. [4, 5] has found that from these three structures the twist (C2) structure is the most stable structure. Both the Twist and Envelope structures have similar energies that differ less than 0.03meV, but the planar (D5h) structure has 50meV less than the other two structures and are therefore considered to be less stable. Due to the low energy differences between the twist and envelope structures, only slight distortions are required for the transformation from one of the two to the other. The energy barrier is found to be less than 0.1meV.

Vibrational frequencies are a way to identify the different structures within the CPS compound or solution. The twist and envelope structures have the lowest vibrational frequencies at 2.6 and 3.8cm^{-1} respectively. These frequencies correspond to the transformations between the two structures. Since the planar structure is only a second-order stationary point which is much higher in energy, it is less stable. Other vibrational frequencies correspond to parts of the CPS structure. The Si-H bond has a frequency from 2100 to 2200cm^{-1}. The H-Si-H bond can move in three different ways corresponding to three different vibrational frequencies: Scissoring occurs from 850 to 950 cm^{-1}, rocking from 300 to 400cm^{-1}, and wagging at 725cm^{-1}. The breathing frequency of the
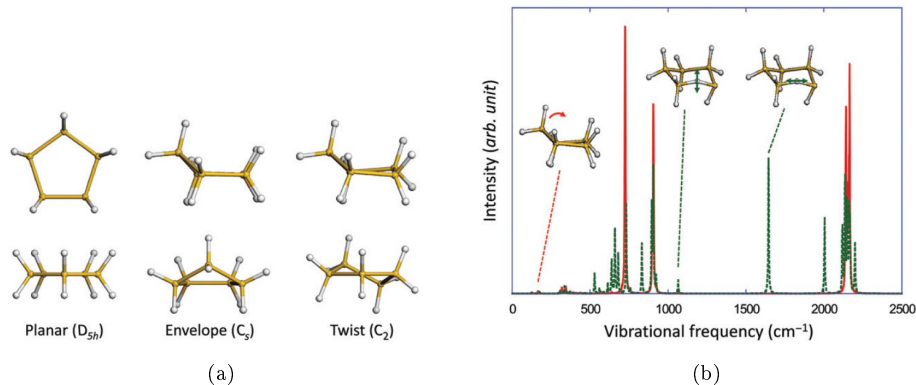
Figure 2.9: Three main structures of CPS (a). Infrared spectra displaying vibrational frequencies associated to the CPS, red lines indicating the twist and envelope structures. The green dotted lines indicate intermediate structures after the formation of the Si-H-Si bridge bond (b). [4]

pentagonal ring itself is at 344.8cm^{-1}. For pure CPS, no vibrational frequency should be found in the region from 1000 to 2100cm^{-1}. Vibrational frequencies are displayed in Fig. 2.9b.

Solvents

Although the CPS can be used unaltered during the solution deposition on a specific substrate, in some cases it may be desirable to modify some of the fluid properties. As mentioned before, exposing the compound to UV photopolymerizes some of the CPS molecules to polysilane chains which are in turn dissolved in the unconverted CPS. The amount of exposure relates to the amount of polysilane chains produced that make the resulting liquid change some of its material properties.

Another option is to use an organic solvent that can be used together with CPS to form a less viscous and more wettable fluid. Some requirements of the solvent should be met such as: The solvent should not react with the CPS during any phase of the processing, and vapor pressure should be in between 0.001mmHg and 200mmHg. A pressure lower than 0.001mmHg will result in too slow drying which would increase the possibility of the solvent remaining in the final film decreasing the silicon film quality. A pressure higher than 200mmHg leads to a fast evaporate which makes a uniform coating of the film very difficult. Finally, the boiling point of the solvent needs to be less than 300°C so that for the resulting amorphous film production during its annealing step, no solvent is remaining that can disturb the quality of the silicon film. [6] For more information about the solvents and the reasoning behind the choices, based on agglomeration energies, the reader is referred to [34].

Research so far

Various research has been done to characterize the properties of CPS. There is still a lot to find out about the compound. Limited research has been conducted in the fabrication of solution processed liquid silicon devices. Fig. 2.10 shows the characteristics of chemical vapor deposition, spin-coated and inkjet printed TFTs from liquid silicon by [1]. The mobilities are a lot higher than those of most organic TFTs that have a mobility close to a-Si:H which is $1cm^2/Vs$. The lower inkjet mobility of 6.5 cm^2/Vs was claimed to be due to poor crystallinitiy and rough surface. The spin-coated liquid silicon TFT had a mobility of 108 cm^2/Vs. Still, this mobility is limited by random grain boundaries found in the channel region that greatly deteriorate transistor performance.
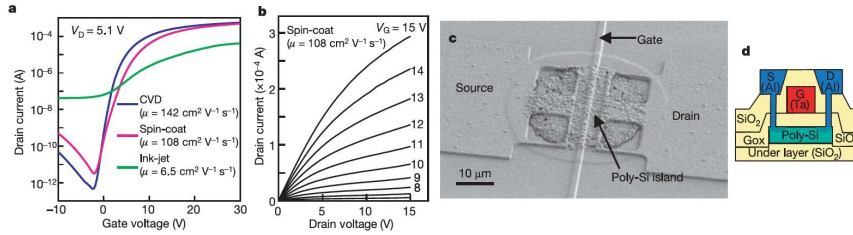
Figure 2.10: TFTs constructed with liquid silicon using inkjet printing, spin-coating, and chemical vapor deposition. Transfer characteristics in (a), output characteristics in (b), image of the TFT using SEM (c), and the schematic of the TFT structure (d). [1]
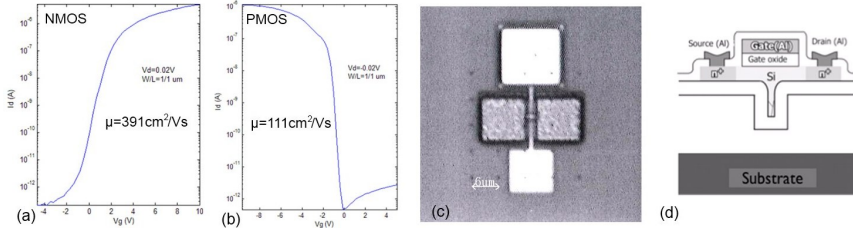
Figure 2.11: Single-Grain TFTs constructed with liquid silicon using spin-coating. NMOS and PMOS transfer characteristics in (a) and (b) respectively, SEM image of the SG-TFT in (c), and the SG-TFT schematic in (d). [2]

[2] shows the location control of these random grains, and created SG-TFTs with spin-coated liquid silicon. The achieved mobilities were 391 cm^2/Vs for electrons and 111 cm^2/Vs for holes. Fig. 2.11 shows the transfer characteristics of both PMOS and NMOS.

In both works, solution deposition methods that are incompatible with roll-to-roll processing have been used. In addition, a second thermal annealing step had been conducted in order to remove sufficient hydrogen atoms for an error

free laser crystallization. This second thermal annealing step makes the whole process still incompatible to plastic substrates.

Therefore, in this work, the liquid silicon material has been spread by the precursor of gravure printing: doctor blade coating. This method is compatible with roll-to-roll fabrication. In addition, the second thermal annealing step has been replaced by an Excimer Laser pre-annealing step which is known to unalter the properties of underlying layers such as the plastic substrate.

Chapter 3

Doctor Blade Coating of Liquid Silicon

In a gravure printing system the blade is known as the soul of the printer. It is a tool used to remove excess ink that has been covering the surface of a certain patterned substrate, and define the patterned areas containing ink and the non-patterned areas that are clean as a result of the blading. The excess ink may be reused and the patterns on the roll or substrate are transferred to a target surface. Due to its direct influence to the printing result, any defects on the blade will significantly influence the final result. In electronics this may be the difference between working and failing of an IC.

In this work, the blade has not been used as a scraping tool but as a spreading tool. In this way, an excess layer is left on top of the substrates while the patterns are filled. For the production of Single-Grain Thin-Film Transistors (SG-TFTs), the position of single crystal grains are controlled by grain filter cavities that need to be filled with the liquid silicon. The excess liquid silicon film formed on top of the patterned layer is needed for the grains to grow into during Excimer Laser crystallization as well as the protection of underlying layers. The thickness of this layer partly determines the maximum shootable laser energy density and therefore the maximum obtainable grain size. A layer thickness of at least 100 nm is desired to be able to shoot energies similar to [2].

In this chapter, the main goal was to use the doctor blade coating method for the deposition of a uniform amorphous silicon layer using the liquid silicon material. First the theory enabling this uniformity is discussed. This section is followed by the experimental part, introducing a list of equipment that has been used as well as the general production method in Section 3.2. Followed by a section explaining the initial experiments for evaluating some of the liquid silicon characteristics. Next, the main experiments for the formation of the amorphous silicon layer is presented, and finally conclusions and recommendations are given.

3.1   Theory

3.1.1   Doctor blade coating

Forces applied on fluids such as the case for doctor blade coating are strongly related to the viscosity of the liquid. The viscosity is defined as the measure of resistance of a fluid that is undergoing shear or tensile stress. For fluids, viscosity is commonly referred to as the thickness of a liquid due to the difficulty of liquid motion.

Fluid properties can be classified in a system where a material is placed in between two large parallel plates. The material is assumed to adhere to the plates. The bottom plate is fixed and a force is applied on the top plate in the parallel direction of both plates. The way the material responds to a shear force applied on the top plate can be used to classify properties of the fluid. The situation is sketched in Fig. 3.1
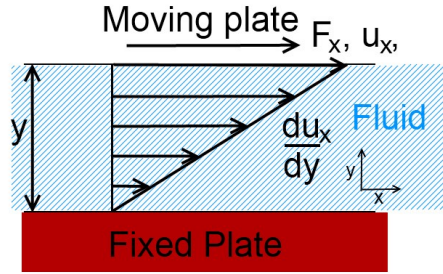
Figure 3.1: Schematic of a system of two parallel plates applying shear force on a medium present in between the plates.

A flow within the medium material is a result of shear stress. This flow is a combination of different layers that move at different velocities as a result of shear stress between the layers. The opposing force to this shear stress is defined as the viscosity. In this way, a velocity gradient exists from the top plate to the bottom plate. This shear flow and velocity gradient defines the fluid. The relation between the applied force and the velocity gradient is described as:

$$\overrightarrow{F_x} = \mu A \frac{\overrightarrow{u_x}}{y} \tag{3.1}$$

In which $\overrightarrow{F_x}$ is the applied force on the top plate, A is the area of the plate, $\overrightarrow{u_x}$ is the displacement, y is the distance between the plates, and μ is the proportionality factor also known as the dynamic viscosity. In terms of shear stress $\overrightarrow{\tau_x}$:

$$\overrightarrow{\tau_x} = \mu \frac{\overrightarrow{\partial u}}{\partial y} \tag{3.2}$$

The rate of shear deformation $\overrightarrow{\frac{u_x}{y}}$ is equal to the shear velocity $\overrightarrow{\frac{\partial u_x}{\partial y}}$ and is also known as the shear strain or relative displacement $\overrightarrow{\gamma_x}$.

Different types of fluids have different proportionality constants or viscosities. A fluid in which a relative rate of movement is proportional to the applied force is known as a Newtonian fluid. In this system μ is a constant. This type includes most common fluids such as water, air, glycerin, oils, etc.

A non-Newtonian fluid is one where the shear stress and shear rate are not proportional but are related. μ in this system is not a constant and is a function of either shear stress $\overrightarrow{\tau_x}$ or shear strain $\overrightarrow{\gamma_x}$. More complex structured fluids are included for this fluid type such as polymers or solutions, suspensions, emulsions, etc. Liquid silicon is assumed to be a non-Newtonian fluid. [35]

The viscosity of liquid silicon can be increased by exposing the base liquid CPS to UV. The UV produces polysilane chains that will lead to a more viscous liquid. The increase in viscosity will result in difficulty in doctor blade coating the material. In doctor blade coating, the situation is slightly different; The top moving plate is replaced with a plate perpendicular to the bottom plate. The plate also digs into the liquid layer allowing the liquid to be transported in this method. A high velocity will result in a low shear velocity or relative displacement as shown by Eq. 3.2. A movement of the blade in one direction forces the liquid to be pushed in this same direction, however, the liquid has a low relative displacement, which means that instead of being pushed in the bladed direction, it will pile up and escape through the edges of the blade. This will cause bigger tracks than in a situation where the viscosity is low, where the liquid flows easily in the same direction as the blade. The situation is illustrated in Fig. 3.2
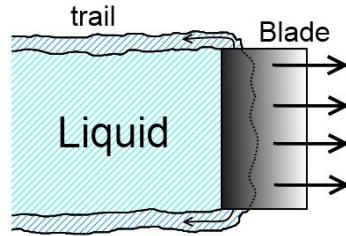
Figure 3.2: Schematic of the top view of doctor blade coating, showing trail formation.

3.1.2 Surface Free Energy

In this section, the theory behind the surface free energies will be given and is based on [36] and [37]. The contact angle (ϑ) is a way to measure the surface energy interactions between a liquid that has been deposited on a solid surface. Fig. 3.3 shows the schematic of the energies present in such a situation.
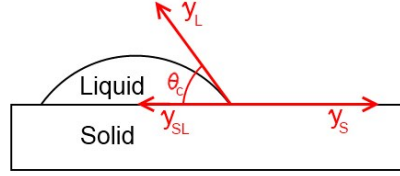
Figure 3.3: Surface energies definition schematic

The more than 200 years old Young equation defines the way these forces interact with each other by:

$$\gamma_S = \gamma_{SL} + \gamma_L \cos\theta \tag{3.3}$$

rearranging gives:

$$\cos\theta = \frac{\gamma_S - \gamma_{SL}}{\gamma_L} \tag{3.4}$$

in which θ is the contact angle, γ_S is the surface free energy of the solid, γ_{SL} is the surface free energy of the solid-liquid interface, and γ_L is the surface free energy of the liquid. Using this definition one can comment on the way the contact angle changes with respect to a change in the various surface energies.

When perfect wetting occurs, the liquid is spread over the solid surface without being able to form an observable contact angle. In this case the contact angle is equal to 0°. An increase in the contact angle will result in a decrease in the term $\cos\theta$, which will mean that either the surface free energy of the liquid increases or the surface free energy of the solid decreases when keeping the surface energy of the interface relatively constant. The opposite is needed for a decrease in contact angle. In this case, the force of attraction between the molecules in the liquid and the molecules of the solid become larger than the attraction between the liquid molecules themselves, therefore the liquid will spread over the surface.

Using Eq. 3.3, the variables can easily be obtained and computed as long as γ_{SL} is known. Various studies have been focusing on an additional relation between γ_{SL}, γ_S, and γ_L, so that γ_{SL} can be made a function of γ_S and γ_L, also known as the equation of state.

Berthelot was the first to study this relation by relating the adhesion work of the interface (W_{SL}), to the cohesion work of a solid and the cohesion work of the liquid (W_{SS} and W_{LL}):

$$W_{SL} = (W_{SS}W_{LL})^{0.5} \tag{3.5}$$

using the Dupre equation on the work of adhesion, and two other relations with the surface free energies:

$$W_{SL} = \gamma_S + \gamma_L - \gamma_{SL}, \ W_{SS} = 2\gamma_S, \ W_{LL} = 2\gamma_L \tag{3.6}$$

a definition of γ_{SL} in terms of γ_S and γ_L had been constructed which is also known as the Berthelot hypothesis:

$$\gamma_{SL} = \gamma_S + \gamma_L - 2\left(\gamma_S\gamma_L\right)^{0.5} \tag{3.7}$$

which forms the base of following theories attempting to accurately relate γ_{SL} to γ_S and γ_L.

Grifalco and Good introduce the parameter ϕ in which the type of interfacial interactions is further defined:

$$\gamma_{SL} = \gamma_S + \gamma_L - 2\phi\left(\gamma_S\gamma_L\right)^{0.5} \tag{3.8}$$

Neumann et al. derive three equations defining γ_{SL} , the first one was based on thermodynamics, and the other two were based on the Berthelot hypothesis:

$$\gamma_{SL} = \left\{\left(\gamma_S\right)^{0.5} - \left(\gamma_L\right)^{0.5}\right\} / \left\{1 - 0.015\left(\gamma_S\gamma_L\right)^{0.5}\right\} \tag{3.9}$$

$$\gamma_{SL} = \gamma_S + \gamma_L - 2\left(\gamma_S\gamma_L\right)^{0.5}\exp\left\{-\beta_1\left(\gamma_L - \gamma_S\right)^2\right\} \tag{3.10}$$

$$\gamma_{SL} = \gamma_S + \gamma_L - 2\left(\gamma_S\gamma_L\right)^{0.5}\left\{1 - \beta_2\left(\gamma_L - \gamma_S\right)^2\right\} \tag{3.11}$$

Where $\beta_1 = 0.0001247$ and $\beta_2 = 0.0001057$, both are experimentally determined.

Partition to SFE components

Fowkes initiated the idea of a partitioning of the SFE into components due to various interfacial interactions. In this way the SFE of the solid is a sum of various interactive components:

$$\gamma_S = \gamma_S^d + \gamma_S^p + \gamma_S^h + \gamma_S^i + \gamma_S^{ab} + \gamma_S^o \tag{3.12}$$

the d, p, h, i, ab, and o, stood for the dispersion, polar, hydrogen bond, induction, acid-base, and remaining interactions respectively. The individual components can be computed in various ways such as the Fowkes method, Owens-Wendt method, and the Van Oss-Chaudhury-Good method. They all require the measurements of multiple liquids. A second requirement is that one of the liquids is a dispersion liquid such as diiodomethane.

In this work we have measured multiple liquids: CPS, UV-exposed CPS, and CPS with cyclooctane solution, however, none of these are full dispersion liquids and can therefore not be used to compute the individual components of the SFEs.

3.1.3   a-Si film formation from liquid silicon

In the experiments, liquid silicon material is used to produce an amorphous silicon film out of a liquid. The term liquid silicon in this context differs from the liquid silicon used in [1] and [2], and applies to any liquid that has been used in this work to form the desired amorphous silicon film. This includes pure CPS as well as a mixture of CPS and an organic solvent, as well as a either of the liquids, exposed to UV. The description of the film formation is given using CPS since this forms the base material.

The compound CPS can be used to form an amorphous silicon film after various processing steps. The compound is liquid at room temperatures, transforms at plastic compatible temperatures and may be used to crystallize into a higher quality silicon. Due to this property it can be seen as bringing quality to solution processing.

The compound reacts strongly to oxygen and water. Processing can therefore not occur in oxygen and water rich ambient for a high quality a-Si film formation. Although vacuum is not required, as is the case in conventional processing, an ambient of an inert gas such as nitrogen should be used [6].

When the temperature of the compound is increased to above 300°C, the hydrogen bonds break and leave the material, and as a result, pure silicon is left [4, 5]. One specific issue in this scenario is the fact that the boiling point of CPS is much lower than this decomposition temperature. Simply heating the compound to the high temperature will therefore evaporate most of the CPS so that almost no a-Si layer can be formed. In order to decrease the volatility of the material, ring-opening polymerization is required [30, 7].

Photopolymerization   The compound can be photopolymerized by exposing it to UV light of a certain range of wavelengths that can break the Si-Si bonds (53kcal/mol). The CPS ring structure opens and can transform into $-(SiH_2)_5-$ radicals. Wavelengths in between 360nm and 420nm give the best results [6, 11]. Wavelengths shorter than 300nm can result in the formation of components that are insoluble and in addition cause difficulty in forming a high quality amorphous film. Wavelengths above 420nm polymerize the compound slowly. Using wavelengths of the specified range will also prevent breaking the chemical bond of an organic solvent that may be optionally used together with CPS. This prevents impurity carbon atoms from getting mixed into the silicon network [34]. According to Dr. Shimoda, a wavelength of 365nm gives the best results.

The UV light will structurally cause a deviation in the envelope construction of CPS, in which the Si atom outside the Si plane deviates at a vibrational frequency of 73.5cm-1 [4]. The UV exposure opens these rings and the resulting opened structures can subsequently join other opened CPS structures end-to-end to form long chains called polysilanes that are non-volatile. More Si-Si bonds can however be broken by the UV exposure, making the availability of single long polysilane chains low. The silicon radicals that are produced by the breaking of the Si-Si bonds can react to oxygen at the surface forming Si_2O_3 after 5 minutes of UV exposure, and $Si(SiO_2)$ after 15 minutes of UV exposure[7].

The resulting silane compound radicals are insoluble in most common organic solvents, however it has proven to be soluble in the original low order silane compound of CPS, as well as a mixture of CPS with a common organic solvent [7, 8]. In this way, during UV exposure the created polysilane chains are immediately dissolved in the precursor. UV exposure of CPS can make the liquid more viscous at first. After sufficient UV exposure, the liquid transforms into a white solid. This happens when the average chain length of the polysilane chains go up to 400 monomer elements [34]. The length of the polysilane chains due to this UV polymerization have a great effect on the viscosity, wettability, melting point, boiling point, and adhesion to the substrate, and will increase these values as the chain length increases. The reactivity with oxygen will become lower. [34]

The UV exposure of the compound may also break Si-H bonds (76 kcal/mol). This will cause complications in the production of polysilane chains, and will lead to non-linearities in the chain structure, especially in the beginning of the exposure process. More bonds break with increasing exposure times. It has been shown that after 5 minutes of UV exposure already most of the Si atoms have lost one hydrogen atom. After 15 minutes of exposure time, hydrogen atoms cannot be detected anymore. This effect is shown by x-ray photoelectron spectroscopy (XPS) of the Si 2p spectrum in Fig. 3.4a. The basis of this experiment lies in the fact that when a hydrogen atom is attached to a silicon atom, the binding energy will increase by 0.3 eV for every binding. The peak of 99.68 eV is accounted to the neutral silicon. The peak at 99.08 eV corresponds to silicon among other silicon atoms, so the removal of most of the hydrogen atoms. The other peak at 102.48 eV relates to the generation of unsaturated surface states due to UV exposure. After 15 minutes of UV exposure the surface is fully oxidized to $Si(SiO_2)$ and a electron binding energy of 103.15 eV results, which also confirms the lack of hydrogen in the film. [7]. Fig. 3.4b. shows the results of gel permeation chromatography (GPC) where the size of the produced polymers are visualized as the broad peak formation.

Thermal Annealing Although most hydrogen atoms are removed during the UV exposure process, there is still a need to transform the polysilanes to a three dimensional amorphous network. For this an elevated temperature is required that is higher in energy than the binding energies of Si-Si and Si-H. Temperatures less than 300°C are insufficient to decompose the polysilanes, and it will be impossible to construct a quality silicon film. The upper limit of the temperature is defined by the substrate. Although for the construction of polycrystalline silicon, an annealing temperature of higher than 550°C is required, exposing the amorphous film to Excimer laser is an alternative way to transform the amorphous material into polycrystalline silicon, resulting in higher electrical properties without having to expose the substrate to such high temperatures [2, 6, 11]. Previous works [1, 2] have constructed an amorphous silicon layer from liquid silicon at an anealing temperature of 430°C. A second thermal anneal step was used for dehydrogenation before Excimer Laser crystallization

(a)   (b)
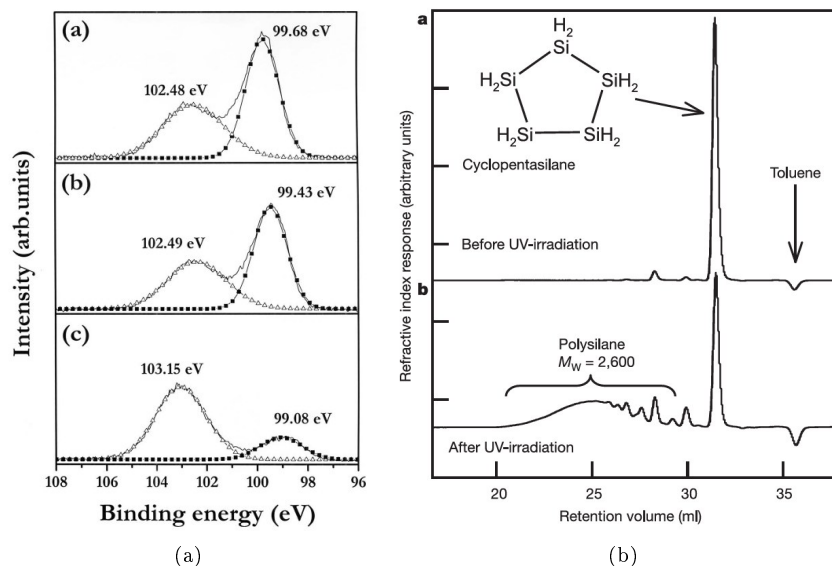
Figure 3.4: Si 2p XPS spectra of a-Si film for different UV exposure times of CPS: a. 3, b. 5, and c. 15 minutes (a) [7]. Gel permeation chromatogram of liquid silicon (b). CPS in toluene in a. and UV-irradiated CPS in toluene in b. [1] The broad peak indicates the polysilanes of various molecular weights.

at 650°C. Both of these temperature are aimed to be reduced to a maximum processing temperature of 350°C.

3.2   Experimental

An overview of the equipment used for the process of this work is introduced. After that, the general processing steps are explained and the variables and boundary conditions are listed. The cyclopentasilane material is highly sensitive and needed to be treated with care. For the production the Glovebox, UV lamp, Hot-plate and spin-coater are used. For the measurements the RAMAN spectroscope, Optical microscope, SEM, FTIR and DekTak profilometer were used.

3.2.1   Equipment

MBRAUN GmbH Glovebox with Gas purification platform MB20/MB200

The *Glovebox* is a sealed box that can limit the levels of oxygen and water. In this way, materials sensitive to these components, such as CPS, can be processed within an inert atmosphere such as nitrogen. The box has a window on one side

with gloves incorporated in it for the operation of tools within the box by the user, while the chamber keeps its controlled atmosphere. Oxygen and water levels can be monitored and are controlled by recirculators and the pumping of the inert gasses.

Key features of the *Glovebox* include a gas purification system (MB 20-G) with control panel, the antechamber, and a pressure gauge. The gas purification system removes the oxygen and water content by continuous circulation using catalysts. A sealed chamber (antechamber) allows the transportation of tools and materials in and out of the *Glovebox* without changing the atmosphere inside. A pressure gauge adjusts the pressure inside the *Glovebox* as the pressure changes from using the gloves. Typically a positive pressure is employed by default since air will be pushed out of the box at all times. [38, 39] A schematic image of the *Glovebox* is displayed in Fig. 3.5.

[6, 11] note that the production of the amorphous silicon film with CPS can be done for oxygen levels under 10ppm. In most of our experiments the level of oxygen has been limited to under 0.1ppm. Only after fabrication of the amorphous silicon film are the substrates transported out of the *Glovebox* for further processing and measurements.
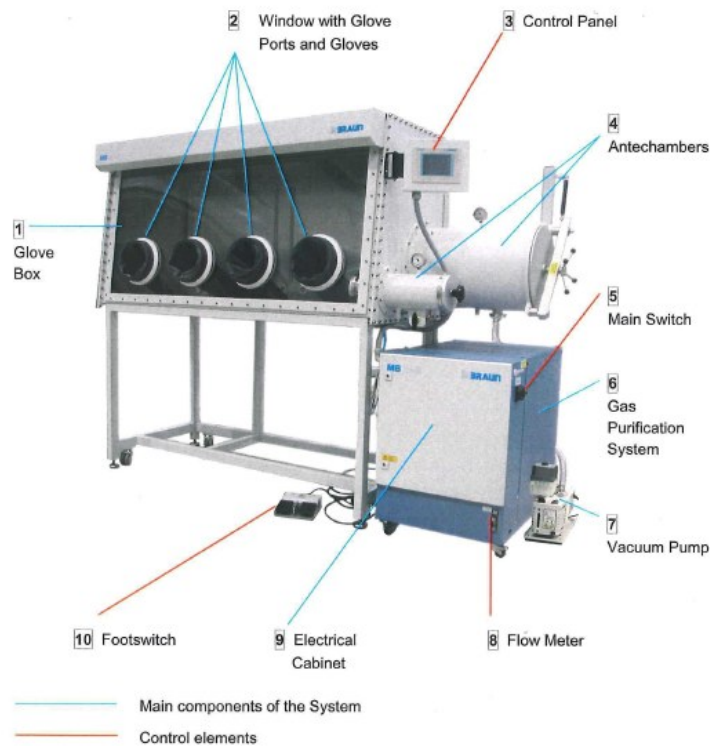
Figure 3.5: MBRAUN Glovebox [39]

UV AHAND 250GS

UV light has been used to photopolymerize the CPS. This photopolymerization makes the liquid deposited on the substrate surface less volatile, and therefore prevents total evaporation of the liquid during final annealing for the formation of the amorphous silicon film. Two filters are available of which the black light filter was used. The intensity of the produced wavelengths are displayed in Fig. 3.6a. According to the T. Shimoda group, the CPS reacts best to a UV wavelength of 365 nm which is within the range of the UV light used our experiments. Two precautions have to be taken when using this UV light source:

1. The UV requires some warm-up time, during this time the UV does not have its maximum intensity so exposing the liquid for a bit more time may be useful.

2. The distance from the liquid to the UV is quite important as the intensity of the light drops exponentially. Fig. 3.6b displays this exponential drop

(a)   (b)
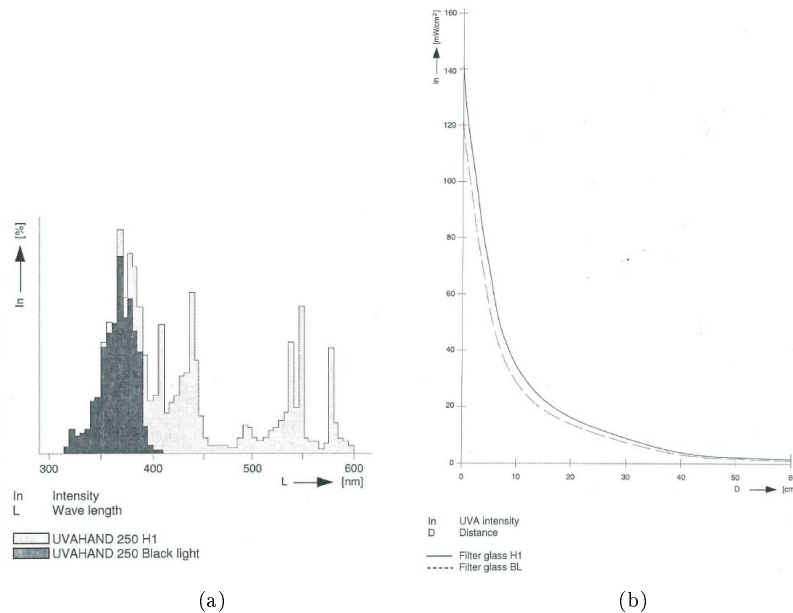
Figure 3.6: UV AHAND 250GS wavelength over wavelength in (a) and intensity over distance in (b).[39]

Hot plate

For temperature treatment of the wafer, for example for thermal annealing, a hot plate has been used since it is small enough to be placed inside the glovebox.

It is able to reach high appropriate processing temperatures while the user is allowed to observe changes of the heated sample. Overshoot of approximately 10 ˚C is a problem with this device even for temperature increases of 10˚C. Since the release of hydrogen atoms during annealing produce silicon radicals and dangling bonds, the liquid silicon material is prone to contamination even in a controlled atmosphere with limited levels of oxygen and water. A quartz lid has therefore been used when annealing the substrate to the high temperature so that no air can enter the amorphous film during heating and release of hydrogen atoms cause a slight overpressure inside the lid.

Optical Microscope

An optical microscope has been used as a preliminary analysis of the wafer. Images could be taken by a mounted camera on top of the microscope. From these images a first impression can be made from the resulting film after annealing, but also from laser crystallisation for the next chapter.

SEM

The scanning-electron microscope gives a more thorough analysis of the way the patterns on the substrate are filled by the solution. It is a high resolution microscope that can produce images in the nanometer range. The basic working is the collection of various signals that are formed when a focused beam of high energy electrons are incidented to a sample. The large amount of kinetic energy of the electron is during absorption of the sample transformed into: secondary electrons, backscattered electrons, diffracted backscattered electrons, photons, visible light and heat. Secondary electrons and backscattered electrons are the most important elements for the imaging of the sample. A cross-section of the wafer is viewed by carefully breaking the wafer with the resulting amorphous film from the liquid silicon compound. This not only shows the filling of the basic patterns, also grain filters are analyzed in this way during the first experiments. The downside of this experiment is that the broken wafer cannot be used for further processing. [40]

Renishaw's inVia Raman Microscope

The optical microscope only gives away the position of the liquid silicon by a change in color. To be sure that this change in color is accounted to the deposited solution, RAMAN spectroscopy is used. The basic working of this tool is identification of a vibrational frequency shift of reflected light from a sample, compared to the original laser source incidented on a sample. This frequency shift is also known as the RAMAN effect and is based on the molecular deformation of the sample into oscillating dipoles due to the electromagnetic wave from the excitation source. The periodic deformation results in the material specific vibration of the molecules. By far, most of the re-emitted photons are subject to *Rayleigh scattering* that has the exact same frequency as the original

light source and is of no use for measurement purposes. Only 0.001% of the reflected light is the result of *Stokes effect* and needs to be filtered. [41]

With this method, the difference between amorphous silicon and crystalline silicon can be visualized. Crystalline silicon will re-emit a narrow peak at a vibrational frequency of 521cm^{-1} due to a high uniformity of bond angles and bond lengths in the material. Due to a wide array of bond angles, energies and lengths as well as dangling bonds, amorphous has a wider peak in the vibrational spectra positioned at 480cm^{-1}. Since CPS is transformed to an amorphous silicon film on top of a crystalline silicon wafer the two peaks can be distinguished and it can therefore be determined if there has been an amorphous silicon formation. The light source used for this type of measurement may crystallize the amorphous silicon itself so a low intensity of 125 µW has been used for the measurement. [42]

Veeco Dektak 150 Profilometer

The two-dimensional, profile of any surface can be visualized by using the Dektak 150. It uses a high quality, low force stylus (Low-Inertia Sensor, LIS 3) that runs in a straight line across a surface and plots the changes in height of the stylus while it encounters various patterns on the target surface. A resolution of 1 Å can be achieved, at the lowest range setting of 6.5 µm, which was commonly used in this work since pattern depths were less than 500nm. Due to the limited range setting, accuracy issues were inevitable. The force of the stylus was set at 1mg. A video camera allowed the manual positioning of the stylus.[43]

FTIR Spectrometer

Fourier Transform Infrared spectroscopy is a tool that can measure the amount of certain atomic bonds present inside a film. In this work, the bounded hydrogen content is measured within the a-Si film formed from liquid silicon. A source of infrared radiation is sent to through a sample which absorbs some of the radiation. This molecular absorption and transmission is measured. The absorption peaks are related to the vibrational frequencies of certain bonding types (vibrations with a transition dipole moment). In this way, the bonded hydrogen can be measured by sensing the distinctive wagging and stretching vibrations of the monohydride (Si-H), the dihydride (SiH_2) and the trihydride (SiH_3). The wagging mode of the configurations (e.g. the degenerated rocking and wagging of Si-H and SiH_3, and the pure rocking for SiH_2) are all located at 640cm^{-1}. The amount of bonded hydrogen present inside the film (N_H) is related to the integrated absorption of the predefined absorption peak. In case of the wagging mode:

$$I_{640} = \int \left(\frac{a}{\omega} \right) d\omega \tag{3.13}$$

$$N_{H_{640}} = A_{640} \cdot I_{640} \tag{3.14}$$

I_{640} is the integrated absorption of the 640cm^{-1} absorption peak, α is the absorption coefficient found from the measurement, ω is the vibrational frequency, and A_{640} is the proportionality factor which related to the strength of oscillation. This proportionality factor is experimentally determined for which the constant $1.6\cdot10^{19}$cm^{-2} is commonly used for a-Si:H. In this work the I_{640} of different UV exposure times and thermal annealing procedures are evaluated. Note that only bound Hydrogen atoms are obtained in this way. [44, 45]

3.2.2 Working procedure

Initial experiments were conducted using a template procedure from which many variations have been tested for the optimization of the film formation process. This template is based on [2]:

1. A crystalline silicon wafer is prepared on top of which TEOS is deposited using PECVD and is patterned.

2. On top of the substrate a predetermined number of drops of 100%CPS will be deposited by means of a pipette.

3. The drop will be spread by a doctor blade that will lead to a filling of any patterns that are present on the surface.

4. After having spread the CPS across the full wafer, the excess is left on top of the wafer to form a protective layer for the Excimer Laser process.

5. The substrate will then be exposed to UV lighting for 10 minutes, during which the CPS on top of the substrate polymerizes to polysilanes, preventing the film from evaporating during the annealing step.

6. The wafer is placed on the hot-plate, and is covered with a quartz lid to protect the film from oxidizing during this annealing step while allowing the evaporated hydrogen to escape. This hot plate is heated to 200˚C.

7. After 1 minute of thermal treatment of 200˚C, the temperature of the hotplate is increased to 430˚C in 10 minutes.

8. After 1 hour of 430˚C thermal annealing, the wafer is slowly cooled down to room temperature.

Changes to this basic procedure have been applied to understand how the fluid behaves and which procedure gives the best results. Besides the 100% pure CPS that has been used in many of our experiments we can use other variations on the liquid silicon material for the creation of the amorphous film.

The variations to the liquid silicon that we have used include pure CPS exposed to UV for different numbers of minutes, as well as the CPS mixed with the organic solvent cyclooctane with 20%wt. of CPS against the solvent. UV exposure of this mixture has also been used for a similar liquid silicon as used

in [2]. The time of the UV exposure is varied but it is ensured that the resulting fluid does not solidify as it is the case for long UV exposure times.

Many different changes can be made within this template procedure. Table 3.1 lists these varieties.

The initial approach was to try various combinations on a substrate to see what combination gives what type of effect. This was followed by a number of repetitions of the best results and attempts to optimize the best obtained results.

3.2.3   Boundary Conditions

The experimental methods we used had a number of limitations. These limitations slowed down the optimization process and made repeating processes inevitable as well as inconsistent.

Blading Many different variables existed during the blading of the liquid silicon on the substrate. This was primarily due to the physical inconsistency since blading was not automated but done by hand. Speed, force, angle of blade, blading directions, vibrations from the hand were all variables that could not be kept as a constant and should always be accounted for.

Impurity Wafers as the target substrates transported into the glovebox from the open air have some oxygen or water molecules sticking on the surface. This would influence the way the liquid silicon is spread on the wafer as well as the purity of the deposited material. Another important aspect was the way the 100% CPS was stored for usage. This was in a brown jar on top of a shelf inside the glovebox. The glovebox although limited in water and oxygen content, could cause degrading of the material over time due to not only the molecules in the atmosphere, but also temperature changes from the hot-plate placed inside the box. Transportation of tools inside the glovebox increases the oxygen and water content to 15ppm at most.

Equipment Inaccuracies during measurement can be misleading for the judgment of the final result. Primary judgment in many cases come from the optical microscope. Roughness of the surface although visible optically through changes in colors, was not detectable using the profilometer or other tools that we have used.

3.3   Characterization Experiments

Before attempting to get the best amorphous silicon films, some basic characteristics of the liquid silicon material should be identified. In this section, some important aspects of the liquid are presented: Thickness of the film, the effect of different types of liquid silicon, the surface free energies of various surfaces that we have used, the RAMAN proof that the liquid indeed transforms into amorphous silicon, and FTIR results for the effect of the variations to the standard procedure to the bounded hydrogen content.

Table 3.1: Processing varieties from liquid silicon to amorphous silicon film

Material usage
The type of liquid silicon material. Either pure CPS or a certain dilution of CPS with cyclooctane before deposition on the wafer. Also the UV pre-exposure times can be varied to change the viscosity of this base material or other properties of the fluid.
The type of material used for the blade can change the way the fluid is spread on the substrate. A hydrophillic blade will cause the fluid to stick more to the surface of the blade whereas a hydrophobic blade will push the fluid away from the blade. The mechanical stiffness of the blade will also change the spreading characteristics
The surface of the substrate can be modified to increase or decrease adhesion of the fluid, or a combination of both. Some treatment can modify the roughness of the surface, others simply result in a change in surface tension of the source fluid.
Temperature
The time the substrate is annealed at the final temperature can be extended for a better quality amorphous silicon film, although it is desirable to decrease this time for production throughput reasons.
The ramp up and cooldown of the wafer during annealing can be speeded up or slowed down. Speeding the temperature change up will give a negative influence on the film due to the sudden shock of temperature difference that the film is exposed to. It will however decrease processing time.
The maximum annealing temperature can be increased to increase the quality of the silicon film, or decreased to make it possible to produce the film on top of a plastic substrate such as polyimide.
Pretreatment of the substrate surface can change the adhesion characteristics due to the molecules that are by default sticking to the surface.
Heating the substrate during deposition and spreading to a slightly elevated temperature will change the adhesion properties.
UV exposure
Exposing the fluid to UV will photopolymerize CPS into polysilanes that dissolve in the non-transformed CPS. This will make the fluid less volatile and therefore prevent the film from evaporating during annealing. A longer exposure time will lead to more CPS transforming into polysilanes, as explained in Section 3.2.2 .
Not only is UV exposure a way to make the liquid silicon less volatile, the fluidic properties will change as well. Exposure will make the liquid more viscous which will give a different effect when spread on the substrate after UV exposure of the CPS.
Blading
Speed of blading
Force applied on the substrate during blading
Angle of blade to the surface
Direction of blading with respect to the patterns
Moment of blading after drop deposition on the substrate

3.3.1 Film breaking

The very first of the observations was one that focuses on the thickness of the deposited liquid silicon material. Some problems with the film occurred for areas on the substrate with a lot of liquid silicon. This was not necessarily a direct cause of the thickness of the layer, but the gradient of the layer seemed to have quite some impact on the film. This was observed when pattern depths had increased leading to a bigger change in step height of the resulting amorphous silicon film. The deeper patterns lead to observable pattern edges after film deposition. These visible edges were the first parts that cracked during baking. On the same wafer a smooth area was observed that did not break during annealing. Areas where the gradient exceeded a certain level resulted in the cracking of the layer. This was the case for four situations:

1. Excess liquid silicon that has been pushed to the edge of the wafer have a bigger thickness and are more prone to thickness variations and therefore breaking in many cases initiate at these excess areas.

2. Trails of the liquid silicon material caused by the blade are locally thicker and will break first during thermal annealing.

3. Patterns on the substrate that are relatively deep and cause a deformation of the deposited film in step-height differences will break at these step heights.

4. Edges of the wafer or areas defining a covered and an empty area may cause breaking of the film at the junction, this however is not a strong source of these cracks.

DekTak images such as Fig. 3.7 prove that the thickness of the film is not particularly a problem, but the thickness variations are the cause of the breaking of the layer. The layer leading towards the empty space, which is where the crack formed, is getting thicker, while the thickness of the surrounding layer itself is in all four cases different. The broken particles had been removed using Isopropanol (IPA) and left an area without liquid silicon which was useful as a reference for the DekTak.

The amorphous silicon layer had various colors that indicate to some extent the roughness of the layer. Cracked areas on the other hand created many small silicon particles that changed its color visibly during thermal annealing, without using the optical microscope. These colors do not indicate the surface roughness, but the quality of the silicon layer as more polysilane structures break and form cross connections with neighboring polysilanes to form an a-Si network. The transition went from colorless to white at around 200°C, yellow from approximately 200° to 300°C , maroon from around 330°C, and finally silver after some time at higher temperatures. The exact temperature on which the transition occurred was undefined since it is also dependent on the duration of heating.
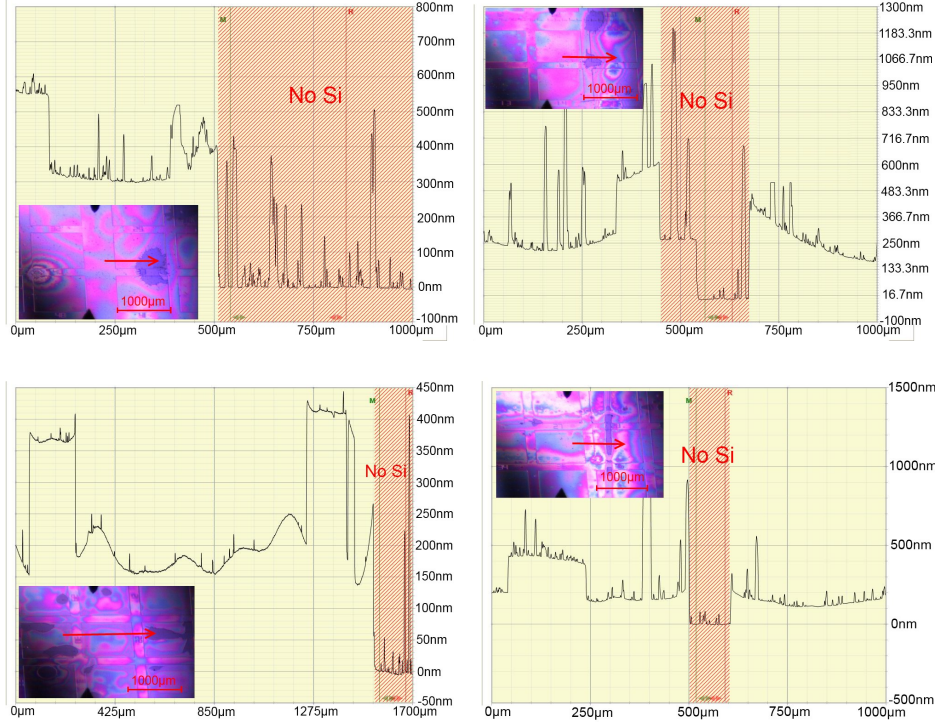
Figure 3.7: DekTak graphs with profiles from various surfaces on which liquid silicon has been transformed into amorphous silicon. The area where the amorphous silicon has been removed is where the layer was broken.

3.3.2   Liquid Silicon

The term liquid silicon in this work is used for a liquid material that can be converted into a solid amorphous silicon film using the procedure as described in Sec. 3.2.2. This means that there are many variations that can be used to the base 100%CPS material. The liquid used in [1] and [2], are both solutions of 100%CPS with cyclooctane that has been UV irradiated before being spin-coated. In this work, experiments have been conducted on the UV irradiated 100%CPS and the 100%CPS mixture with cyclooctane solution and pure CPS.

The advantage of using the cyclooctane solution is the increasing wettability characteristic of the liquid silicon. While UV exposure makes the liquid more viscous and thicker, the organic solution can make the liquid less viscous. Using a CPS-cyclooctane mixture, during thermal annealing the cyclooctane will evaporate leaving only the CPS that has been converted to polysilanes during photopolymerization. A number of issues exist when using the organic solution:

1. The evaporation of cyclooctane means that a lot more liquid needs to be

     deposited to get a similar amorphous film thickness as when using pure CPS. When only small amounts are used, as possible for blading, the solution quickly dries out.

2. The mixture introduces carbon atoms in the film that degrade its quality, although the boiling point of cyclooctane (149°C) is slightly lower than that of CPS (194°C).

3. When using only a little amount of the liquid silicon, which is possible for doctor blade coating, the organic solution dries rapidly. For spin-coating this problem does not exist, as large amount of the liquid silicon is deposited and spread across the wafer in a matter of seconds. In doctor blade coating however, drying will occur during every movement of the blade causing uniformity issues.

4. Grain filter cavities filled with the mixture of CPS and cyclooctane result in amorphous silicon that has shrunk inside the filter. As the cyclooctane evaporates, part of the amorphous silicon is already solidified and cannot refill the grain filter. Smaller cavities inside the grain filter will cause issues during laser crystallization.

Due to these issues, this work does not use any organic solution for the production of the liquid silicon SG-TFT.

    Exposing the CPS to UV, will make the liquid more viscous. A longer exposure time results in more polysilane production while at the same time being dissolved into the source CPS material. Varying this exposure time can change the properties of the liquid silicon such as viscosity, volatility as well as wettability. Increasing the viscosity through UV exposure has lead to track formation when doctor blade coating which is undesirable. Omission of this step results in the evaporation of CPS before the decomposition to a silicon film.

3.3.3   Surface Free Energy

The way a liquid reacts to a solid surface is dependent on the surface energies associated to both materials. These surface energies can be obtained by measuring the way a droplet is formed on the solid surface, i.e. the contact angle. A liquid can in this way obtain controlled spreading as is also used in offset lithography printing.

    Three surface modification techniques as well as a number of different substrates have been tested. The modification techniques are: 0.55%HF dip for 4 minute which is a common way to remove native oxide from a silicon wafer at a rate of 15nm/min, O_2 plasma and Argon plasma that bombard the surface, making it rougher. The HF dip does not significantly deform the patterns on the substrate, and Argon is a heavier alternative to Oxygen. Fig. 3.8 shows the different contact angles of pure CPS. The two thermal oxide surfaces indicate different sessions. It is important to note however that in most cases the contact angle reduced over time indicating a dependence on the time that the liquid is in
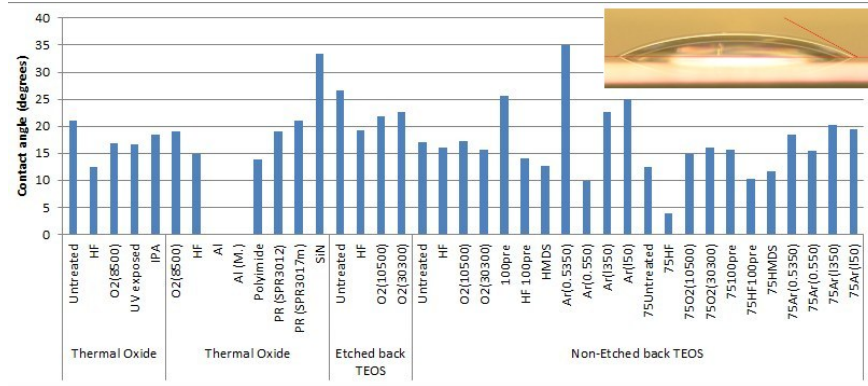
Figure 3.8: Contact angle graphs, different surface modifications on different types of oxide, using pure CPS.

contact with the surface. The experimental data is based on the contact angles approximately 1 to 2 seconds after droplet deposition. The main conclusions that could be derived from these were:

Temperature An elevated temperature of the substrate has a big effect on the wettability of the liquid silicon. This is both because it is more difficult for the molecules within a droplet to stay together due to thermal motion, and because the liquid reacts in some way with the oxide surface. Both effects allow the liquid to spread over time.

Surface treatment 0.55%HF dip for 4 minutes gave the best wettability properties compared to most of the plasma surface modification types. Adding the elevated temperature of 75°C shows that the HF treatment gives better wettability than high pressure, 550W Argon, that shows a lower contact angle at room temperatures. The plasma treatment, bombards the surface with either Oxygen or the heavier Argon molecules which make the surface more rough allowing more of the liquid silicon molecules to react to the surface. The HF however makes the surface more smooth which allows an easier spreading. Varying the plasma conditions for Oxygen plasma gave only limited variations to the final contact angle.

Liquid Silicon The variations of the liquid silicon material from the base CPS compound has different effects on the contact angle. A 20wt.% of CPS in cyclooctane reduces the contact angle on all surface to zero. UV exposing the base CPS material makes the liquid more viscous, which lead to a higher contact angle on all surfaces.

Material The surface material, although for SG-TFT a TEOS surface is required, for the final gravure printing cylinder, other material types may be used. Aluminum showed the highest wettability of liquid silicon, whereas silicon nitride gave the highest contact angle of 33.4°.

From the contact angles, the surface energies of the various surfaces can be computed since the surface energy of the liquid (CPS) is calculated in [46] to be 32.5 mJ/m².

In this work 3.10 has been used to determine the surface energy by rearrangement in 3.3:

$$(\gamma_S/\gamma_L)^{0.5} \exp\left\{-\beta_1\left(\gamma_L - \gamma_S\right)^2\right\} = 0.5\left(1 + \cos\theta\right) \tag{3.15}$$

By obtaining γ_L of CPS from [46] (32.5 mJ/m²), and by measuring the contact angle of CPS on various surfaces, the surface free energies of these surface can be calculated using Matlab.
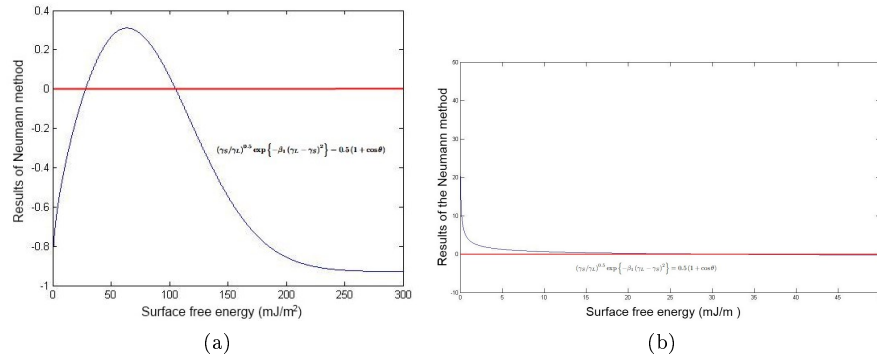
Figure 3.9: Surface Free energy figures using 3.15. Extracting theγ_S (a), and the γ_L (b) by sweeping the respective parameters.

Sweeping the function for various values of γ_S and equating this to the line of $0.5(1 + \cos\theta)$, two solutions can be obtained. The first solution is found to be correct by comparing an the effect of an increasing contact angle which should decrease the surface free energy of the surface, which was only the case for the first of the two solutions. A graph of the plot is shown in Fig. 3.9a. matlab graph needed. The final results are presented in a table in Appendix D, while the graph is presented in Sec. 3.3.3. In the same way, after finding the various γ_S parameters, an unknown γ_L can be computed, by using the same surface modifications for a different liquid. Sweeping the liquid in this case gives the correct result. In this work, CPS that had been exposed to 2 minutes of UV was found to have an average SFE of 33.5 mJ/m². The graph obtained from sweeping γ_L is shown in Fig. 3.9b

Fig. 3.10 shows the results of computing the surface free energies for all surfaces used in our experiments. Notice that the surface free energy increases when the contact angle decreases. The contact angle for aluminum was 0°, however using Eq. 3.10, a maximum equal to the surface energy of CPS was obtained. The actual SFE of aluminum is slightly higher than this number.

Using the same equation (Eq. 3.10), the SFE of another liquid that has been tested on the same surface can be calculated. A second liquid has been used
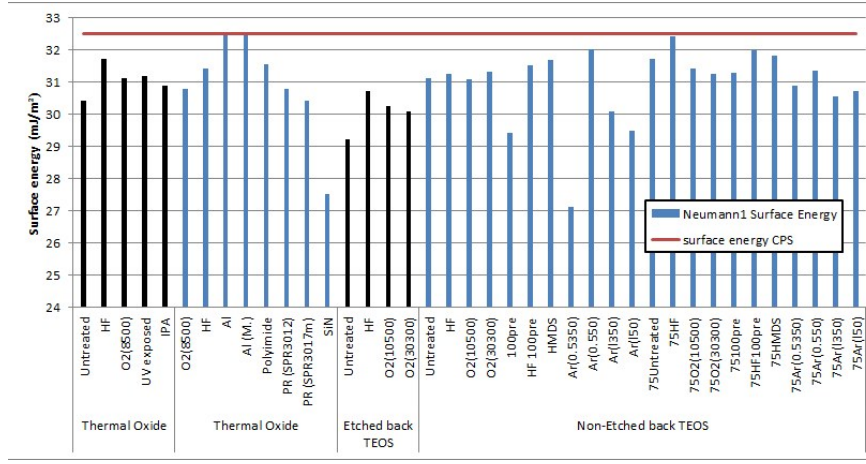
Figure 3.10: Surface energies calculated using Neumann's method

for one series of contact angle experiments: CPS exposed to 2 minutes of UV. From the results an average SFE of 33.5 mJ/m² has been obtained.

3.3.4 Blade types

Although SFEs show some important effects of the liquid reacting to various surfaces, in the spreading process it dominantly comes down to using either a flexible blade or a rigid blade. The flexible rubber blade, when used with little force, allows some spreading of the liquid, however, as soon as a minor force is applied, it digs into patterns and removes some of the liquid from inside the patterns, allowing only little liquid to remain inside the patterns. Bigger and shallow patterns in this way are more prone to lose their liquid silicon than compared to smaller and deeper patterns. Rigid blades such as silicon, glass, titanium nitride, silicon nitride, did not show this removing property when similar forces were used as the rubber blade process. It is however difficult to remove excess when using these types of blades. Automated blading may give accurate excess removing results as is currently used in gravure printers.

Fig. 3.11 shows the difference between silicon blading, the combination of silicon and rubber blading, and rubber blading with force. This shows that using the force applied on the rubber blade has a big impact on the final result.

SFE energies have limited influence on the blade type since none of the blade types have a large contact angle, and since the liquid sticks onto the surface of the blade during every spreading movement. Over time the contact angle decreases, and more and more liquid silicon adheres to the blade making the type of the blade insignificant. The elasticity of the blade proves to be the dominant factor in this manual spreading process.

(a)   (b)   (c)
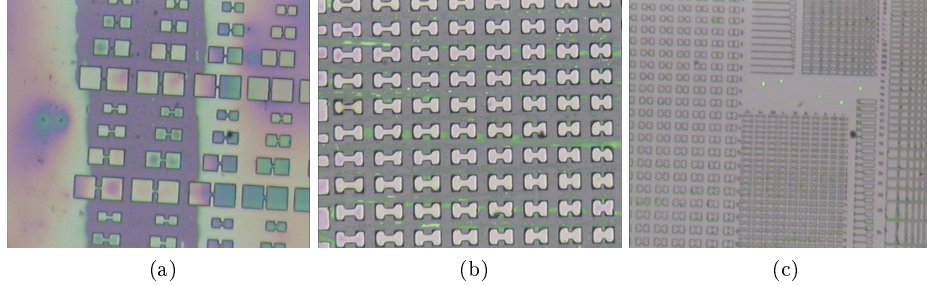
Figure 3.11: Blade type results of silicon only (a), silicon and rubber (b), and rubber with additional applied force (c)

3.3.5   Post-deposition variations

Variations to the procedure after the liquid silicon has been spread, are the steps of photopolymerization under UV and thermal annealing. Variations in both the duration of UV, the duration of the maximum temperature during annealing, and the maximum temperature itself can influence the amount of hydrogen that is contained inside the final silicon film. A reduced maximum temperature however should ensure that the film still transforms into amorphous silicon. Although [2] used 430°C, [7] uses a lower maximum annealing temperature of 350°C. At this temperature, some plastics such as polyimide may survive, and can therefore be incorporated in this fabrication procedure.

RAMAN spectroscopy confirms that the film was successfully transformed into amorphous silicon after using the reduced temperature. All following experiments were therefore conducted at the lower temperature. Fig. 3.12 shows the results of RAMAN spectroscopy, where the broad peak indicates the a-Si and the narrow peak at 521 cm^{-1}indicates the crystalline silicon. Both peaks are visible in the first figure since the light can go through the thin a-Si layer.

The FTIR is used to measure the hydrogen content of the film produced with various UV exposure times. Using MatLab, the area of the peak has been used to extract the integrated absorption at the wagging frequency of 640cm^{-1}. The proportionality factor for an a-Si film produced from liquid silicon is unknown, therefore the areas under the 640cm^{-1} peak of the samples are compared. Fig. 3.13 shows the content of the different process variations. An increased UV exposure time results in a lower integrated absorption which is proportional to the hydrogen content. 20 Minutes of UV exposure has been used in most experiments.

3.4   Film spreading recipe

Two types of wafers were used in the experiments. Although both wafers have the same deposited layers of TEOS on top of a crystalline silicon substrate, and
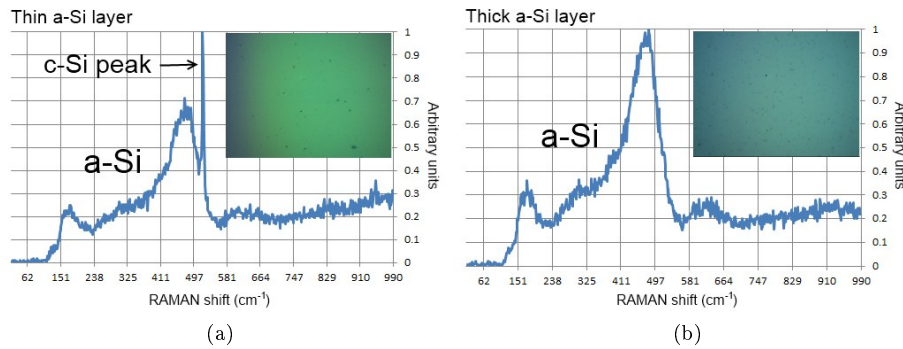
Figure 3.12: RAMAN spectroscopy result of a thin a-Si film (a) and a thick a-Si film (b), both annealed at 350°C for 1 hour.
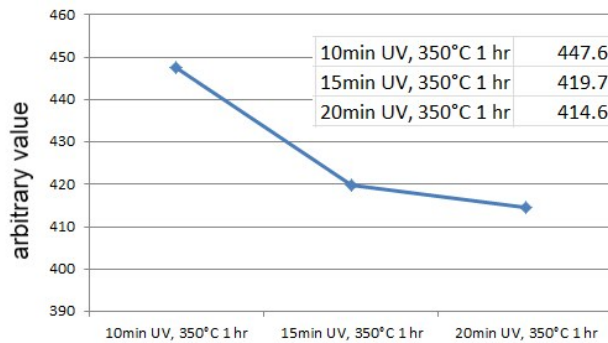
Figure 3.13: FTIR graph of absorption peak integrals at 640cm^{-1}, for three UV exposure conditions

although both wafer types have matrices of grain filters spread across the surface, one of the two wafers is flat and the other has 250nm deep 1 by 1 mm square patterns inside which the grain filters are positioned. This has been done since blading on a flat surface could lead to a layer that is too thin since essentially the blade is scraping the liquid over the surface. Therefore, the squares could ensure that the layers on top of the grain filter cavities is somewhat thicker. The laser could be aimed at these squares.

A proper film production using doctor blade coating is desired. The results from blading are compared to the spin-coating method used in other works [1, 2]. Also the combination of blading and spin-coating, although incompatible with roll-to-roll processes, have been experimented with. A thickness of at least 100nm on top of the surface is desired to be able to produce grains similar to [2] since this forms the protective films against the laser for underlying layers, as well as a source for the grain seed to grow into large grains. A thick uniform

layer is therefore desired during the optimization of this process.

3.4.1   Spin-Coating

Few spin-coating tests were conducted on the available wafers, since spin-coating in general costs quite some amount of material. Flat wafers filled with matrices of grain filters have been used for uniformity reasons. A spin-coated wafer by Dr. Shimoda's group resulted in a layer of approximately 100nm thick. Although we a higher thickness was desired, when repeating their experiment with the same RPM we obtained a much lower thickness. The liquid silicon material was pure CPS dissolved in cyclooctane (20%wt.) and exposing this to a few minutes of UV. This had been spin-coated at 2000RPM, and a final film of approximately 50nm was found. This is assumed to be due to the little time of UV exposure. The alternatives of pure CPS and UV pre-exposed CPS were used in subsequent experiments for the reasons stipulated in Sec. 3.3.2, as well as to improve the thickness of the layer.

(a)   (b)   (c)
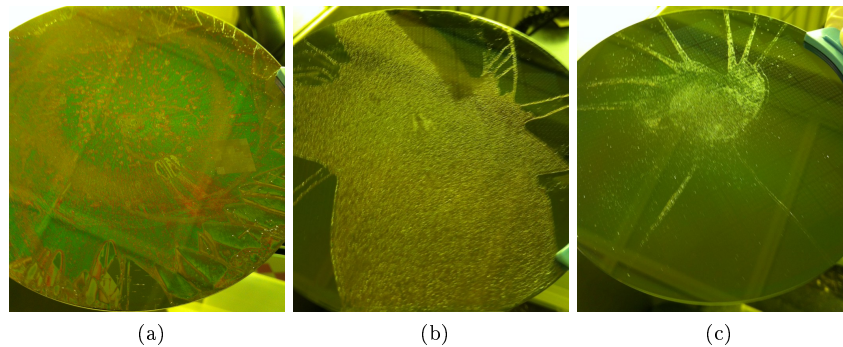
Figure 3.14: Spin-coating experiment results. Double coating of CPS and UV pre-exposed CPS (a), 20 minutes UV pre-exposed CPS only (b), 20 minutes UV pre-exposed CPS only with 0.2μm filter (c).

First, to increase the thickness, multiple spinning was considered. The first layer of pure CPS was spun at 2000RPM, followed by a second, much thicker layer of UV pre-exposed CPS spun at 1000RPM. This second layer, although it attached better to the surface due to the already existing thin CPS layer, resulted in a less uniform layer, and did not spread out across the full wafer. No cracks were formed on the wafer, so it was hard to measure the thickness. During the Excimer Laser ablation test, where energies have slowly been increased in order to find the energy at which the film ablates, we found a level that was similar to the level of ablation of one of our bladed wafers with a thickness of just 30nm.

For the next experiment, one single spin-coating event with a thicker, 20 minute, UV pre-exposed CPS layer, spun at the limited speed of 1000RPM has been conducted. This decrease in RPM, although it would lead to a less uniform

spread of the liquid, the irregularities caused by the first spinning event in the previous experiment caused the limited spread of the liquid silicon material. This decrease in spin speed will result in a thicker layer and even if it would not cover the whole wafer, we wished for it to cover at least some limited number of dies.

The second experiment, as expected, did not cover the wafer well even though an increased amount of UV pre-exposed CPS had been used compared to the previous experiment. The covered area broke completely due to the thickness variations combined with the large amount of different sized polysilanes that cause the final layer to lack uniformity and spreadability. Although the thickness of the cracks was approximately 400 to 450nm as observed from the DekTak profilometer, the test of filtering out different lengths of polysilanes had not been executed before. Some parts of films from this experiment had a thickness of 50 to 100nm.

The third spin-coating experiment had been conducted by using the exact same UV pre-exposure time from the second experiment of 20 minutes, and filtering various sized polysilanes out with a 0.2μm filter. Only little liquid had been deposited due to the filter which reduced the total amount. This little liquid first of all resulted in a worse wafer coverage, and also created a layer that had cracked all over.

From these experiments the CPS with pre-exposed UV lead to many errors in the resulting film. Using CPS only for spin-coating will result in a thickness which is too low. A combination of a pre-existing layer such as used in the first of the listed experiments, should help cover a bigger area with the liquid silicon material. This is due to the time-dependency of the liquid with the TEOS as found in the SFE experiments in Sec. 3.3.3. But to prevent using a lot of CPS material for this initial layer, the layer can be bladed with limited number of droplets to at least cover the whole wafer once. The three spin-coating experiment results are displayed in Fig. 3.14.

3.4.2 Blading

Blade types have been investigated in Sec. 3.3.4 and it was found that the rigid blade type was a good way to spread the liquid silicon and fill the patterns, whereas a flexible blade type could be used to remove excess liquid. A combination of the two lead to the 1 by 1 mm squares losing their contents due to the size of these squares and the rubber blade. The resulting thickness was approximately 30nm. The combination had also been tested with less force on the rubber blade and omission of the rubber blade. Cracks in the latter process were only observed in limited parts, and revealed a thickness ranging from 200 to 300nm which was our desired thickness. It was also found that the resulting layer did not fill the squares but simply formed a layer with a similar step height. Grain filters however did get completely filled displayed in Fig. 3.16.

Care has to be taken when a step height in any part of the wafer is present since this in many cases leads to a crack in the resulting a-Si layer. Although the surface modification techniques on the blade would have limited effect, the sur-
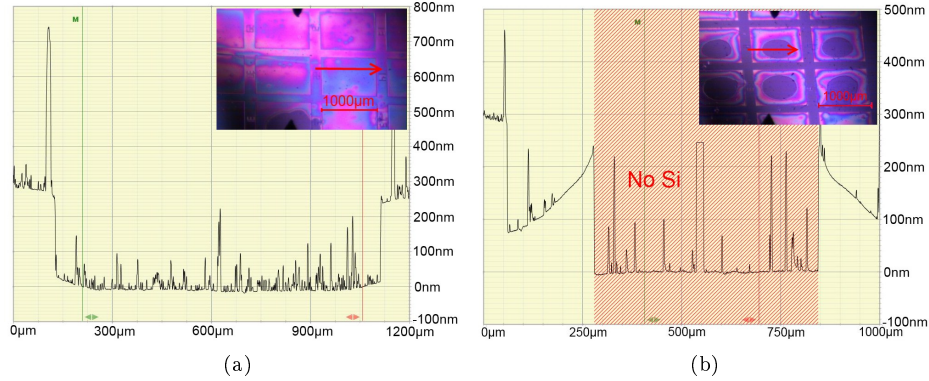
Figure 3.15: Profiles of a-Si layers deposited on the wafer with 1 by 1 mm 250 nm deep square patterns. Fully covered layer in (a), and bulged square coverage in (b).

face of the substrate was treated with 0.55% HF for four minutes, that showed together with the spreading at an elevated temperature to give lowest contact angle and therefore the highest wettability. This means that layers prefer to smoothen out over the surface rather than forming a droplet, avoiding the thickness gradient that results in the film cracking.

Increasing the number of drops may help against step heights from patterns, however, the thicker layer also induce trails from the blade, as well as thicker excess around the edges when these are not removed off the substrate. Both effects lead to breaking of the film, and therefore, the amount deposited on the wafer should be limited.

Wafers have been exposed to a 100°C before liquid silicon deposition since this step would remove any water molecules attached to the wafer that would influence the quality of the final film.

Square patterned wafer

The wafer with square patterns are prone to cracking at the edges of the squares. Using this type of wafer however, resulted in a thicker layer when compared to flat wafers. Also, the liquid adhered slightly better to this patterned surface.

Limited wetting, square patterned wafer, may result in the filling of these squares without forming a continuous film over the wafer surface. Optically this seems to be a good property, however, these areas break very easily since they are only local films with a bulging behavior towards the center of the square as shown in Fig. 3.15b, and should therefore be avoided. Blading multiple times helps form a continuous film, however makes the film also prone to blading trails.

Experiments where the spreading temperature was set at 75°C show a good final result with a final thickness ranging from 100 to 300nm. An issue in

(a)
(b)
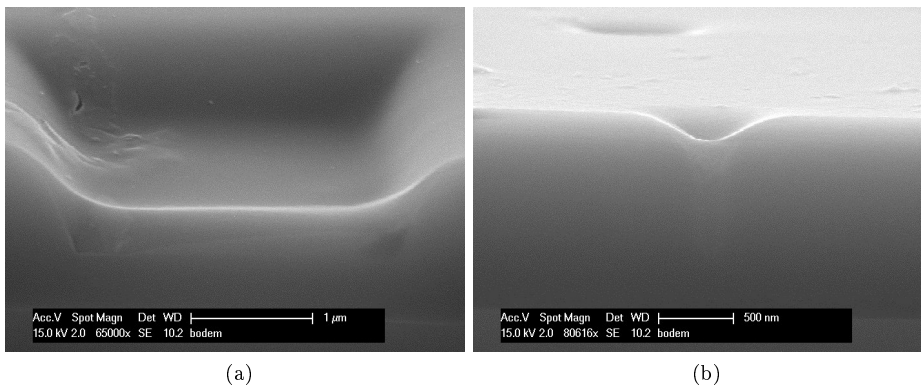
Figure 3.16: SEM images of liquid silicon covering a pattern instead of filling it (a), and the filling of the grain filter (b)

the process was that spreading the liquid across the surface and sustaining the covered surface was still difficult although easier than when spreading at room temperature.

Additional tests were conducted with increased spreading temperatures to 90°C and 110°C. As the temperature is increased, the liquid deposited on the wafer slowly evaporates. An increased temperature also greatly reduces the surface energy of the substrate and the liquid silicon material shows very good wetting. Care has to be taken however that only limited number of blading strokes should be used since the film becomes thinner as it is spread, and trails start to form on the surface when this layer is thin enough, which would lead to a poor film quality. The faster evaporation at 110°C caused the edges of the square wafers to appear, therefore the slightly lower temperature of 90°C showed good, reproducible results although thickness of the layer was limited to approximately 100nm. Some of the experiments on this wafer type are displayed in Fig. 3.17.

Flat wafer

When using the flat wafer for the doctor blade coating of liquid silicon without spreading modifications, it was found that the resulting thickness was quite low. In addition, the smooth surface made it more difficult for the liquid to sustain a continuous film, only after multiple blading attempts did the liquid adhere to the surface, forming a continuous layer. Blading should be done carefully on this wafer type, especially when spreading the liquid at room temperature. An elevated temperature however, leads to a better wetting of the liquid on the surface. Cracks on the flat wafer can now only be formed by the excess liquid and trails from the blading due to the lack of patterns on the surface. This also allowed a slightly higher spreading temperature of 110°C. The increased wettability allowed minimal blading for full surface coverage. A relatively thin

<center>(a)   (b)   (c)</center>
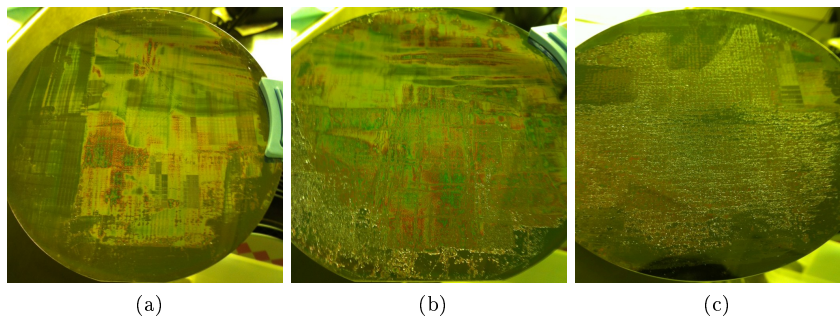
Figure 3.17: Some blading experiment results for the formation of a film. Silicon blade spreading and rubber scraping with partly hard rubber scraping (a), silicon blade spreading with partly mild rubber scraping (b), edge formation and cracking in 500nm square wafer with a small part showing a uniform layer (c).

layer of approximately 100nm resulted, with good reproducibility.

Due to the lack of patterns, an additional spin-coating step could be used to create a thicker layer on top of the surface.

3.4.3   Combination

The thickness of the layer when only spin-coating is quite low, whereas the thickness of the layer when using blading on a flat surface is also relatively low. A combination of the two can help increase this thickness. Initially, when the substrate is bladed, the film covers the surface. A second, spin-coating step allows a better adhesion of the additional CPS droplets on the wafer so that more of the wafer surface is covered during this subsequent step. Trails from blading should be minimized to ensure a better wafer coverage when spinning. This additional step resulted in a film thickness of approximately 250nm. Some of the results are displayed in Fig. 3.18.

3.5   Conclusions and Recommendations

Conclusions

A general procedure has been followed in the formation of an a-Si film from liquid silicon. Some initial experiments had been carried out for the characterization of the film, before optimizing the layer formation.

1. Creating a layer of liquid silicon with excess for a buffer layer gives some difficulties in uniformity issues and cracking of the layer during thermal annealing. The cracking is in many cases a result of layer step-height differences, as observed from excess layer bladed to the edge of the wafer,
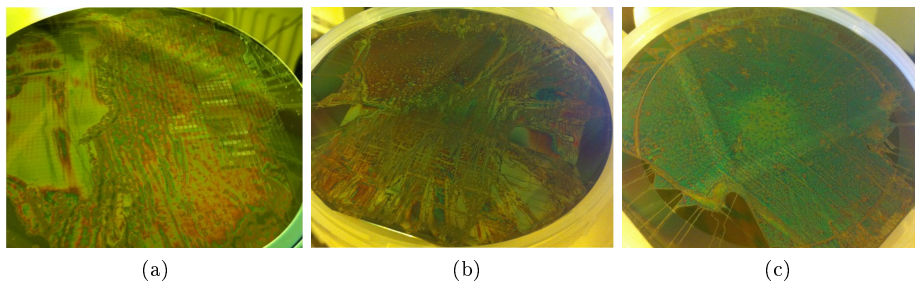
Figure 3.18: Results of the combined coating methods blading and subsequent spin-coating at 500RPM (a), 1000RPM (b), 1000RPM on a polyimide substrate (c).

the edge of the film in general, trails of thick CPS from the blading, and film deformation due to substrate patterns.

2. Liquid silicon is a material using the base compound CPS, and may include the irradiation of UV, the mixture with the organic solvent cyclooctane, or a combination of the two. In this work, it has been found that using the organic solvent can cause various issues such as: evaporation and drying issues, carbon contamination, blading uniformity issues, and shrinking in the grain filter cavities. UV exposed CPS has been found to increase the surface energy of the liquid and makes it more easier for the blade to create tracks. Pure CPS has been used for most of the experiments.

3. Contact angle measurements have shown that the Surface Free Energy (SFE) for the surface modification of 0.55% HF dip for four minutes gives the highest wettability combined with an elevated temperature

4. Blade types, although the liquid has various effects on different materials, is dominantly dependent on its elasticity, especially because the doctor blade coating is done manually. An elastic blade can drag out the liquid from inside the patterns, and a rigid blade allows a proper spreading of the liquid across the wafer but has difficulty in removing the excess.

5. RAMAN shows that thermal annealing the liquid silicon at 350°C already gives the desired amorphous silicon result and is therefore used in many of the experiments.

As single spin-coating resulted in limited film thicknesses, and multiple spin-coating to uniformity issues as well as CPS spillage, using this method only, was found to be unsuitable for the creation of a quality film. Blading proved to give reasonable results, and reproducible results in some process configurations. A combination of first blading followed by spin-coating to improve uniformity and thickness gave a good result due to the time-dependency of the CPS on the substrate surface and the improved adhesion before spin-coating.

An increased number of droplets improve the coverage of the liquid across the wafer. A continuous layer is more quickly formed, however, thick tracks can be produced by blading this large amount of liquid that can break. Using less liquid silicon, may cause difficulty in covering the full wafer so multiple blade strokes may be necessary but will in its turn cause tracks on the film that are prone to breaking or create a low quality film. Elevated temperatures will lead to a thinner film and make it easier to leave tracks. A solution to all this is by increasing the spreading temperature to approximately 100°C so that the wetting and creation of a continuous layer is possible with limited blade strokes. This increase in temperature can however cause slight evaporation of the film but is not a big issue.

The best results were obtained with:

- 250nm deep 1 by 1 mm square wafer, 4 minute 0.55% HF dip, 100°C pre-annealing, 70°C blading of 45µl CPS

Thicknesses was approximately 200nm. Reproducibility however was poor. A reproducible result could be obtained with:

- Flat grain-filter-only wafer, 4 minute 0.55% HF dip, 100°C pre-annealing, 110°C blading of 45µl CPS

- 250nm deep 1 by 1 mm square wafer, 4 minute 0.55% HF dip, 100°C pre-annealing, 90°C blading of 45µl CPS

The resulting thickness in both cases is approximately 100nm. Although thicker layers were desired, these layers are good enough for the SG-TFT processing and does not use a spin-coating step that wastes a lot of material.

Recommendations

For the layer formation, it is very important to use fresh CPS. Oxidized CPS results in a high possibility of cracks due to oxygen molecules present inside the amorphous silicon layer that disturb the film integrity during annealing.

Any sign of trails by the blade that appear locally thicker on the film may be removed since this layer will crack undoubtedly and may degrade a neighboring silicon layer.

A further investigation is required in thermal annealing of the film. Cracking is a result of a difference in thermal expansion coefficients. Slowing down the heating process may prevent cracking altogether. A way of removing local thick areas has however a higher priority.

Automated blading may help the issues of tracks formed by the blade since a small blade is currently being used to be able to be held by hand but which has only the size of a fourth of a wafer. The blade should currently therefore be used at least in four strokes. A machine that could uniformly spread a blade of the size of a full wafer should be able to remove the trail formation issues.

Chapter 4

Low Temperature Annealing and Crystallization

Excimer Laser Crystallization (ELC) is a liquid phase crystallization method and is a way to crystallize an a-Si film into polysilicon. Another crystallization method is the Solid Phase Crystallization, however, the intragrain defect density is higher and therefore mobilities of the final devices would be lower than when using ELC.

The basic working of the ELC process is the use of a high power short wavelength pulsed light source. The shortness of the wavelength ensures a shallow absorption depth of the laser in the a-Si film (approximately 6.6nm associated to the absorption coefficient of about $1.51 \cdot 10^6 \mathrm{cm}^{-1}$) . In addition, there is a low spacial coherence of the light source, which therefore makes the process fast and suitable for the crystallization of thin films without having a thermal impact on underlying layers that may have thermal constraints such as in the case for plastic substrates or for 3D-IC purposes.

Within the Excimer laser electrons collide with a rare gas such as Kr or Xe which in turn get into an excited state or even become positively ionized. These excited atoms will form dimers with halogen molecules such as F or Cl. Within several nanoseconds the excited molecule will fall back to its ground state and will in the process emit UV light. The molecule in its ground state will immediately dissociate and the whole process will repeat itself. Excimer comes from the "excited dimer" that is produced in this process and is the cause of the UV light emission.[47, 48]

Crystallization occurs when the molten a-Si layer cools down since the melting point of c-Si is much lower. Crystallization of the a-Si produces heat that enables subsequent crystallization of amorphous layers.

A crystal seed is left a the bottom of the cavity as the layer on top gets molten by the laser. This allows a single crystal to grow from inside the grain filter to the surface area. The thicker the area, the more the grains can grow when high laser energies are used. The a-Si layer serves also as a protection of

underlying layers. This amorphous layer however should not contain a lot of hydrogen due to the following errors that can occur:

Hydrogen effusion Any hydrogen present within the amorphous silicon film can effuse due to the laser irradiation and may destroy some parts of the film. Since the liquid silicon material is produced from a hydrogenated silicon compound, and due to limited annealing temperature, a significant amount of hydrogen atoms can be left in the film that can cause defects by this out-diffusion of the hydrogen.

Film agglomeration Partial dewetting may occur and lead to film decomposition into beads which is known as agglomeration. The main source of this dewetting are the fluctuations of the silicon film that are severe enough to reach the underlying oxide layer. These fluctuations are influenced by the pulsed-laser annealing caused by non-uniformities in the spatial profile of the laser pulse and intensity fluctuations from the homogenizer. Also the interference of the incident beam with laterally scattered beams as well as the surface tension gradient have an impact on this defect.

Ablation is related to excessive agglomeration and is known as the explosive release of hydrogen. A major issue in this work is indeed the hydrogen content of the amorphous silicon film produced from the liquid silicon material.

These errors can destroy the final film and decrease the single grain quality of the final transistor. When a polyimide substrate is used, it can have disastrous effects due to subsequent TFT processing steps that will significantly harm the polyimide layer through the broken a-Si film. Using the Excimer Laser, the right laser recipe is needed to be constructed to reduce the hydrogen content. It was shown in [2] that the hydrogen content of the amorphous silicon film formed from liquid silicon is still a significant amount and will lead to ablation issues and poor crystallization results. In the process of [2], a second thermal anneal was used to decrease this hydrogen content, however due to thermal constraints when using plastic substrates it is important to reduce this annealing temperature.

In this chapter, the pre-anneal theory is first discussed. This is followed by the experimental process which includes: the equipment, the approach, and the results. Finally conclusions and recommendations are given.

4.1 Pre-anneal effects on Hydrogen concentration

It was believed that multiple shots with low energy densities may improve the film quality by decreasing the hydrogen content without ablating and result in large grain sizes. In [49] this pre-irradiation had been tested on a 100nm PECVD amorphous silicon film. Indeed ramped shots, with a lower energy density than compared to the single pulse film deteriorating energy density, improved the

maximum shootable energy density. One shot for every energy density level had been used, and the results are shown in Fig. 4.1. The results show that as the film is exposed to more shots at lower energy densities, that the maximum shootable energy before significant film deterioration increases.
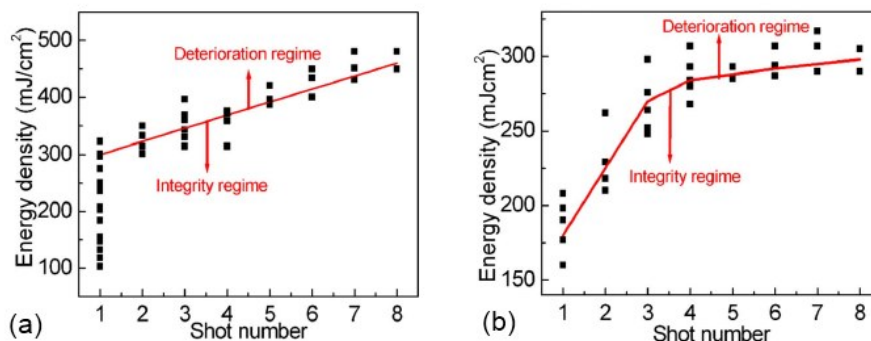
Figure 4.1: Maximum shootable energy before which the silicon film starts cracking as a function of the number of Excimer Laser shots. Pretreatment at 300°C (a) and untreated a-Si film (b) [49]

The effect of laser pre-annealing is visualized in Fig. 4.2 where a sample without pre-annealing is compared to one with pre-annealing. A single shot of 500 mJ/cm² has been used on the first sample. This is a relatively high energy and destroys most of the film due to the many Hydrogen atoms that effuse and break loose from the a-Si film. The second sample is one that is has been irradiated at lower energy densities for multiple shots (90 shots at 100 mJ/cm²), showing the film becoming slightly darker and rougher due to the minor hydrogen effusion. The third sample shows a pre-annealed sample with a maximum laser energy density of 550 mJ/cm², clearly less dark and crystallized due to the pre-annealing effect.
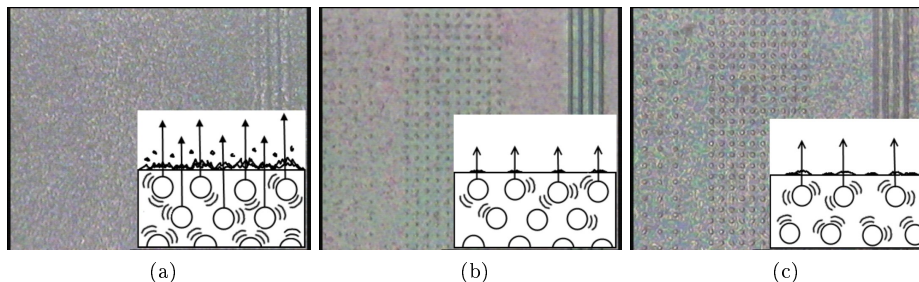
Figure 4.2: Demonstration of laser pre-annealing benefits. Single shot without pre-annealing at 500 mJ/cm² (a), 90 shots at 100 mJ/cm² (b), and a pre-annealed sample with maximum laser energy density of 550 mJ/cm² (c)

4.2 Experimental

4.2.1 Excimer Laser setup

The Exitech M8000V System
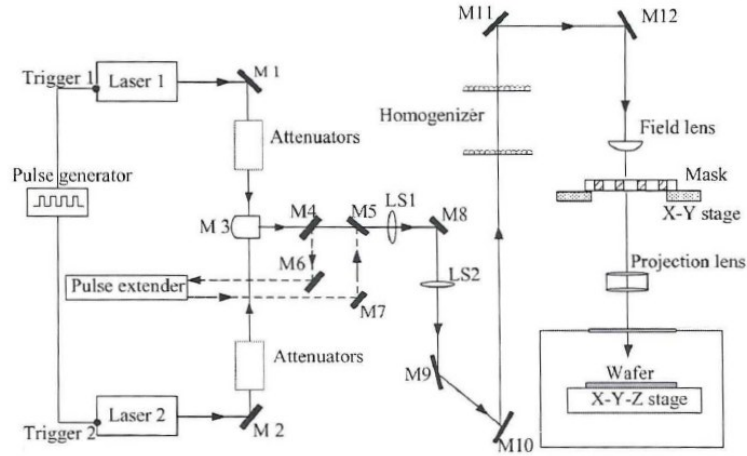
Figure 4.3: Exitech M8000V Excimer Laser system schematic [48]

The schematic setup of the Exitech M8000V System for Excimer Laser Annealing is shown in Fig. 4.3. The gasses used for the laser is a mixture of Xe and Cl_2, that will form the dimer of XeCl for the irradiation of a 308nm wavelength beam. In this setup, two Lambda Physik LPX 210 laser sources are used and are combined by mirror M3 in the figure. Attenuation of the energy density of either beam occurs before their combination. After their combination the beam can either go through a pulse duration extender, or continue to lenses LS1 and LS2.

Although the total setup would produce a beam with a pulse duration of approximately 25ns, the duration can be extended by timing of the two laser sources or by adding a pulse duration extender shown in the image by mirrors M4 to M7. The idea behind this setup is that mirror M4 and M6 sends the combined beam to the pulse extender that consists of numerous semi-transparant mirrors. Each mirror deflecting part of the beam and transmitting another part to a next semi-transparant mirror. This would result in a chain of deflected beams with slight delays that will in total produce a beam that has a longer total pulse duration of 250ns.

Lenses LS1 and LS2 are used to guide the beam to the homogenizer. The homogenizer is a tool to produce a beam with a uniform spatial profile. This

beam continues to the Field lens that sends the beam through a mask for the alignment of light paths, to a projection lens for the final exposure on the wafer surface. The wafer is placed on an X-Y-Z stage for accurate wafer position control, and is covered by a quartz plate to protect the projection lens from ablation of the sample film.

This setup still may produce some uniformity issues that result in a problem in repeatability of the exposed results. This makes it all the more difficult when the film is lacking uniformity. Small energy density differences of 10mJ/cm² have therefore been avoided and replaced by steps of 50mJ/cm².

4.2.2   Approach

In this work, a similar process to [49] is used, however, many more shots at lower energy density levels were believed to help reduce the hydrogen content before ablation. Some issues in this process was the non-uniformity of the film, and the non-uniformity of the laser.

An initial test had been conducted to recognize the energy density at which the film deteriorates significantly when a single shot is used. A few tens of mJ/cm² lower than this maximum energy, a large number of shots have been fired to the substrate after which the energy density has been ramped up and the number of shots had been decreased. The optimum type of recipe can be obtained from these results. These different recipe types include: single shot recipe, ramped single shot recipe, linear decrease recipe, exponential decrease recipe, and variations in step size for the exponential shot recipe. A visual representation of three of the recipe types are indicated in Fig. 4.4 .
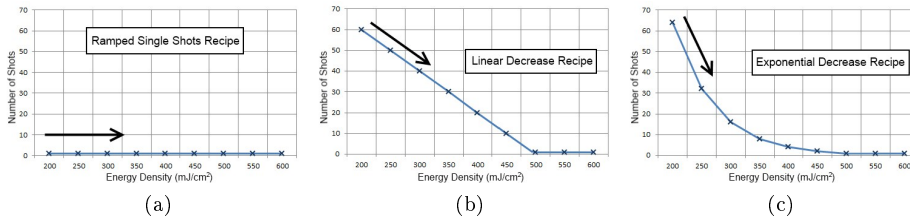
Figure 4.4: Visual representation of the recipe types ramped single shot (a), linear decrease (b), and exponential decrease (c).

By far, most a large number of recipes have been tested on one particular wafer on which the CPS had been doctor blade coated and spin-coated,. This wafer was primarily used to obtain conclusions from identical a-Si film thicknesses. Although the absolute results cannot be identical to wafers with other liquid silicon thicknesses, the relative results are still relevant.

4.2.3 Results

Optical Microscope Results

Fig. 4.5, shows the final conclusions derived from optical measurements. The bars show at which energy density the film shows the first signs of deterioration, where the dark blue bars indicate the long pulse results, and the red bars show the short pulse results. The red and blue markers indicate the maximum obtained grain size using the specific type of recipe for short pulse and long pulse respectively.

(a) (b)
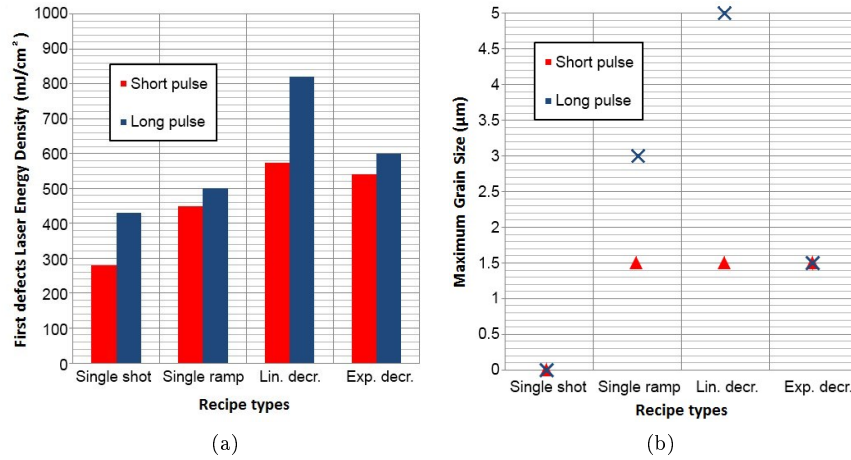
Figure 4.5: Laser energies from which the film starts to show signs of defects for every laser recipe type(a). Maximum grain size obtained for the particular recipe type (b).

Pulse duration

For short pulse duration (25ns), it has been observed that the energy at which the layer significantly deteriorates is at approximately $E_{1,max} = 260\text{-}300$ mJ/cm² when pre-annealing has been omitted. For the long pulse duration (250ns) this limit is extended to approximately 420-440 mJ/cm². Extending the pulse duration will decrease the cooling rate of the molten silicon which would result in bigger grains. It will also help against film deterioration as observed by the extended shot density limit.

Step size

In the laser recipes, an increasing energy density was used for the crystallization of the film. The step size between two energy density levels should be approximately 50 mJ/cm², since smaller step sizes are inaccurate due to the

inconsistency of the laser energy. Bigger step sizes usually deteriorate the film earlier and may approach the level of a single shot recipe. A final jump from a series of 50 mJ/cm² should not exceed 150 mJ/cm².

Recipe types

Using this first deterioration energy with the single shot tests, various recipes can be tested. [49] obtained good results with ramped single shots, however, increasing the number of shots at lower energy densities could lead to better removal of the hydrogen atoms while maintaining the quality of the film. Single shots, ramped single shots, exponential decrease shots, and linear decrease shots, have been compared. Single shots gave the lowest maximum shootable energy and in many cases could not form grains before film deterioration. Ramped single shots gave reasonable results with maximum grain sizes in the short pulse configuration similar to the two remaining recipe types, however, the deterioration of the film occurs earlier. The exponential decrease of shots was compared to the linear decrease of shots, and although similar results were obtained for the short pulse configuration, the long pulse configuration showed better results for the linear decrease recipe. This is mainly due to the starting energy of the exponential decrease recipe, which was too low. This resulted in a fast decrease of shots to 1, so that the nature of the recipe approached the level of ramped single shot recipes.

Starting energy density

The starting energy for all recipes should be below the deterioration energy, $E_{1,max}$, obtained for the single shot experiments. Comparing the starting energies, an energy density at about 100 mJ/cm² lower than $E_{1,max}$ would lead to similar results compared to energies starting a lot lower than this. Starting energy density of only a few tens of mJ/cm² lower than $E_{1,max}$ results in bigger grain sizes, however, deterioration of the film occurs at an earlier stage. Fig. 4.6 illustrates that when $E_{1,max}$ is found to be 260 mJ/cm², using the first pre-annealing energy density at 200 or 150 mJ/cm² has only little influence to both the deterioration energy and the grain size. Using the slightly lower energy of 250 mJ/cm² however will increase the maximum grain size as well as an earlier initial deterioration energy. This has also been found for linear decrease of the shot number, as well as in the long pulse series.

The results of the long pulse linear recipe that gave the biggest grains are shown in Fig. 4.7. The recipe starts at 350 mJ/cm², so only slightly lower than the $E_{1,max}$ with 70 shots, that have been decreased with 10 shots every time and increased energy densities at steps of 50 mJ/cm² until 800 mJ/cm². Finally a jump has been made to 950 mJ/cm².
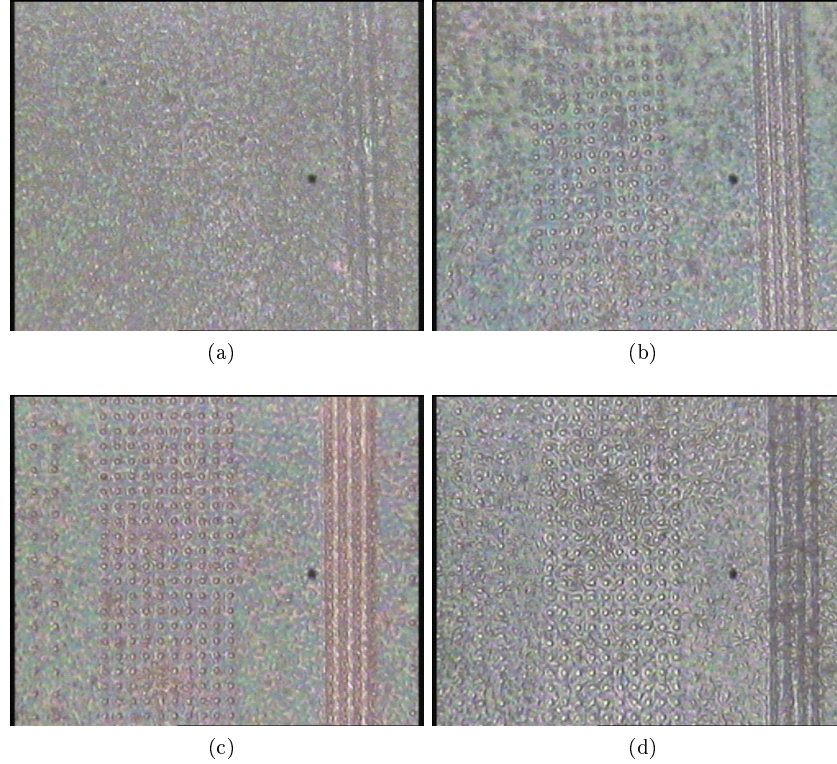
Figure 4.6: Excimer laser irradiation results short pulse. Single shot (a) against an exponentially decreased number of shot with increasing shot densities of 50 mJ/cm² starting at 150 mJ/cm²(b), starting at 200 mJ/cm² (c) and at 250 mJ/cm² (d), with a maximum of 500 mJ/cm² for all cases.

Elastic Recoil Detection (ERD)

The hydrogen content can be quantitatively measured using Elastic Recoil Detection (ERD). It is an ion beam analysis technique that determines the absolute concentration values of light elements within a thin film. An ion beam of several MeV energy is irradiated on a sample, in this case the a-Si film. The light elements that are present in such a film are recoiled in forward direction and can be detected. The energy spectrum of the ejected atoms can be used to obtain the concentration depth profile of the sample. The scattered ions that move in the same direction from the incident beam are blocked by using a foil that allows the recoils to pass through. [50, 51]The ion beam does not go through the substrate, and has a probing depth of 400nm in silicon using the equipment of [51]. Fig.4.8 shows the schematic of the ERD setup.

Six samples are prepared for this analysis, at an $E_{1,max}$ of 500 mJ/cm²: 100 shots of 100 mJ/cm², 100 shots of 300 mJ/cm², 100 shots of 450 mJ/cm², linear

(a) (b)
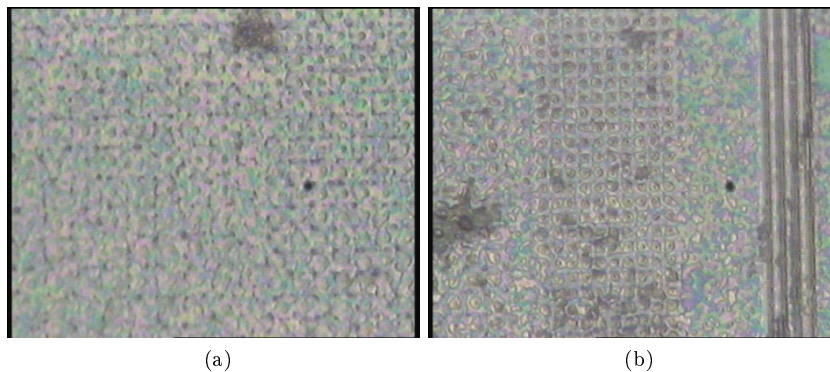
Figure 4.7: Excimer laser irradiation results long pulse. Linear recipe for which the biggest grain sizes have been obtained. 4 and 3 micron pitch image (a), and 3 and 2 micron pitch image (b).
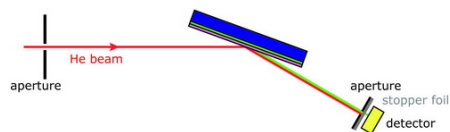
Figure 4.8: ERD setup schematic[50]

decrease from the 100 shots of 300 mJ/cm² to 450 mJ/cm², 650 mJ/cm² and 850 mJ/cm². [results will be obtained by beginning of June]

Rutherford Backscattering Spectroscopy (RBS)

A similar ion beam analysis technique is the Rutherford Backscattering Spectroscopy, a tool used to measure atoms ranging the periodic system. A beam of He2+ ions at an energy of 1 to 2 MeV is incidented on a sample placed in a predetermined angle. The backscattering energies of the ions can be detected from which the concentration depth profiles can be obtained. The backscattering energies are directly related to the mass of the particle and the depth of collision [50, 52]. A probing depth of approximately 2 micron is possible using the setup from [50]. Fig. 4.9 shows the schematic of the RBS setup.

The system is used to detect atoms heavier than hydrogen in the amorphous silicon samples. Carbon concentration and oxygen concentration are measured for three different samples: a reference sample annealed at 350°C and UV cured for 20 minutes, a sample with only 10 minutes UV curing, and a sample with an increased annealing temperature of 430°C. [results will be obtained by beginning of June]
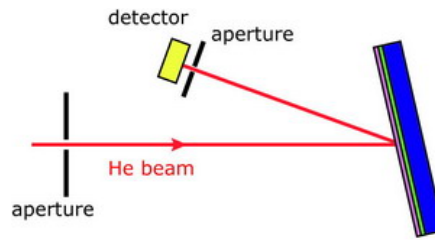
Figure 4.9: RBS setup schematic[50]

4.3   Conclusions and recommendations

Conclusions

Excimer laser pre-annealing has proven to increase the maximum shootable energy density. Various laser recipes had been tested which showed generally that a long pulse duration significantly helps to increase the maximum shootable energy as well as the maximum grain size due to the heating rate and cooling rate respectively. The recipe showing the best results were those that were shot with a large number of shots at low energies, and a linear decrease in the number of shots as the energy densities were increased by 50 mJ/cm².

Recommendations

For Excimer Laser Crystallization it is important to consider as little film deterioration of the film as possible when working with an underlying polyimide layer within the substrate, even if this would result in smaller final grain sizes. The laser recipe type of exponential decrease should be further investigated for long pulse configurations since it may still produce quality grains.
Other methods for increasing the grain size should be tested, such as the heating of the layer during irradiation to reduce the cooling rate.

Chapter 5

l-Si SG-TFT on Polyimide

As the liquid silicon layer fills the grain filter cavities, and forms amorphous silicon during annealing. The samples are exposed to Excimer laser for hydrogen removal and crystallization. The position of the single crystal grains are accurately controlled by the grain filters, and within these grains, monocrystalline silicon channels can be formed for high quality devices.

So far reports have been made of liquid silicon devices that have been spin-coated and inkjetted without grain location control in [1] and spin-coated with grain location control in [2]. The latter have produced TFTs at temperatures incompatible with plastics such as polyimide due to the annealing of the liquid silicon layer for transformation into an amorphous silicon network and the removal of hydrogen atoms that can have detrimental effects during laser crystallization.

In this work, the annealing temperature of the transformation from liquid silicon to an amorphous silicon network has been reduced from 430°C to 350°C, and the hydrogen removal has been conducted with a laser pre-annealing treatment similar to [49]. With this decrease of temperature, the compatibility to polyimide has been realized and devices both on polyimide as well as devices without the additional polyimide layer have been constructed and measured.

5.1 Transistor structure

A schematic of the device fabrication process is given in Fig. 5.1. The process is similar to [2], and uses a μ-Czochralski process for the controlled growth of the crystalline silicon grains. Notice that in this schematic the polyimide layer has been left out after step 1, although both processes, with and without this layer, have been used for our final devices. Step 7a is used when the polyimide layer has been omitted, whereas step 7b is used for when a polyimide layer had been implemented in the process. For the protection of this layer, additional aluminum has been used to protect the underlying polyimide layer during the activation of implanted dopants through Excimer laser.

5.1.1 Fabrication procedure
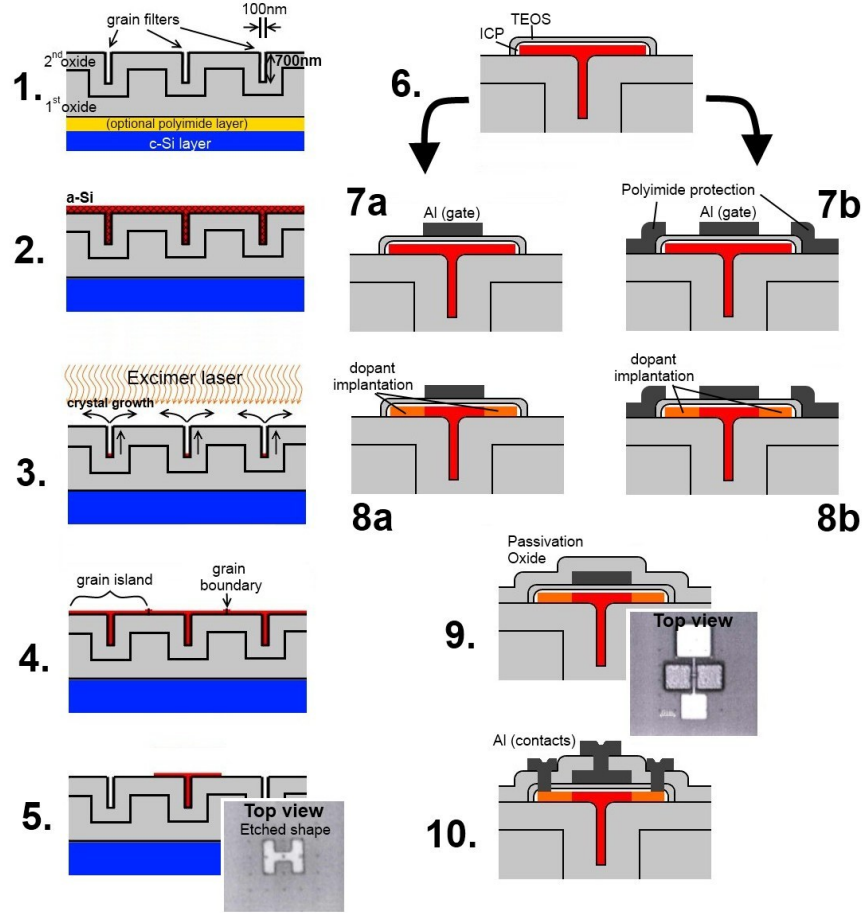
Figure 5.1: SG-TFT fabrication process both with (b steps) and without (a steps) an additional polyimide layer. The polyimide layer has been omitted in this schematic after step 1, however step 1 shows its designated position.

1. Using a crystalline silicon wafer as the supporting substrate material, a polyimide layer may be spin coated on top of this wafer. Using plasma-enhanced chemical-vapor deposition (PECVD) two oxide layers have been deposited on top of this base layer in the machine Novellus Concept One using tetraethylorthosilicate ($Si\{OCH_2CH_3\}_4$ or TEOS) at 350°C. The first 750nm thick 1μm wide oxide layer has been patterned to form big, controllable cavity sizes by using anisotropic reactive-ion etching (RIE) in a C_2F_6-CHF_3 plasma. The second 800nm oxide layer has been deposited

by the same PECVD process to decrease the cavity size to a grain filter level. The grain filters have a depth of 700nm and a diameter of 100nm.

2. According to the process described in Chapter 3, an amorphous film is manufactured from the bladed liquid silicon material. A thickness of approximately 200nm is desired using pure CPS, 20 minutes of UV exposure, and thermal annealing at 350°C for 1 hour in an nitrogen ambient with oxygen and water levels in below 0.1ppm.

3. Using the Exitech M8000V System for Excimer Laser Irradiation of the amorphous silicon layer, the top amorphous silicon layer is molten until a crystal seed is left at the bottom of the grain filter. The laser induces crystallization as explained in Appendix E

4. Crystal growth in every grain filter induced by the Excimer Laser will continue at high energy densities, until either a defect of the film occurs, or the crystal growth collides with a crystal grown from a neighboring grain filter. This collision causes a halt to the grain filter size increase and will form grain boundaries at those positions.

5. Grain islands are formed with RIE. These islands are positioned in a way that the channel region exists in the single crystalline area produced from one single grain filter.

6. For the production of a gate oxide layer, to types of oxide are formed on top of the crystalline silicon area. Using inductively coupled plasma (ICP), high quality oxide is grown at a mere 250°C with less plasma damage on the oxide than when using PECVD TEOS. This made out the first 14nm of the gate oxide layer for a good semiconductor-oxide interface. After this first layer, PECVD TEOS has been used for another 22nm oxide at 350°C to speed up the process.

7. The aluminum gate has been sputtered on top of the gate oxide by using the Trikon Technology Sigma 201 cluster tool at room temperature. The aluminum has a 0.1% silicon content to prevent spiking due to diffusion, and has a thickness of 675nm. For the polyimide version (7b) the aluminum used to protect the underlying polyimide layer should not contain any silicon for accurate removal of the layer after dopant activation.

8. The aluminum gate pattern has been used as the mask for self-alignment of the ion implantation of the source and drain regions. For PMOS, $1 \cdot 10^{16}$ ions/cm² boron atoms at 20keV were used, and for NMOS TFTs, $1 \cdot 10^{16}$ ions/cm² phosphorus atoms at 70keV were implanted. Both dopant types were activated using Excimer laser with an energy density of 300mJ/cm² at room temperature.

9. The total device structure is passivated again using PECVD TEOS, for protection of devices and insulation between conductors.

10. Finally, contact holes are etched, followed by aluminum via deposition for local contacts. The patterning has been done by using photolithography and Al sputtering.

5.1.2   Polyimide

In this work the polyimide layer is produced using a Polyamic Acid Durimide 150A, that is transformed into a fully stable polyimide after thermal curing. The structure of the Durimide is shown in Fig. 5.2a.[53]

Polyimide is a polymer of imide monomers, the structure of an imide is shown in Fig. 5.2b. It is the combination of two acyl groups bound to nitrogen. In the durimide structure, both nitrogen atoms will replace the nearby OH group while losing one hydrogen atom to form the imide structure during thermal curing. An aromatic heterocyclic polyimide is the result. [54]

(a)   (b)
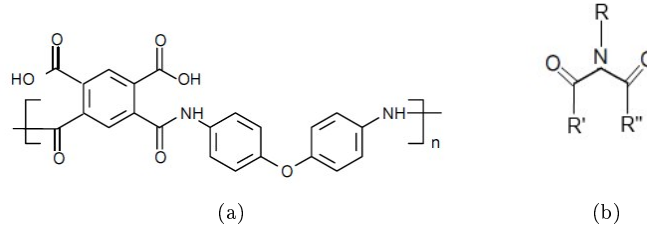
Figure 5.2: Chemical structure of the Polyamic Acid Durimide (a)[32], and the Imide monomer

The polymeric structure is known for its excellent mechanical properties, thermal stability, and chemical resistance. This is due to the strong intermolecular forces between the polymer chains.

The polyimide used in this work has a glass transition temperature of 371°C, and a thermal decomposition temperature of 597°C. The reader is referred to [53] for more information on the material.

5.2   TFT characteristics

When measuring the final devices, it is important to look for transistor characteristics that determine the quality of the fabricated devices. The devices are based on MOSFETs in which a current is controlled by means of a voltage difference at the gate. In this section, parameters such as: field effect mobility, subthreshold swing, threshold voltage, and off current are determined from the transfer characteristics, $I_D V_G$, and output characteristics, $I_D V_D$ graphs. I_D is defined as the current that is passing through the channel, V_G is the voltage

applied at the gate while the voltage difference across the channel is kept constant, and V_D is defined as the voltage applied at the drain contact assuming that the source contact is set at 0V (ground). [47, 48]

Field Effect Mobility

Mobility is related to the carrier transport through a material as a result of an induced electric field, and is one of the most important parameters of the transistor. The current that runs through the device has various operating modes and is defined by Eq. 5.1.

$$
I_D = \begin{cases} \mu_{FE,n} C_{ox} \frac{W}{L} \left[(V_{GS} - V_{th}) V_{DS} - \frac{V_{DS}^2}{2} \right] & Linear\,region \\ \frac{\mu_{FE,n} C_{ox}}{2} \frac{W}{L} (V_{GS} - V_{th})^2 & Saturation\,region \end{cases} \tag{5.1}
$$

Where I_D is the drain current; μ_n is the electron field-effect mobility; C_{ox} is the oxide capacitance; W and L are the width and length of the channel respectively; V_{GS} is the gate to source voltage; V_{th} is the threshold voltage and V_{DS} is the drain to source voltage.

From the saturated region, the mobility can be extracted by measuring the slope of the $I_D V_G$ curve while keeping the drain voltage at a constant saturated level:

$$
\mu_{FE,n} = \left(\frac{\partial \sqrt{I_D}}{\partial V_{GS}} \sqrt{\frac{2L}{C_{ox} W}} \right)^2 \Bigg|_{V_{DS} = level\,of\,saturation} \tag{5.2}
$$

Subthreshold Swing

The subthreshold swing (S) is a parameter that defines the quality of the turn-on characteristics of the device. It can be obtained from the weak inverting regime, which occurs at $V_{GS} < V_{th}$. In this regime the swing is defined as the gate voltage required to increase the drain current by an order of magnitude. This parameter determines the semiconductor/dielectric interface trap density and is defined as:

$$
S = \left[\frac{\partial \ln (I_{DS})}{\partial V_{GS}} \right]^{-1} \tag{5.3}
$$

$$
S = \frac{kT}{q} \ln 10 \left(1 + \frac{C_{depl} + C_{it}}{C_{ox}} \right) \tag{5.4}
$$

In which k is the Boltzmann's constant; T the temperature in Kelvin; q is the charge; C_{depl} is the capacitance of the depletion region; C_{ox} is the capacitance of the gate-oxide, and C_{it} is the capacitance of the interface states which is in parallel to the depletion capacitance.

Threshold Voltage

The property that defines the gate voltage on which the device turns on is the threshold voltage. This voltage needs to be sufficiently low for the device to be operational with limited supplying energy. It is physically defined as the formation of an inversion layer on the semiconductor-oxide interface that allows charge carriers to move from the source and drain regions.

Off-current

The off-current is the current flowing through the channel while no voltage is applied at the gate. This current should be as low as possible to obtain a proper switch-like function.

5.3   Results

[Results will be obtained by mid June]

5.4   Conclusions

[Results will be obtained by mid June]

Chapter 6

Excess Liquid Silicon Removal for Gravure Printing

Chapter 3 has discussed the doctor blade coating of liquid silicon onto a patterned substrate: a process that can be regarded as a precursor of the gravure printing system. The process allows the liquid to be spread across the patterned surface without the need of removing any liquid that is not filling a pattern.

Excess liquid silicon removal is another precursor of gravure printing which requires any excess liquid to be scraped off the patterned substrate. The result is that the liquid will only fill patterned cavities filled with the specific liquid. The final transition towards gravure printing would require this substrate with the liquid to be pressed against a target surface.

The focus in this chapter was on spreading the liquid silicon while filling patterns and removing excess liquid in non-patterned areas.

6.1 Experimental Results

The substrates used in this chapter are different from the ones used in Chapter 3 in the cavity patterns produced in the TEOS layer. The wafers do not have any grain filters but various pattern sizes ranging from a few tens of micrometers to a square of 1 by 1 micrometer. The shape of most of the patterns are like the letter "H" which is a common structure used for the production gates or the channel region. The depth of these patterns have been varied from 0 to 1000 nm. Many of the experiments however, were conducted using a depth of 250nm which is a typical thickness for a semiconductor layer. Grain filters are omitted since the aim of this work looks at producing a transistor using the filled cavity, or by gravure printing the pattern on a target substrate. In both cases, the grain filters are not required.

The desired result is either a completely filled pattern, a pattern that is only filled in the corners, or a bulging/dewetted pattern. Although the latter two can not be used directly for gravure printing ends, these results allow further

modification while using the surrounding structure for self-alignment purposes for example.

The general procedure used for these experiments for the formation of a-Si from liquid silicon is the same as the one described in 3.2.2. Again numerous variations have been tested for obtaining the optimum result. The characterization results obtained in 3.3 are a good starting point for the following experiments.

6.1.1   Excess removal

Excess layers, or thick layers, have shown to be problematic in doctor blade coating experiments when they result in cracks during thermal annealing. In this work, additional precautions have to be taken in order to get a desired result of filled patterns and a clean surface in non-patterned areas. The excess has to be removed in some way using the blade.

The surface free energy of the blade has negligible effect on the blading result for the available blade type varieties. A big difference exist however in blades of different elasticity. The rubber blade allows a good manual removal of the excess layer in non-patterned areas when a sufficient force is applied, since the flexibility of the blade allows it to adapt to the surface. It however, also leads to the removal of the liquid in some of the filled patterns. A rigid blade on the other hand is problematic for the manual scraping of the excess due to the direct effect of any inaccurate hand motion. The patterns however do not lose most of their liquid and therefore this second type of blade is good for spreading, whereas the first type is good for removing excess. A combination of the two blade types will give the desired result, where the rubber blade is carefully used for scraping after the rigid blade spreads the liquid.

The blade angle differences have no observable effect, and the position of the blade determines partly where the liquid from within the pattern is pushed towards on a non-patterned area. It also determines the direction of the trails that may lead to cracking. The blade angle is set approximately vertical for all experiments and the blade direction is also set in one direction imitating the conventional gravure printing system.

Another problem exists for the film within a pattern when the excess layer is not removed. The excess connected to the film within the pattern, pulls the film out during thermal annealing causing a strong deformation of the film inside the pattern, as can be observed from Fig. 6.1 . This is the result of a difference thermal expansion coefficient. The effect is not as strong in bigger and shallower patterns as well as in grain filter sized patterns.

Since the excess is removed in many of areas on top of the wafer, small droplets that are still left may combine to form a droplet that cracks during thermal annealing. This effect is visible in Fig. 6.2, and can only be helped by accurate removal of the excess.

Deformation may also occur inside a pattern without excess. This effect will be discussed in Sect. 6.1.2.

(a) trails covering filled patterns   (b) medium sized structures   (c) large area structures
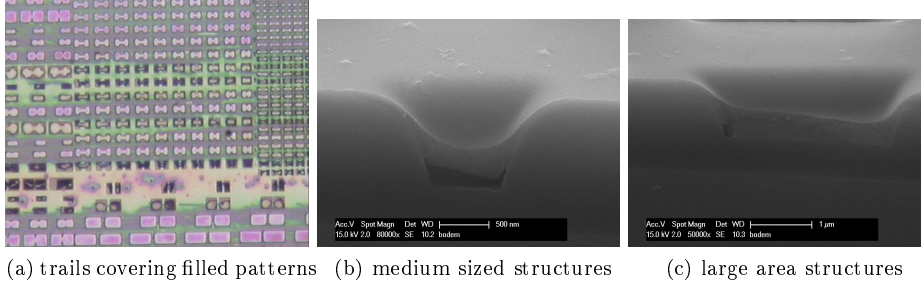
Figure 6.1: Films within patterns getting pulled out by the excess layer connected to the film inside. Optical microscope view (a), a SEM image of such a pattern (b), and a SEM image of a bigger pattern (c).
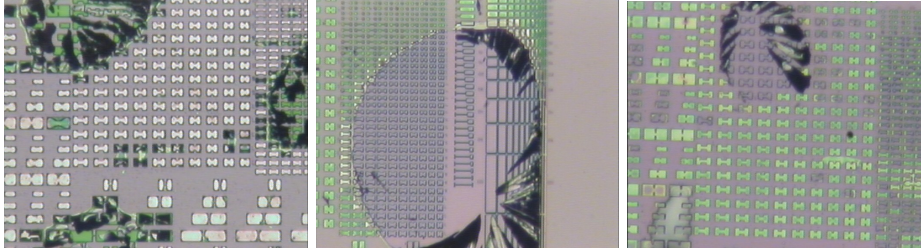
Figure 6.2: Bubble bursting of CPS due to excess CPS on top of a filled pattern.

6.1.2 Pattern deformation

The change in surface energies between the liquid and the substrate can lead to the liquid to change its shape into either more spherical or flatter shape. The change to a more spherical shape is called dewetting, due to commonly known wettability of liquids to surfaces for which a low wettability is associated to a more spherical shape. This change in shape of the liquid can be used in advantageous scenarios in processing transistors. It can for instance be used for self-alignment. During the formation of an amorphous silicon network through annealing of the UV exposed liquid silicon, this dewetting may occur in a similar fashion as shown in Fig. 6.3. The opposite of dewetting may be regarded as wetting, so the liquid spreading out over a surface with minimum thickness. We use the term reverse dewetting for the situation in which a pattern once filled with liquid silicon has formed a hole in the middle, while the silicon has spread to the edges or corners of the pattern. This effect can also be observed in Fig. 6.3 and can also be used for self alignment purposes.

Although some of the images from Fig. 6.3 appear to be dewetting, this is in fact not dewetting but simply a change in shape due to thermal expansion mismatch of the amorphous silicon material and the silicon dioxide. This explains the darker areas formed around the spherical shape. The corners are the

(a) Regular filling (b) Dewetting appearance (c) Reverse dewetting

(d) wetting combination 1 (e) wetting combination 2 (f) wetting combination 3
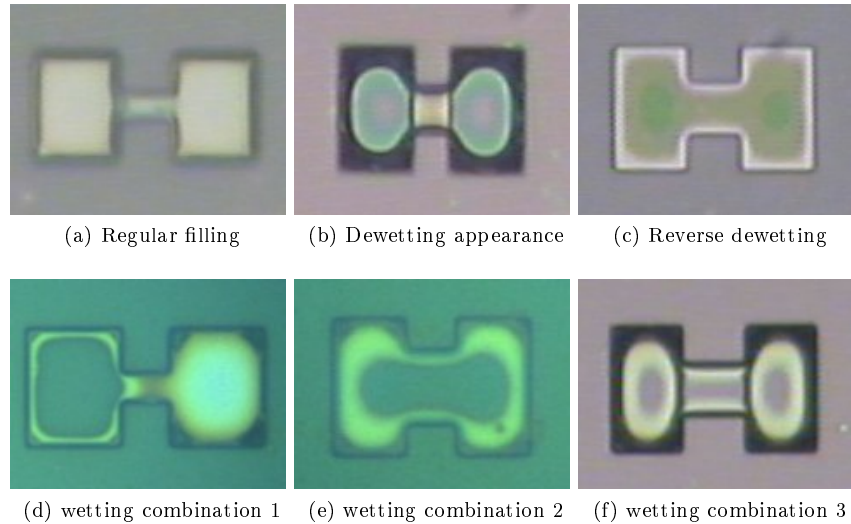
Figure 6.3: Different ways of pattern filling.

most prone to be lifted up followed by the edges of the pattern due to the way the patterns are etched. This effect can be seen from Fig. 6.4. As the figure shows, many of the dark areas are related to the deforming behavior. RAMAN spectroscopy confirms the darker areas to be amorphous silicon as well, as can be observed from Fig 6.5.

(a)   (b)   (c)
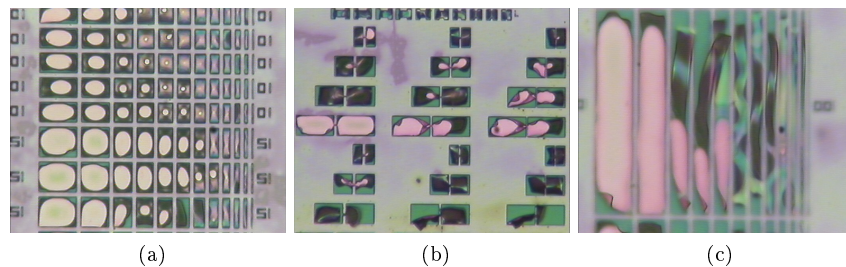
Figure 6.4: Deformation of supposedly dewetted patterns.

This gave the idea that the holes are not filled as much as we had hoped for. The situation that we were aiming for as well as the situation we have at present are visualized in Fig 6.6a. It is unlikely for a situation in which the pattern is completely filled to be deforming to the extent of Fig. 6.4, the layers that appeared to have filled the patterns are therefore relatively thin.

By using the DekTak we have confirmed that the thickness of the amorphous film inside the pattern was limited to a few tens of nanometers as can be seen

(a) non-patterned surface   (b) Pattern sphere   (c) Pattern outside sphere
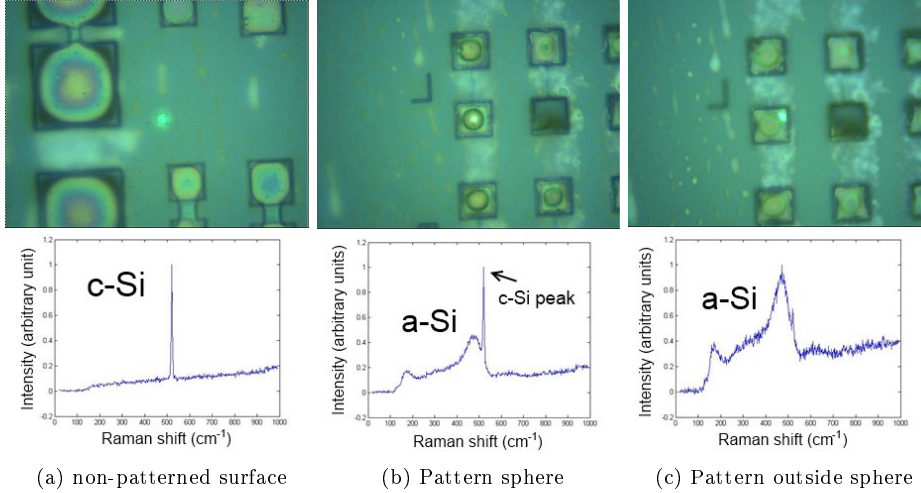
Figure 6.5: RAMAN spectroscopy measurements of filled and dewetted patterns.

from Fig. 6.6c.

Deeper patterns have a higher possibility of deformation due to the shape of the pattern. The more shallow patterns are more prone to lose their CPS by blading. Fig. 6.7 shows the effect of various pattern depths.

Not only the depth of the patterns may lead to this effect, but also the area of the patterns. Large area patterns are relatively easier to lose their CPS since the flexibility of the rubber blade may scoop more of the CPS out of such a large area pattern. Fig. 6.7a shows this effect.

6.1.3 Time Dependency

Films that are spread after deposition of a number of droplets show that there is a difference in properties in the droplet area and the liquid spread area. A time dependency was observed in a film of liquid silicon that is left for some time, and a neighboring film that has just been spread. This has also been observed in the contact angle tests, where the contact angle decreased over time.

This time dependency resulted in a better adhesion of the liquid silicon to the surface, making it more difficult to remove the excess layer as can be seen from Fig. 6.8a and b. Deformation of the patterns become also less likely as adhesion increases over time, as shown in Fig. 6.8 c. This adhesion is the result of a reaction between the liquid material and the oxide surface of the substrate. It is desirable for the layer of liquid silicon material inside patterns, but not desirable for the excess layer in non-patterned areas. An experiment where a drop of liquid silicon was moved across the surface by inclining the substrate, also confirmed this; at higher speeds the liquid leaves a track of small droplets while at lower speeds it leaves a thick uniform film.
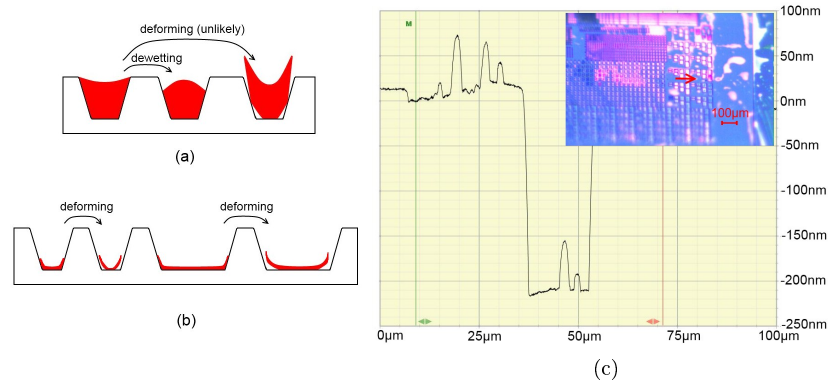
Figure 6.6: Dewetting against deformation schematic when properly filled (a) and when poorly filled (b). The proof of a thin layer within the 250nm deep pattern (c).

(a) 270nm depth   (b) 800nm depth   (c) 1100nm depth
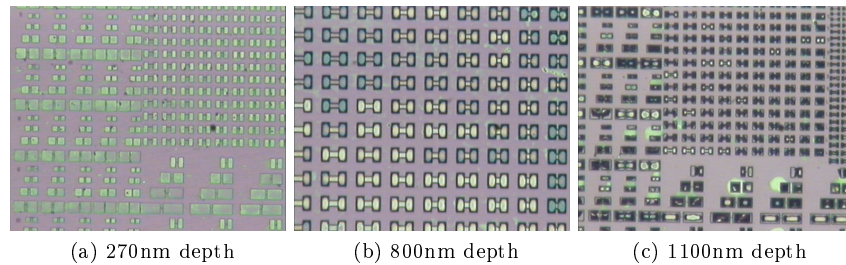
Figure 6.7: Effect of pattern depth on liquid silicon

6.1.4 Liquid silicon

Mixing cyclooctane with CPS increases its wettability to the surface. Removal of the excess is problematic, and the evaporation of the organic solvent results for the same amount of liquid only a thin layer of a-Si. A higher concentration of CPS or more liquid will help create a thicker layer, however, the cyclooctane also introduces carbon atoms inside the final a-Si layer and is therefore avoided. In addition, drying of the mixture during blading introduces difficult in spreading of the liquid across the wafer.

UV increases the viscosity of the liquid silicon due to the photopolymerization process that produces polysilane chains. At a certain point the liquid solidifies into a white substance. Solidifying a liquid silicon layer deposited on top of a patterned surface will not make it easier to remove the excess by a rigid blade, breaking this excess layer off from the layer inside the patterns. The film within the patterns get dragged out of in a relatively solid state, as can be observed from Fig. 6.9b.

(a) (b) (c)
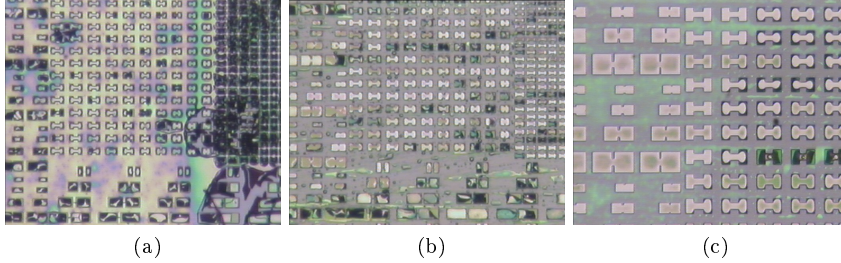
Figure 6.8: Results of time dependency experiments, good adhesion in the initial thick layer area (a), area outside this initial layer after (b), and the transition from initial layer to the bladed area outside (c).

It has been observed that wafers on which UV exposed CPS had been deposited had overall more cracks throughout the area due to the increase in viscosity of the liquid that lead to more tracks and deformations in the resulting film as the liquid is thicker. In general, the UV exposed CPS is more difficult to spread which may be due to the increase in viscosity and surface energy, but it also may be due to the evaporation of the liquid during exposure of UV light that at the same time generates some heat.

(a) (b) (c)
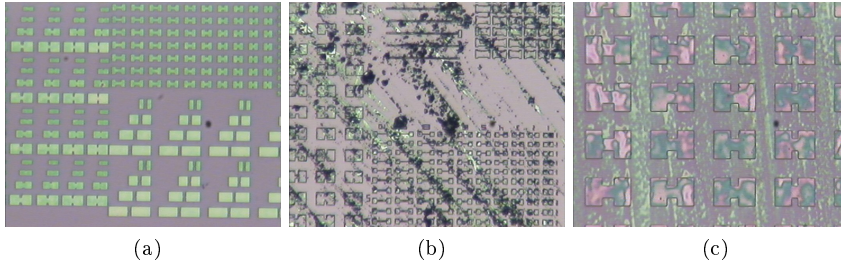
Figure 6.9: Various UV exposure times. No UV exposure before blading (a). 10 minute UV exposure before blading on top of a wafer (b), but many intermediate exposures during blading (c).

Finally, exposing the wafer with the liquid silicon, multiple times with UV, and scraping the excess off after every exposure, some of the patterns were filled in a strange way, which is assumed to be due to more and more of the UV exposed CPS filling the patterns. Although this method may improve the way the patterns are filled, it was also observed that after every UV exposure, it did not became easier to remove the excess liquid. Also, the physics behind this method lies in the solidification of the CPS inside the pattern, while more and more new CPS material fills the pattern at the same time with intermediate solidification steps. This may also cause integrity problems. The pattern filling for this situation is depicted in Fig.6.9c.

6.1.5   Surface modification

Two types of surface modifications had been used, both relying on very different types of etching. The first one is plasma oxidation in which the substrate is placed into an oxygen plasma that bombards oxygen atoms onto the surface of the wafer which makes the surface rougher. The other type is wet etching by using a low concentration of HF for a short period of time, a commonly used technique to remove native oxide of a silicon wafer. This wet etching type will cause the surface to allow the liquid silicon to flow and therefore increase the surface energy of the substrate.

Oxygen plasma settings were set at 500W for 8 minutes. The plasma resulted in the adhesion of excess outside the patterns. These excess layers outside the patterns however were segmented instead of combined. This was also visible from some of the droplets that were visible on the surface. These droplets formed a cluster of smaller droplets around the main droplet. This property did not help with removing the excess by blading since parts of the excess could break off during scraping rather than forming a bigger droplet that follows the blade. Fig. 6.10 gives the results of some of plasma oxidized experiments and Fig. 6.11 elaborates the blading scenario compared to the regular substrate surface. Silicon dioxide surfaces is considered to give a good adhesion of to amorphous silicon films, an increase in roughness increases the adhesion of the silicon atoms to the oxygen film.

(a)　　　　　　　　(b)　　　　　　　　(c)
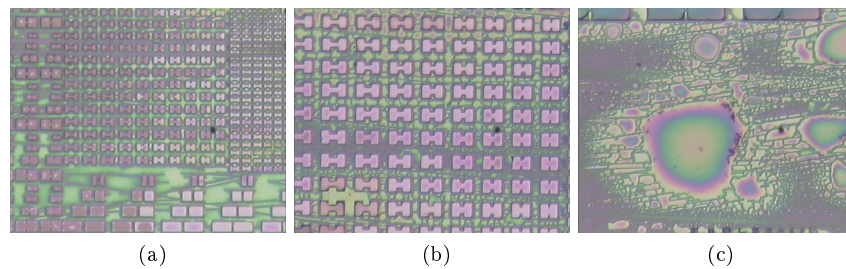
Figure 6.10: Blading results on plasma oxidized surface.

For the wet etching setup, a concentration of 0.55% HF has been used for 4 minutes after which the wafers had been rinsed for approximately 5 minutes and have been spin dried. The low concentration and relatively low time is used to ensure that the patterns will not significantly change their shape. This setup is also used for the removal of native oxide on a c-Si wafer at an etch rate of 15 nm/minute [55]. Segmentation of the droplets similar to the plasma oxidized experiments were not found. Fig. 6.12 shows some of the results that we have obtained from the experiments. As the figure suggests, the liquid is better spread across the surface, however a conclusions about the excess removal is still premature. The wettability of the liquid silicon increases also in this case.
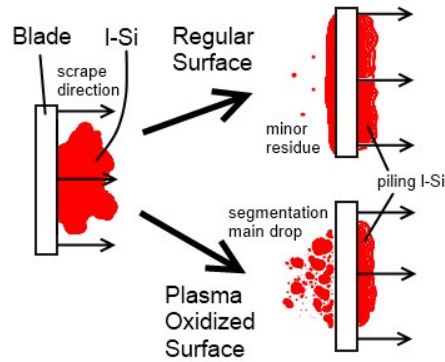
Figure 6.11: Difference in blading of the excess on regular surface and plasma oxidized surface.
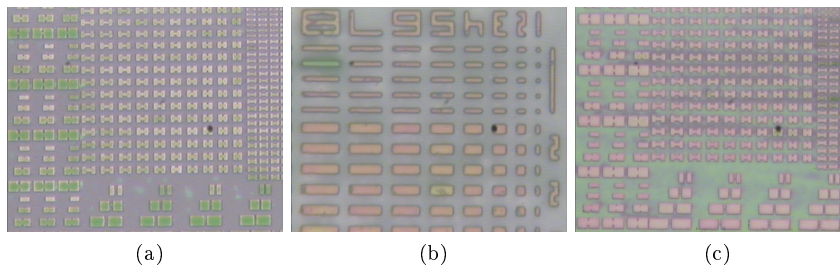
Figure 6.12: Blading results on HF dipped surface.

6.2 Conclusions and Recommendations

Conclusions

The results from the experiments in this chapter has helped gain understanding of the way the liquid silicon behaves to the filling of various patterns, while removing the excess layer.

1. The excess film can cause errors such as cracks, caused by liquid silicon trails from the blade or film uniformity issues. In addition, the excess film can pull the solidified structures from within the patterns out. Grain filter patterns and large area patterns are not prone to this pull-out effect, caused by the difference in thermal expansion coefficient of the silicon film and oxide surface.

2. The blade is the tool for spreading the liquid silicon as well as removal of the excess layer. Blading direction has an effect on the way the excess layer is spread, however, multiple blading will lead to a lower amount of liquid within the patterns. Furthermore, blade types were investigated

for various contact angles, however, in this process it seemed that the stiffness of the blade plays a dominant role. A more rigid blade allows the liquid to spread without removing it from inside the patterns. The excess is harder to remove in this case. A flexible blade can remove the excess more accurately, however it will also remove liquid inside patterns. Bigger patterns are in this case more prone to losing their liquid. A careful combination of the two could lead to the optimum results. Since the blading process has been done by hand, it is believed that a more accurate automated process could lead to better results for the rigid blade.

3. Deformation of patterns occur when the liquid inside the pattern is too thin and has a poor adhesion to the surface. The film can easily be deformed due to the thermal expansion differences. The pattern geometry can strongly influence the way that it is filled. Shallow patterns are more likely to lose the liquid silicon that was filling the pattern. Patterns with bigger area are also more likely to lose their liquid during blading. Deeper patterns are more prone to deformations due to the cone shaped structure of the pattern.When even less liquid is inside a pattern the liquid can spread to the edges and corners of the pattern forming a ring of silicon that can also be used for self-aligning ends.

4. The liquid silicon has some form of time dependency on the surface of the substrate. Over time the adhesion increases making it harder to remove the excess liquid material, but also preventing deformation within patterns.

5. The liquid silicon used could come in various forms by using pure CPS and varying UV exposure, dissolving it in cyclooctane, or a combination of the two. From the results a preference in usage of pure CPS had been grown due to the fast evaporation times, carbon introduction, and low a-Si thickness of the cyclooctane solution, and the thickness and spreading difficulty of UV pre-exposed CPS.

6. The target substrate surface can be modified to change the wetting and adhesion properties. Two types of etching have been used for this. The first one is a dry etching process, plasma oxidation that appeared to have a strong adhesion that results in segmenting of the droplets. The second type is wet etching by using a low concentration of HF. This resulted in a higher wettability and easier spreading of the liquid silicon. This latter case shows an indefinite result for the removal of the excess.

Optimization of the excess removal process with filled patterns, lead to a thin film inside the pattern that is prone to deformation. At this point the optimized procedure is: silicon blade coating of pure CPS and a subsequent careful rubber blade scraping on patterns with a depth of 250nm. After scraping, leaving the liquid for a few minutes inside the patterns for a better adhesion. HF may be used to improve the spreading behavior, but will not lead to a benefit in excess removal.

Recommendations

An automated blading machine could provide a consistent way of scraping off excess with a rigid blade type, as it is being used in conventional gravure systems. Current manual blading introduces many variables that cannot be controlled and are not present in automated systems.

The main issue at this moment is actually the poor filling of the patterns, and their deformation. Filling can be improved by creating a situation in which a liquid that has poor wettability in non-patterned areas, but can easily enter the patterns and have a strong adhesion to the insides of the patterns. Surface-material wise, this would mean that the surface may be made of silicon nitride or another material with very low surface energy, while the patterns inside can have a surface of HF etched or a modification that leads to high surface adhesion and wettability. It must however be ensured that the adhesion to the non-patterned surface is minimal which is many cases related to a surface with a very low surface energy. The blade itself can also be made from a silicon nitride material to minimize the adhesion of the liquid to the blade.

Either CPS or UV pre-exposed CPS need to be used in this scenario since it is assumed that UV pre-exposed CPS will not be difficult to remove from the surface anymore due to the increase in hydrophobicity of the silicon nitride surface.
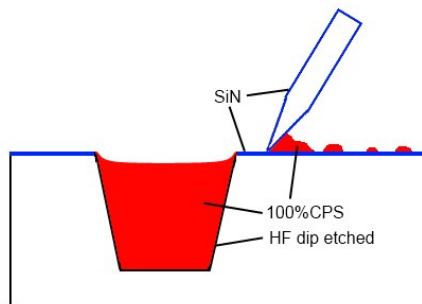
Figure 6.13: Recommended setup mainly based on high adhesion within the pattern, and poor adhesion outside, with a poor adhesive blade.

To prevent pattern deformation, patterns that are once filled need to rest for some time for the liquid silicon to react to the surface within the pattern for a stronger adhesion. When transistors are made from this filled patterns, maximum adhesion is desired and some resting time is therefore required. In the blading process, relatively deep patterns with small areas are preferred. The total situation is illustrated in Fig. 6.13.

Chapter 7

Conclusions and Recommendations

Liquid Silicon is used as a way of taking the advantages of a cheap, low temperature, solution fabrication process, and the high electrical property of silicon transistors. Doctor blade coating is a first step towards gravure printing systems allowing roll-to-roll mass production of electronics. Using location controlled grain filters and Excimer Laser pre-annealing, high quality Single-Grain Thin-Film Transistors can be manufactured on plastic substrates.

7.1 Doctor Blade coating Liquid Silicon

Some basic characteristics of liquid silicon have been investigated, and a method for obtaining a good a-Si layer is achieved. The obtained characteristics are listed:

Excess liquid Excess liquid can induce large stepheights that break during thermal annealing due to thermal expansion. Instances at which these large film gradient can occur are besides excess layers from the large amount of liquid, trails caused by blading, and substrate patterns.

Pure CPS is the preferred material to work with as liquid silicon. Manipulations of this base material can increase its viscosity, or decrease its surface free energy. UV light causes the production of polysilanes within the material that thicken the liquid. These result in a higher possibility of blading trails as well as a poorer wettability. Mixing cyclooctane increases wettability however a number of issues exist: carbon is introduced in the resulting a-Si film, the resulting film evaporates leaving only a thin layer of polysilane content on the surface, a-Si in grain filters shrink due to this, and the solution dries quickly leading to uniformity issues when blading.

Surface Free Energy High wettability of the liquid is desired and can be

obtained by surface modification techniques. Increasing the number of droplets will only create thicker tracks when doctor blade coating which can crack. 0.55% HF treatment for four minutes together with an elevated temperature gives the highest surface free energy (SFE) of the surface resulting in high wettability. Wettability increased over time due to reactions of the material to the surface. Care has to be taken for the evaporation of liquid silicon when spread at elevated temperatures.

Blade types The SFE of the blade is not a dominant factor when doctor blade coating due to the errors that may result from manual blading. Elasticity however gives a significant effect. Flexible blades such as rubber adjust to the surface even if the blade is not positioned accurately. This flexibility enables an ease in removing the liquid, and may also remove liquid from inside the patterns. A more rigid blade allows a better spreading of the liquid across the surface.

Using these characteristics the liquid silicon has been either spin-coated, bladed, or the two have been combined. Spin-coating gives poor adhesion and a lot of wasted liquid silicon. Blading gives good results when a patterned wafer with 1 by 1 mm square patterns are used instead of a flat wafer. For the flat wafer case, blading will result in a thin layer of approximately 30nm. Adding a spin-coating step to this layer improves liquid silicon adhesion and leads to a good layer with a thickness of approximately 250nm. The best results are obtained by using 0.55%HF dip for four minutes on a wafer with 1 by 1 mm square patterns, while spreading 6 drops (total 45µl) at an elevated temperature of 70°C for both types of wafers. A more reproducible result with a thickness of approximately 100nm was obtained when spreading at an elevated temperature of 90°C for the square patterned wafer, and 110°C for the flat wafer. The wafers have been exposed to 20 minutes of UV for photopolymerization, and have been annealed at 350°C for 1 hour.

7.2 Low Temperature Annealing

Similar works of liquid silicon [2] have obtained a SG-TFT using the same material, however a second thermal annealing step of 650°C was used that made the process incompatible with plastic substrates. This second annealing step was necessary for reducing the oxygen content for the subsequent Excimer Laser Crystallization process. Low temperature annealing by using the same Excimer Laser will lead to a maximum processing temperature of 350°C for which polyimide substrates can be used.

Excimer Laser pre-annealing has been investigated by [49] for the removal of hydrogen without film deterioration, and has been further explored in this work. Several conclusions have been made:

Long pulse A longer pulse duration (250ns) lead to higher maximum shootable energies than short pulse duration (25ns). As a result, bigger grains were

produced in this configuration. The reason for this is the decrease in cooling rate.

Step size Laser recipes with a step size of smaller than 50mJ/cm² are prone to laser uniformity and inconsistency issues. Step sizes a lot bigger than 50mJ/cm², takes away the effect of laser pre-annealing.

Starting energy When the starting energy of the laser recipe is a lot lower than the level of first deterioration, the film is less disturbed. A laser energy just below the level of first deterioration will produce more film disturbances, however will result in bigger grain sizes.

Recipe type A large number of energy shots have been shot at the beginning to remove more hydrogen at these low energy levels. The decrease in number of shots have been done linearly and exponentially. For short pulse configuration, the results were similar. For long pulse configuration, the linear decrease recipe resulted in bigger grain sizes due to the fast decay of shot number in the exponential setup.

The recipe that has achieved the biggest grain size of 5µm grains was: a starting energy of 350 mJ/cm² for 70 shots, with steps of 50 mJ/cm² and decreasing shot count by 10 until 1, and a final jump of 150 mJ/cm² at 800 mJ/cm². A lower starting energy density is desired when the polyimide substrate is used to ensure its survival.

7.3 Liquid silicon devices

[Results will be obtained by mid June]

7.4 Excess removal using doctor blade

The next step towards a gravure printing system is the process of using the doctor blade to remove excess liquid in non-patterned areas, after the liquid has been spread across a substrate. The patterns are cavities of various shapes, and these require to be filled completely for the gravure printing process. Other characteristics of the liquid silicon has been analyzed for this type of solution processing.

Excess liquid The excess in this process is slightly different from the excess in the doctor-blade coating section. The excess needs to be completely removed in this process. Any leftovers can produce cracks similar to the previous process. A smooth layer however, which was acceptable in the other process, may pull out some of the middle sized patterns in this process due to thermal expansion. Blade types are preferred to be rubber when excess needs to be removed, however, this blade type may also remove the liquid from inside the patterns, and is generally not a good way

for spreading the liquid. Using a silicon blade for spreading and careful rubber blading for excess removal will give the best results.

Deformation Many patterns were filled with a very thin layer. This thin layer, when adhesion lacks, may easily deform during the annealing step. A deeper pattern is more prone to deformation due to the shape of the pattern. A too shallow pattern on the other hand may lose all of its liquid silicon content.

Time dependency Liquid silicon reacts to the TEOS surface as has also been observed during the SFE experiments. This enables an improvement in adhesion that can prevent deformation during the annealing step. Excess liquid should be fully removed before pursuing a strategy using this time dependency.

Other types of liquid silicon gave similar issues as with the doctor blade coating case. Surface modifications of HF dip and O_2 plasma were used, however none of them showed a significant improvement in filling properties and excess removal. O_2 plasma even improved adhesion of the liquid to the surface. The best results of filling were obtained when pure CPS was spread by silicon blade after which the excess is carefully removed by the rubber blade. These results lead to a thin layer within the patterns, which still needs to be optimized for the production of a completely filled pattern.

7.5   Recommendations

Doctor blade coating

Oxygen contamination of the CPS gives disastrous effects on the formation of the a-Si film. Cracking occurs earlier in the annealing process, and in general a bigger part of the area breaks. The CPS should be refreshed once every two to three weeks.

When blading the liquid silicon, trails from the blade are in some cases visible. These are thick and narrow lines that are the first to break during thermal annealing. The trails may be carefully removed before UV exposure by a tissue to ensure that the cracked trail does not drag neighboring a-Si layers.

Breaking of the layer is the result of thermal expansion. This may be helped by slowing down the annealing temperature process over many hours. This of course is not desirable when considering a roll-to-roll process.

Automated blading can help remove many variables induced by manual blading, and may spread a liquid silicon layer in a consistent way. It is much more accurate, and a large blade should be mounted so that multiple blading is not required in order to spread the liquid over the whole wafer.

Low temperature annealing

Additional precautions have to be taken when handling a wafer with a polyimide substrate. Any damage through Excimer Laser crystallization or annealing can significantly impact the polyimide layer in subsequent processing steps. A lower initial energy density is desired at the cost of the grain size.

The linear decrease came out to be give the best results in the long pulse configuration. The exponential recipe decreased to a shot count of 1 very rapidly in this configuration, as the film could handle much higher energies. This reduction in shot count made the results of the exponential recipe similar to the one with single ramped shots. A much higher initial energy, or higher shot count is required to be able to remove hydrogen in this recipe type at higher energy levels.

Other methods for increasing the grain size should be tested. Heating of the wafer for instance, during laser irradiation, could reduce the cooling rate which leads to the formation of bigger grains.

Excess removal

Similar to doctor blade coating, automated blading will have many benefits in this process. Due to the increased accuracy and stability of the blade, a rigid blade type may be chosen to remove the excess layers.

Main issue in this work during this process was the lack of filling of the patterns, while excess is in many cases not completely removed. Fundamentally, a decrease in wettability in the non-patterned areas is desired, while wettability and adhesion should increase within the patterns. Again the automated rigid blading will lead to less liquid being dragged out of the pattern. Surface modification techniques may however allow even better filling of the patterns in this sense. Using silicon nitride or another material with a lower SFE will lead to better excess removal, whereas HF dip or an alternative with better adhesion would lead to a better filling of the patterns.

Time dependency of the liquid silicon should be explored further. As adhesion increases, film deformation may decreases, which may relate to the cracking of some of the layers.

Appendix A

Market Analysis

A.1 Radical innovation

In the business world, two types of innovation exist within the research department. The first type is called the incremental innovation, where research is based on building upon current existing products. For example, Intel's Pentium III to the Pentium IV processor is an innovation of this type. The products are fundamentally similar; however the latter is simply a better version of the former. This type of innovation is usually safe, and causes a steady increase in product quality. The only risk is that a competitor brings a product on the market that is radically different.

That brings us to the second type of innovation, which is the radical innovation. An innovative product of this type is fundamentally different from its predecessors. It may cause a complete change in the competing basis of a certain industrial sector. An example would be the change from cellular phones, to smart phones, to smart phones with touch screens, every innovative change brings the competing basis to a fundamentally different level. This type of innovation is in most cases hard to achieve and is therefore not a reliable source of increase in product quality

In many cases a company has the choice to invest in many different innovative projects. It is common however to spend the bigger part of the innovative budget in the incremental type of innovation. However, should a company be prepared for future changes in the competing race, a significant share of the budget should go to radical innovation. By doing so, a company is up-to-date and can keep up with its competitors or even become a pioneer in a new revolutionizing product. [56]

That is exactly what the project described in this paper is aiming for. Liquid silicon is still at its infancy, and many researchers either still focus on improving current displays by making them sharper, or faster. Other research is also based on radical innovation, but more in the sector of flexible displays using organic semiconductors.

By exploiting the potential of liquid silicon, the best of both the high quality displays as well as the cheap and flexible organic displays can be achieved. The whole basis of competition within the display sector, or even in any chip fabricating sector, will change. One important claim to consider is the claim of solution processing beating the costs of conventional processing.

A.2   Associated costs

Current organic solution processing has been reviewed. In this case it is often claimed that the main advantage of this type of processing lies in the cheap fabrication method. A careful analysis is required to value this claim. High quality transistors are still hard to achieve with this type of processing, especially when using organic semiconductors. Printing a complete device will have to be compared to manufacturing in the conventional method. In this sense, although printing of organic TFT's loses ground in the quality of transistors, it has a much lower cost per unit area of a substrate. Several important points are discussed [3]:

- Although it is said that solution processing is useful for its lower cost in processing, it will not achieve a lower cost for linewidths of over 1 micrometer. This is because in this regime there are many lithographic tools available that have been highly depreciated. Creating lines with a width of more than a micrometer is therefore cheaper in the case of lithography tooling.

- Although theoretically it is believed that printing can bring an eventual lower cost for the fabrication of devices, the actual process machinery still needs to be developed and made suitable for mass IC production. Although the general idea of the technology is available for other sectors, a machine for accurately printing full devices on a mass scale still needs to be developed. On the other hand, conventional processing of silicon is based on many decades of optimization, and have settled a good solid bases to improve upon. It would be hard to convince these machine owners to move on to the new era of printing chips.

- Process complexity in any case would be reduced in solution processing methods which will decrease the overall costs and increase the throughput of devices fabricated. This is due to its principal idea of additive processing rather than subtractive processing where lithography is used to use masks, develop the masking layer, baking the masking layer, etching, and removing the masking layer. It will lead to a reduction of overall step count, raw material costs and tooling costs. In this sense costs are greatly reduced.

- Low-cost substrates can be handled and potentially, roll-to-roll processing can be used to increase the throughput to a level of mass production. Tools for high registration accuracy is required when multiple layers need

to be deposited on the same respective devices. This again is accounted for the development of the IC printing devices.

- Although cost per substrate area may be much lower when considering conventional processing methods, the cost per transistor, or the cost per function is much higher due to the worse resolution for current printing methods as well as the electronic quality limitations of the organic transistor.

- Cost advantages are depending on specific process flows used

A.3 Applications

Printed electronics make it economically attractive in area-constrained applications rather than requiring functional density[3, 57]

+ displays, sensors (functional density of sensors dominant on size and form-factor of sensing element), RFID tags (operating at relatively low frequencies such that the size of the antenna and passive components dominate overall size of the tag

Easy integration of mutually incompatible and diverse materials on the same substrate

+ various sensor types and tags with multiple functions

Relatively poor performance due to low temperature process, lack of self alignment, poor film quality, large linewidth, low performance materials are used. Frequency of operation should therefore be less than 1MHz and the device should be relatively large.

+ displays, simple sensing elements

RFID focus on lower cost (eliminate expensive chip attach), however, these will have a limited performance

Printed array sensors performance trade-offs, integration of disparate materials on the same substrate

Displays costs per unit area, before only low resolution displays were produced, for high resolution, the electronics should be of higher quality or a compatible back plane technology required.

Appendix B

Printer types for electronics fabrication

B.1   Impact Printers

Impact printers are the oldest type of printers known to man. The many types of impact printers are fundamentally based on a print master which is coated with ink and transferred to a substrate upon contact. This full contact property makes the resulting images highly reproducible. The fact that the process is based on bringing ink and substrate into contact by a specific force will lead to the danger of wear of the master. Nevertheless the process is used nowadays in areas where mass production of the prints is needed due to the speed and reproductive quality of this type. The master therefore needs to be highly stable and carefully optimized. Printers of this type include: letterpress, lithography, screen, and gravure printers [13]. Their main properties are:

+ High speeds can be achieved due to cylinder to cylinder, or roll to roll, printing [13]

+ The process can be converted into a web-fed process, rather than sheet press process. This makes high speeds possible, however, they have longer set-up times, more start-up waste, and it makes it difficult to print on varying formats or substrates. They have a great advantage however in longer print runs. [13]

+ High repetitive quality [13, 10]

- They have defectivity challenges due to the direct contact of the master with the substrate. [3]

- Ink splitting should be taken into account. It is a process where, the ink to be transported is split when the master is released from the target substrate, causing a thinner printed layer than what might be hoped for.
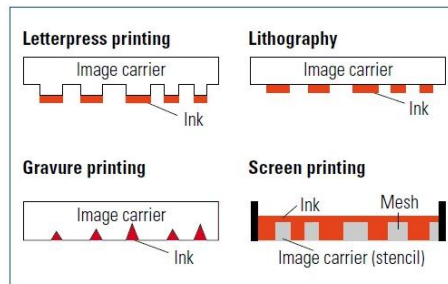
Figure B.1: The master plates for four main impact printers [13]

The differences between the different impact printers is primarily in the way that the master plates are constructed. Fig. B.1 shows different masters that are associated to the different types of impact printers. Letterpress is probably the easiest to understand and is the most well-known type. Patterns that are needed to be transferred to the substrate are on an elevated level on the print master. These raised elements bring the ink into contact with the substrate. The second master in the figure is the lithography printer, where the printing elements are on the same level as the non-printing levels. The surface is modified so that the ink will only adhere only to the printing elements. The third type is screen printing, where the master is patterned by way of making openings through which the ink is pushed onto the substrate according to the shape of the openings. Finally, gravure printing may be considered as the inverse of letterpress printing. The master is patterned by means of small indents filled with ink that can later be transferred on the substrate by means of fluid adhesion. This last type of impact printer will be important for this thesis and a separate section will be dedicated for it.

B.1.1 Gravure Printing

Gravure printing has been known for its outstanding reproductive quality although an expensive master is needed. Today's market share for this type is limited to 10 to 15 percent, and found to be fruitful for very long print runs (>1000000). Gravure printing is typically implemented for high-quality, high-circulation printed packages as well as products which include: magazines, catalogs, plastic films, metal foils, transparent films, carrier bags, security papers, stamps, bank notes. In today's commonly used applications, there are various sizes and speeds in use. [13]

In this master the printing elements are formed in the inverse way of letterpress printing. The elements are recessed in a master with various depths and sizes for an optimum print quality and prevention of pattern deformation upon contact, common in letterpress printing. The entire plate or cylinder is flooded with low viscosity ink. A cylinder is preferably used for a better throughput of the process.While this ink fills the holes of the patterns and forms a film on

top of the patterns as well as non-patterned areas, a high quality blade removes
any excess ink. The excess ink can be reused and the ink that is left in the cells
of the cylinder or plate is pressed against the substrate under a high pressure.
Depending on the type of ink, the force that has been used or the speed of the
process lateral shear forces can cause a pick-out effect where the ink can be
pulled out of the desired printing area. Optimization of this process with spe-
cific ink, force and speed is necessary. [3] A schematic of this process is shown
in Fig. B.2 .
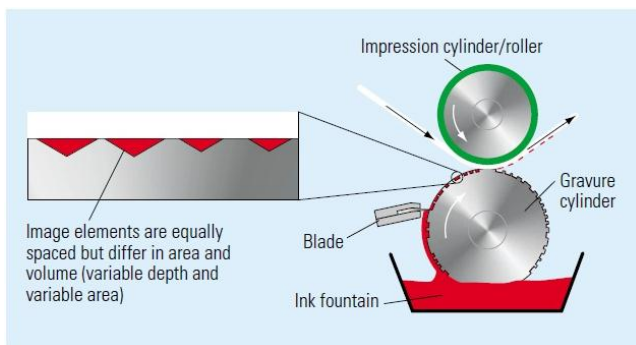
Figure B.2: Gravure printing schematic [13]

The blade, also known as the soul of gravure printing is one of the most
important elements of the whole process. It is a thin, wear-resistant, strip that
ensures the removal of excess ink, and proper filling of the cells and is usually
made of steel. Since the whole cylinder will be pressed against the substrate,
any defects on the blade will have a direct impact on the final result. It is
mounted slightly angled depending on the type of blade or the type of ink that
is used. Due to the constant scraping of the blade and its importance, it must
be changed regularly to avoid the effects of wear.

When aiming at high manufacturing speeds, using an engraved cylinder as
the master is the better way when comparing to a plate master. This cylinder
has recesses for the printing elements, however, these elements can have either
variable depth, variable area, or both for an optimum print quality. For every
different color, whole cylinders are used to maximize throughput. The impres-
sion roller is used as a counter force from the other side of the target substrate.
These rollers should be as small as possible to ensure a narrow printing nip. The
roller needs to be capable of withstanding high pressures without deformation
or deflection. Hydraulic cylinders can offer a solution to this problem. Cooling
is also an issue in these structures. [13]

The inks that can be used have a relatively low viscosity for a high speed
filling of the printing cavities. Although bleed-out can also be a problem for
gravure printing, it is not as critical as it is for screen printing. No binders
are therefore required that thicken the ink, unlike with screen printing. There
is a large range of useful inks that can easily have their viscosity decreased by

creating a solution out of them. Toluene and Xylene are typically used solvents since they are transparent, can dissolve many types of inks and dry fairly quickly. The final ink is kept in an ink pan in which the gravure cylinder is inserted. The cylinder must not form foams or splash inks to maintain a high quality ink filling of the cells. When the ink is transferred to the final substrate, it will not be able to be transferred completely which is also the case for the other impact printers. The ink will split depending on variables such as: thickness of the ink layer, period of contact, contact pressure, rheological ink properties such as viscosity and wetting properties, temperature ratios, surface properties and absorption properties. In the case of gravure printing, two additional variables can influence this ink splitting, such as the shape of the cells and the filling level of the cells.[13]

To summarize, there are a few key aspects of the gravure printing process that make them suitable for the mass production of electronics:

+ Very high image quality [12, 13]

+ Very high speed [3]

+ Very good image reproduction [13, 10]

    + Good uniformity [3]

    + Low line-edge roughness [3]

+ Good compatibility with many materials [12]

+ Wide range of thicknesses possible due to the cell structure [3]

+ Good scalability up to a linewidth below 20µm [3]

- Expensive Cylinder [12, 13]

- Limited by overlay printing registration accuracy (OPRA) [58]

- Separate cells on the cylinder prevent this type of printer to create smooth straight lines. [59]

For the implementation in electronics fabrication, it is important to know the operating regime of the process currently in use. Table B.1 summarizes some of the typical values associated to gravure printing.

Research has been conducted on the printability of electronics using this type of printing[58, 60]. The benefits of gravure printing has attracted many researchers. Already many electronic devices have been proven to be producible with this type of printing such as OLEDs[61, 62, 63] and basic circuit elements [12, 64, 65].

Table B.1: Typical values for gravure printing processes [13]

Web width	2.4m - 3.6m	(publication)
	1.2m - 1.4m	(packaging)
Web speed	10m/s - 15m/s	(publication)
	5m/s - 6.5m/s	(packaging)
Gravure Cylinder circumference	800mm - 1600mm	(publication)
Screen ruling	40 lines/cm - 140 lines/cm (typically	
	60 lines/cm - 70 lines/cm)	
Cell geometry	Width	30 µm - 230 µm
	Depth	10 µm - 30 µm (max 50 µm)
	Cell wall width	3 µm - 5 µm

B.1.2   Other impact printers

Letterpress Printing

The oldest type of impact printer and is the least complex type of impact printing. Typical non-electrical applications that are used today by letterpress/flexographic printing include small-format jobs, business cards, form printing, packaging printwork, labels, carriers and bags.

The print master used to transfer the ink to the substrate is modified in a way that the print elements, so the patterns that needed to be transferred, are raised. The master plate will subsequently be inked and the ink is transferred by applying pressure to the master, onto the substrate. The raised elements on which the ink has adhered will be transferred by force. The schematic is shown in Fig. B.3 [13]

An upgraded version of this type of printing is flexography which uses a relief flexible plate to transfer the ink. This type can be used on many different types of target substrates. [59]

This method has proven to have a fundamental advantage but also a significant disadvantage:

+ The manufacturing method is quite easy and straightforward. [12]

+ Continuous lines can be printed unlike other pixelated printer types such as inkjet, gravure or screen printing. This prevents this type of printer from pinholes, cell blocking, and missing dots. [66]

- The master is prone to mechanical deformation due to the excessive force that is applied on the raised elements. Minor deformations of these elements can lead directly to a change in the shape of the resulting pattern. [12]

- On the edges of the printed areas, a certain pattern is visible due to the squashing behavior of the plate to the substrate. The non-uniformity at the edges may cause issues in electrical systems.[59]
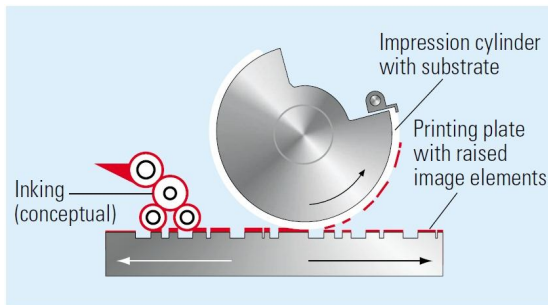
Figure B.3: Letterpress schematic diagram [13]

Flexography has been shows in some instances to be suitable for the printing of continuous lines in electronics in [66], and has helped the development in OLED displays in [67]. Within the electronics industry however, alternative printer types based on letterpress have emerged such as microcontact printing and nanoimprint. Both show promising results in research, and can achieve high resolutions.

(Offset) Lithography Printing

Offset lithography is one of the most commonly used type of printer. Typical applications to this type of printing method include newspapers, magazines, brochures, books, and packaging.

In lithography there is no problem with deformation of printing elements, since no elements are raised. Instead, all elements are on the same physical level, but have different material properties that can either adhere or repel ink. The master plates are usually made of different materials with different chemical and surface properties. An aluminum based surface is covered with a photopolymer which is patterned as the area to which ink will adhere. The whole surface is then covered with a dampening solution which spreads on the aluminum surface due to its high surface energy, but will stick poorly to the photopolymer areas with low surface energy. The surface is subsequently covered with ink that will only spread on the image areas. This surface is then brought into contact with the desired substrate. [13, 59]

Offset printing is related to this type of printing by setting an intermediate carrier for the transfer of ink. The ink is then first pressed against the intermediate carrier, which subsequently brings the ink to the final substrate for the reduction of water brought to this substrate. [13, 59] The schematic is shown in Fig. B.4 .

Although there are some advantages to this method of printing, there is one fundamental limitation [12]:

+ No deformation due to impact
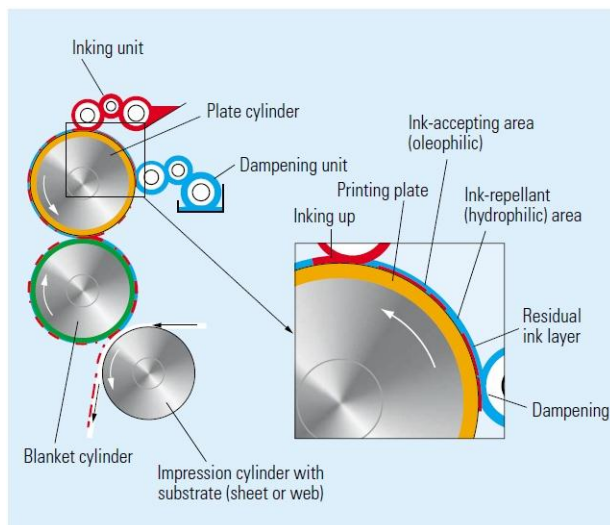
Figure B.4: Lithography/Offset printing schematic diagram [13]

+ The printing quality is high

+ The resolution can be made high

+ plates are easy to make and relatively cheap [59]

- The useable ink is quite limited since it needs to be compatible with various materials and have the right properties.

- High viscosity inks are required

Some limitations for the printing of electronics include: issues with the water based dampening solution that can affect the ink which is could have detrimental electronic properties to the material. Waterless offset lithography can be used which replaces the dampening solution with a silicone layer. The second limitation is that the thickness of the transferred ink is relatively low (1 to 2 µm). Multiple passes of the printing plate may be required. Finally, inks with high viscosity are required.

Screen Printing

For printed electronics, this type of printing is the most mature. The most commonly known application in electronics are printed circuit boards, that have been manufactured in this way for decades. Typically, besides PCBs, screen printing is used in: textiles, t-shirts, toys, equipment, packaging, and large-format advertising posters. [13, 3]

The working principal is based on squeezing ink all the way through a master plate. The master plate is constructed from a fine mesh. The non-printing

elements are coated by a photosensitive screen coating. A squeegee is used to squeeze the ink through the open meshes, while the relatively viscous ink is pushed through the mesh and transferred onto the substrate. Fig. B.5 shows a schematic of the process. [13]
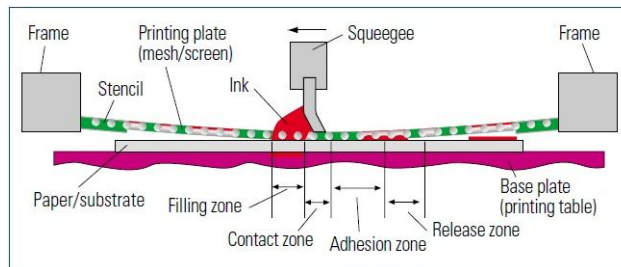
Figure B.5: Screen printing schematic [13]

Although, again no elements are raised that are prone to deformation during impact, there is a significant disadvantage of using screen printing and it lies in the type of ink that can be used as well as its resolution [3]:

+ Can deposit thick films which may be useful in applications such as contact line production

- Resolution is typically worse than 50µm in commercial use

- Research has indicated a resolution of less than 10µm to be achievable

- The viscosity of the ink should be relatively high (>1000cP). This is because excessive spreading and bleed-out needs to be avoided. A low viscosity ink will cause disastrous effects due to these effects. Binders are added to increase the viscosity of the ink. This is generally used in graphic arts, however, for electronics; these binders can destroy semiconductor properties. They can cause excessive leakage currents, dissipation in dielectrics or drop the conductivity of conductors.

Due to the final con, screen printing is applied only in electronic applications where addition of the binders does not lead to unacceptable loss of performance.[3] The main electronic application for this printer type still lies in the production of PCBs, however the production of OLEDs [68, 69] and even OLED displays [70] have also been shown to be possible with this printer type.

B.2   Non-Impact printers

Non-impact printers (NIP) are popular due to their property of printing variable prints easily. This type is not limited to a stable, physically fixed master that should be used many times before being economically feasible. Every print run can be produced in a different way, so we would have a print-on-demand

system. Prints can easily be adjusted digitally allowing the variation of prints per run. This is a huge advantage when researching new materials. There are however some negative sides to be considered. Due to its resetting property, it can produce a greater variation when two of the same prints are produced. The paper is usually held by electrostatic forces instead of grippers which gives limitations to the overall accuracy. Finally, this type is slower than cylindrically printed, web-fed, impact printers. Each print requires a fresh imaging; it will however be unlikely to produce large scale benefits for mass production. From this type of printers, Inkjet is most commonly used for research purposes, and electrophotography is the second most commonly used commercial NIP type. To summarize, the main properties of Non-Impact Printers include:

+ They are not limited to the stability of the physically fixed image carrier. The patterns are digitally preprocessed.

+ They can imprint a different page per print, making optimal use of variability in print runs

- They have however a low repetitive quality, since every print run is regarded as a new print.

- They have the problem of achieving high speeds.

B.2.1 Inkjet

Printing active electronic circuits today is most commonly done by inkjet printing [12, 3] . It offers a quick and easily variable process and therefore a good way to research new materials. In this type of printing, low viscosity inks are used (1-20cP), so again no binders are required as was the case for the screen printing process. No masks are needed for the NIP printers, and by digital manipulation, prototypes can easily be manufactured [10].

Inkjet, unlike electrophotography, does not require an intermediate carrier for transferring the image information. The ink is shot directly onto the substrate either continuously or by drop-on-demand. In the continuous case, the ink is constantly shot towards a substrate as a continuous stream of small droplets. These droplets are charged and directed towards the image by means of an electric field. When an area does not require ink, the droplets are deflected for re-usage. In the case of drop-on-demand, a droplet is only produced when it is required. The ink is shot either thermally by inducing a gas bubble through evaporation and sending the droplet in front of the bubble towards the substrate when the bubble pops. A second way is to induce a bubble piezo-electrically by bulging the material itself for the ink shot. [printer book paddy French] [13] . The schematic is shown in Fig. B.6. The summarized properties are:

+ It uses a digital input for on the fly design changes [3, 10]

+ It is less prone to wear problems compared to impact printer types
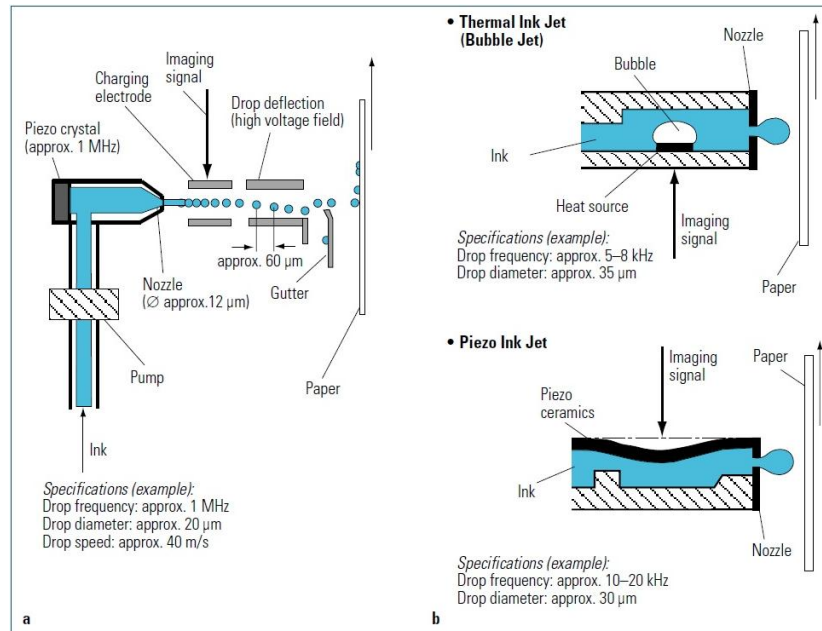
Figure B.6: Inkjet printing schematic [13]

$+$ It is compatible with many different materials [3]

$+$ It deposits in small volumes [10]

- Since the technique depends on droplets, pixelation related issues are inevitable.

- Due to propelled droplets rather than full contact of patterns in impact printing methods, there is a statistical variation in the final position of the droplets.

- Due to the complex drying phenomena of droplets it can produce widely variant printed patterns. Pinholes and sharp edges are the result of this. The non-uniformity of this drying will also lead to non-homogeneous transistor performance. [3] This issue has been solved for a case in [71] which resulted in a high mobility of 16.4 cm^2/Vs

- Distance between deposited drops can change the linestyles of the final result. Small distance between drops will cause bulging, a bigger distance will lead to scallops. One possible solution to this is flash drying which is the rapid drying of drops upon substrate contact. [3]

- Slower than the web-fed cylindrical impact printer types. A higher throughput can only be achieved when multiple nozzles are used in parallel. Misfiring is an issue in these systems [3, 10]

Inkjet is currently widely used for the research of organic semiconductor devices due to the ease and flexibility of the solution process due to its non-impact printing advantages. In the case of these electronic devices, a thermal nozzle can not be used since the heat produced in this process could destroy the properties of the organic semiconductor. A piezoelectric or even an acoustic inkjet printer is used therefore used. Many works have already shown the production of electronic devices using this printer type [27, 72, 71, 73], in some instances all parts of the TFT[74, 75]. Today, subfemtoliter accurate inkjet printers are being used at Someya's Organic Transistor Lab in Tokyo University for extremely high accuracy [72].

B.2.2 Electrophotography

Electrophotography is based on the transfer of ink to a substrate through electrostatic forces. A drum with a specific type of surface can be used on which a controlled light source can create patterns. The light source will induce charged colored particles called toner to be attracted to the specific patterned parts on the surface of the drum. This toner is subsequently fixed on the substrate, after which the drum is cleaned. The individual process steps are visualized in Fig. B.7

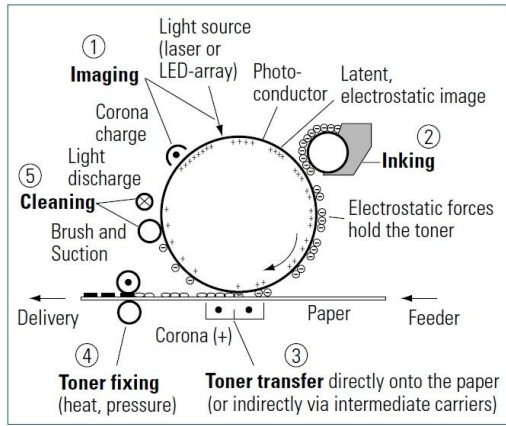Figure B.7: Electrophotography schematic [13]

Electrophotography is the second most widely used Non-Impact Printer type, and is used today mainly as commercial automatic copiers.

Some of the properties of electrophotographic printing are [13] :

+ Can produce higher quality prints compared to inkjet

- Slower than inkjet and more expensive, although [76] reviews this and claims that this difference is quite small

+ Similar to Inkjet printing, there is no fixed master, and a different charge image can be produced after every drum revolution.

- When repetition in prints are required the drum still needs to be recharded after every rotation. Fluctuations in two identical print setups are inevitable due to both image generation with charges, and the transfer of toner to the substrate due to electrostatic forces.

• The type of toner used determines for a large part the quality of the print: particle size, shape, and chemical structure. Both liquid as well as powder typed toner may be used. Conventionally, toners with particle sizes of 6 to 8 um are used.

Although electrophotographic print quality is superior to the quality of inkjet printing, the former is not being used for printing electronics for two main reasons [59]:

1. The toner used for transfer of materials to the substrate needs to be charged and go through an electrostatic field. Conductors and semiconductors will be influenced by this charging.

2. The transferred toner needs to be fixed onto the substrate. This fixation may cause problems in some applications.

B.3 Conclusion

Different types of printers have been introduced in this chapter. Some are more suitable for electronic applications than others. For mass production ends it is important to achieve high quality at under high production speeds. Table B.2 qualifies the various printers according to important aspects from the electronic device manufacturing point of view. Notice that electrophotography has been left out of the table due to lack of electronic device applications.

When comparing impact printers to NIPs the biggest difference is the digital input with the NIPs. Because of this property, they are excellent for highly variable printing processes, and therefore quite useful for research purposes. They lack however in throughput, and therefore although very useful for research, may not be the best option for mass production.

Impact printers on the other hand are aimed for mass producing runs, using roll-to-roll, web-fed processes. Screen printing achieving limited resolution may not be useful for electronic ends although contacts in PCBs are still manufactured in this way and there may be a certain reliability to this quality. Offset lithography is also a viable option, however, there are limited works that have investigated the fabrication of electronics using this type of printing, this may be due to the poor compatibility of the inks that can be used as wettability is a prime focus. Flexography has the issue of pattern deformation, although the masters are relatively easy to make, the main advantage lies in the printing of continuous lines, unlike gravure, inkjet or screen printing. Finally, gravure

Table B.2: Comparative analysis of the various printer types

	Typical Resolution	Ink Viscosity	Main advantage	Main disadvantage
Gravure	+	low	Excellent reproducibility and fidelity	expensive master
Flexography	±	low	continuous line printability	pattern deformation
Offset Lithography	+	high	fast and accurate	limited ink compatibility
Screen	-	high	reliable	low resolution
Inkjet	+	low	digital input	low throughput

printing has gained quite some attention due to its high reproducibility and fidelity over long print runs. In addition, the throughput is high and many types of inks may be used. The cost of creating the master is relatively high, however, print runs exceeding over 1,000,000 runs, compensate for the costs and make this type of printing rather inexpensive.

For electronics, many different printers may be used but are suitable for perhaps various parts of the transistor. A combination of printing types may be the most efficient way to create low cost large area electronics. One particular printer type, gravure printing, has proven to be the most interesting for mass production ends. For research however, it is more useful to produce easily manipulable devices, and therefore the non-impact printer type inkjet printing, is the most suitable for the early stages of printing electronics due to its digital input and high resolution.

Appendix C

Thin-Film Transistor

Thin-film transistors are different from conventional MOSFET's and BJT's in one essential aspect: they can be built on top of a certain substrate. Today many of the applications of these devices are especially large area displays. In these products the devices are manufactured on top of a glass substrate and operate by directly influencing the emission of light through the display. In this example, it is not essential to create the devices at lower temperatures due to the temperature stability of the glass substrate. Solution processing in this case is still however desirable for larger area displays, flexible displays, and cheaper displays.

In essence, thin-film transistors are a type of MOSFET's built on top of a substrate. Today, many of the displays are created using hydrogenated amorphous silicon (a-Si:H) as the semiconductor. It is important to notice that most of the devices in this Appendix are focused on organic semiconductors since these are the main type of solution processable semiconductors and therefore the direct competitor of the liquid silicon material. Organic semiconductors were preferred due to their solubility with many common solvents without losing their original semiconducting function. These organic semiconductors have fundamental limitations to their stability, and therefore the impact of different device configurations and processing methods to the final device is quite big, whereas this would not be the case for conventionally processed TFT's. Solution processed devices which is necessary for the printing of devices is mainly focused from an organic TFT point of view.

C.1   OTFT Characteristics

For the organic transistor, current flow is limited as well as their reliability [2, 8]. The main charge carrier transport occurs in the first 50 angström of the organic semiconductor layer, away from the semiconductor-dielectric interface [9]. This interface is therefore essential for the quality of the device. The thickness of the semiconductor layer ranges typically from 200-500 angström. Thinner films

could fail due to incomplete surface coverage [9].

The deposition of the semiconductor layer in this type of transistor becomes crucial. There are three important points about deposition conditions [9]. The first one is the deposition rate; it can directly affect the crystallinity and morphology of the resulting layer. A high deposition rate leads to high nucleation densities. These nucleation densities are related to the grain sizes within a film. A high nucleation density corresponds to a high concentration of small grains. A highly crystalline film that consists of larger grains, gives better characteristics of the final device, as is the case for the different crystal structures of silicon based devices. Bigger grain sizes are therefore desirable, since grain boundaries deteriorate the current flow of the device. Additional energy is required for the charge carriers to move from one grain to the other. High deposition rates are in this case not desired; however it could also induce the formation of a different packing order which may improve the device performance. The surface of the substrate and substrate temperature also has a great impact on the formation of the film. Substrates with grooves in a particular direction may induce an ordering of the organic molecules in a way that improves the charge carrier transport. Finally, post-deposition treatments can also help improve the device performance.

C.2   Transistor Configuration

The basic construction of TFT's can be divided into four groups depending on the position of the gate, semiconductor and contacts. Each has its own advantages as well as disadvantages and will briefly be described below. Again it is important to consider the organic variant of these devices. These devices are shown in Fig. C.1.

- Top-Gate-Bottom-Contact

- Bottom-Gate-Top-Contact

- Bottom-Gate-Bottom-Contact

- Substrate-Gate-Bottom-Contact

Notice that the combination of Top-Gate-Top-Contact has been left out. This is primarily due to the poor reliability of the organic semiconductor. In most cases it is undesirable to build upon an organic semiconductor as thermal sensitivity and contamination may impact the semiconductor characteristics and therefore the properties of the final device.

The different gate positions relate to some important device characteristics. A top-gate (staggered) configuration compared to the bottom-gate (inverted-staggered) configuration gives:

+ The spacing between source and drain and therefore the essential channel length can be determined early on the design, as the contacts are deposited at an earlier stage.
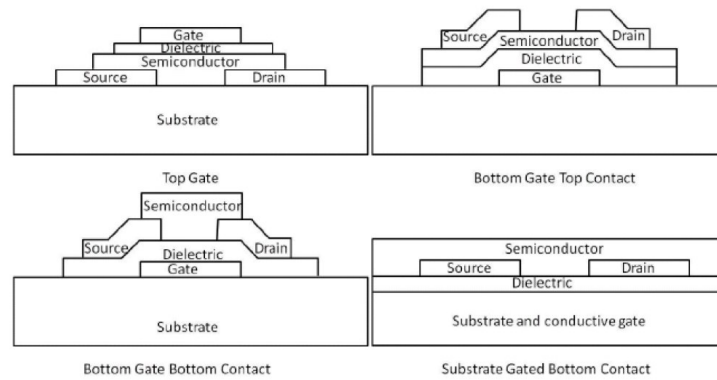
Figure C.1: Various TFT structures [12]

+ Since the gate layer is deposited later than the semiconductor layer, the gate dielectric will cover the semiconductor layer. This will give the advantage of encapsulation of the sensitive semiconductor layer.

+ Due to its inverted staggered configuration, the contact resistance to the gate is much lower.

A bottom-gate configuration will bring some other advantages on the other hand:

+ The semiconductor layer will be deposited later on, which helps for the thermal sensitivity of this layer. There are also less processing restrictions in this way for avoiding contamination of the semiconductor.

+ The choice of dielectric and deposition is much less critical in this case to avoid changing the semiconductor characteristics of the already deposited semiconductor layer.

+ The interface between semiconductor and dielectric layers are not determined by the roughness of the semiconductor layer which is generally relatively rough.

+ Higher mobility devices can be achieved in this configuration.

The position of the contacts also differs in the performance of the final device. It may be confusing to define characteristics based solely on the position of the contacts regarding the semiconductor film. A better way to characterize the contact position is with respect to the semiconductor-dielectric interface. Some general statements to the contact positions are listed below.

• For devices with the contacts placed close to the semiconductor-dielectric interface. The charge carriers don't have to travel a long path to reach channel on the semiconductor-dielectric interface. Contact resistance is therefore lower in this configuration. [72]

- It is undesirable to have the semiconductor placed before the contacts are placed due to the instability of the organic semiconductor that may therefore be influenced by the subsequent contact deposition.

Although some of these characteristics are only limited to the processing of organic transistors, it is important to know what the alternative for liquid silicon solution processed devices can provide. Some of the information in this section may also apply to liquid silicon devices, although it is relatively more stable. In the final design of the device, the exact worst configuration for organic transistors will be used due to the way liquid silicon Single-Grain Thin-Film Transistors are constructed.

Appendix D

SFE Results

	Surface modification/type	Contact angle	SFE (mJ/m²)
Thermal Oxide	Untreated	21˚	30.4
	HF	12.5˚	31.7
	O_2(8min500W)	16.9˚	31.1
	UV exposed	16.6˚	31.2
	IPA	18.4˚	30.9
Thermal Oxide2	O_2(8min500W)	19˚	30.8
	HF	14.9˚	31.4
	Al	0˚	32.5
	Al(Marangoni)	0˚	32.5
	Polyimide	14˚	31.6
	PR(SPR3012)	19˚	30.8
	PR(SPR3017m)	21˚	30.4
	SiN	33.4˚	27.5
Etched back TEOS	Untreated	26.6˚	29.2
	HF	19.33˚	30.7
	O_2(10min500W)	21.8˚	30.3
	O_2(30min300W)	22.6˚	30.1
Non-Etched back TEOS	Untreated	17˚	31.1
	HF	16.1˚	31.3
	O_2(10min500W)	17.2˚	31.1
	O_2(30min300W)	15.7˚	31.3
	100˚ pre-anneal	25.7˚	29.4
	HF + 100˚ pre-anneal	14.2˚	31.5
	HMDS	12.8˚	31.7
	Ar (0.5p350W)	34.9˚	27.1
	Ar(0.5p50W)	10˚	32.0
	Ar(lp350W)	22.6˚	30.1
	Ar(lp50W)	25˚	29.5
	Untreated 75˚	12.5˚	31.7

	Surface modification/type	Contact angle	SFE (mJ/m²)
	HF 75˚	3.92˚	32.4
	O_2(10min500W) 75˚	14.8˚	31.4
	O_2(30min300W) 75˚	16.08˚	31.3
	100˚ pre-anneal 75˚	15.6˚	31.3
	HF + 100˚ pre-anneal 75˚	10.4˚	32.0
	HMDS 75˚	11.8˚	31.8
	Ar(0.5p350W) 75˚	18.4˚	30.9
	Ar(0.5p50W) 75˚	15.4˚	31.4
	Ar(lp350W) 75˚	20.2˚	30.6
	Ar(lp50W) 75˚	19.4˚	30.7

Appendix E

Excimer Laser Crystallization

E.1 Crystallization process

Two types of crystallisation occur in the ELC process. [47, 48]

Explosive Crystallization

The melting point of a-Si is a few hundred degrees lower than crystalline silicon (1414°C). This difference in melting point lies at the core of the explosive crystallization process. When the a-Si is molten, it is rapidly cooled with respect to the crystalline silicon, which will cause crystallization of the liquid into polysilicon areas (only at very high cooling rates and lack of crystalline fractions will the liquid solidify back into an amorphous solid). The heat produced by the crystallization of the silicon liquid will further melt the remaining a-Si which again proceeds to solidify due to the supercooled surrounding. In this way the molten layer moves deeper into the total film leaving a trail of fine polysilicon grains behind. The whole process is self-sustaining and is continued until there is a sufficient loss of heat that is required for the further melting of a-Si.

Melting and Solidification

When a certain threshold is reached by the laser, the fine polysilicon grains that were previously formed by explosive crystallization, remelts at the surface. This remelting of the polysilicon is not as severely supercooled as is the case for explosive crystallization. Therefore the solidification rate is much lower, which results in a reduced number of granular planar defects, and an increased grain size.

At this second remelting energy a difference between complete melt and incomplete melt can be recognized. In the event of a complete melt, there are no crystalline seeds left for regrowth. Therefore, before solidification may occur, homogeneous nucleation is required. These nucleï will stabilize under certain thermal conditions. After the formation of nucleï, the film will solidify rapidly.

The nucleation rate is strongly dependent on temperature, and will result in a final film in which small grains coexist with larger ones. In a near complete melt condition, some fine polycrystalline grains from the explosive crystallization survive. Solidification will initiate at the remaining polycrystalline grains due to heterogenous nucleation rather than the homogenous nucleation. Grain size will increase significantly and will grow beyond the film thickness. This process is called superlateral growth.

Keeping these processes in mind, grain sizes can be enlarged by increasing the lateral growth interval. This can be done by reducing the cooling rate of the molten silicon. Heating of the substrate, extension of the pulse duration, or simultaneous irradiation of the sample from the front and backside are some of the possible options. Shooting multiple pulses at a sample can also increase the grain size due to the growth of preferential orientation of the grains.

E.2   Crystallization problems

Some issues when producing the crystalline film may also occur:

Random grain boundaries Grains that are grown from different seeds can collide. During crystallization the silicon will expand due to the density difference between solid and liquid phase silicon. The higher density solid silicon has little effect in the vertical growth direction, however, horizontally the liquid will be pushed by the crystallizing solid silicon. At the interface between two growing grains the liquid will built and prevent further growth. This results in high defect density grain boundaries and should be avoided when constructing polycrystalline silicon TFTs in this way.

Breakdown growth The rate of growth of the crystalline silicon may be too high which may lead to misplacement of atoms that result in stacking faults and twins and may even lead to complete breakdown. Orientation of the crystal highly influences this type of error.

Thermal stress Rapid cooling may induce thermal stresses that will result in planar defects during lateral growth. Tensile elastic strain in the silicon builds up until yielding of the material occurs. Again crystallographic orientation is important for this type of error.

Film cracks These are formed as a release of thermal stress due to steps in the film that have been lithographically produced. The difference in thermal expansion rates of silicon and silicon dioxide lie at the source of this problem.

Hydrogen effusion Any hydrogen present within the amorphous silicon film can be effuse due to the laser irradiation and may destroy some parts of the film. Since the liquid silicon material is produced from a hydrogenated

silicon compound, and due to limited annealing temperature, a significant amount of hydrogen atoms can be left in the film that can cause defects by this out-diffusion of the hydrogen.

Film agglomeration Partial dewetting may occur and lead to film decomposition into beads which is known as agglomeration. The main source of this dewetting are the fluctuations of the silicon film that are severe enough to reach the underlying oxide layer. These fluctuations are influenced by the pulsed-laser annealing caused by non-uniformities in the spatial profile of the laser pulse and intensity fluctuations from the homogenizer. Also the interference of the incident beam with laterally scattered beams as well as the surface tension gradient have an impact on this defect.

Ablation is related to excessive agglomeration and is known as the explosive release of hydrogen. A major issue in this work is indeed the hydrogen content of the amorphous silicon film produced from the liquid silicon material.

Bibliography

[1] T. Shimoda, et al. "Solution-processed silicon films and transistors", Nature vol. 440, 6 April 2006, pp. 783-786

[2] J. Zhang, R. Ishihara, H. Tagagishi, R. Kawajiri, T. Shimoda and C. I. M. Beenakker, "Single-Grain Si TFTs using Spin-Coated Liquid-Silicon", IEDM11, 2011, IEEE, pp. 339-342

[3] V. Subramanian, et al. "Printed Electronics for Low-Cost Electronic Systems: Technology Status and Application Development", Department of Electrical Engineering and Computer Sciences, University of California, Berkeley, IEEE, 2008.

[4] A. Sugiyama, T. Shimoda, and D. H. Chi, "Ab initio study of the polymerization of cyclopentasilane", Molecular Physics, vol. 108, No. 12, 20 June 2010, pp. 1649-1653

[5] P. V. Dung, P. T. Lam, N. D. Duc, A. Sugiyama, T. Shimoda, D. H. Chi, "First-principles study of the thermally induced polymerization of cyclopentasilane", Computational Materials Science 49, 2010, pp. S21-S24, Elsevier

[6] H. Iwasawa et al. "Silane Polymer and Method for Forming Silicon Film", US Patent 2009/0215920 A1, Aug. 27, 2009

[7] D. L. Kim et al. "The Effect of Ultraviolet Exposure on Solution Process of Silicon Thin Film", Electrochemical and Solid-State Letters, 12, 2009, pp. E23-E25

[8] [book] David B. Mitzi "Solution processing of Inorganic Materials", John Wiley & Sons, Inc., Hoboken, New Jersey, 2009

[9] M. M. Ling and Zhenan Bao, "Thin Film Depostition, Patterning, and Printing in Organic Thin Film Transistors", Department of Chemical Engineering, Stanford University, American Chemical Society, 2004.

[10] J. Verilhac et al. "Step toward robust and reliable amorphous polymer field-effect transistors and logic functions made by the use of roll to roll compatible printing processes", Organic Electronics 11, 2010, pp. 456-462

[11] C. Y. Woo, C. Y. Ho, K. H. Seok, L. Y. Hee, "Solar cell manufactured using amorphous and nanocrystalline silicon composite thin film, and process for manufacturing the same", European Patent Application, EP 2 040 310 A2, March 25, 2009

[12] Alejandro de la Fuente Vornbrock, "Roll Printed Electronics: Development and Scaling of Gravure Printing Techniques", Electrical Engineering and Computer Sciences, University of California at Berkeley, Dec. 29th, 2009

[13] [book] Helmut Kipphan, "Handbook of Print Media, Technologies and Production Methods", Springer- Verlag, Berlin Heidelberg New York, 2001

[14] J. Perelaer, et al. "Printed electronics: the challenges involved in printing devices, interconnects, and contacts based on inorganic materials", J. Mater. Chem., 2010, 20, 8446-8453

[15] [Book] L. Solymar, D. Walsh, "Electrical Properties of Materials", Oxford University Press, 7th edition

[16] [Book] D. R. Gamota, P. Brazis, K. Kalyanasundaram, J. Zhang, "Printed Organic and Molecular Electronics", Kluwer Academic Publishers, ISBN: 1 4020 7707 6

[17] H. Ebata, T. Izawa, E. Miyazaki, K. Takimiya, M. Ikeda, H. Kuwabara, and T. Yui, "Highly Soluble [1]Benzothieno[3,2-b]benzothiophene (BTBT) Derivatives for High-Performance, Solution-Processed Organic Field-Effect Transistors", J. Am. Chem. Soc. 2007, vol. 129, no 51, pp. 15732-15733

[18] T. Endo, T. Nagase, T. Kobayashi, K. Takimiya, M. Ikeda, and H. Naito, "Solution-Processed Dioctylbenzothienobenzothiophene-Based Top-Gate Organic Transistors with High Mobility, Low Threshold Voltage, and High Electrical Stability", Applied Physics Express 3, 2010, 121601

[19] T. Uemura, Y. Hirose, M. Uno, K. Takimiya, J. Takeya, "Very High Mobility in Solution-Processed Organic Thin-Film Transistors of Highly Ordered [1]Benzothieno[3,2-b]benzothiophene Derivatives", Applied Physics Express, vol. 2, 2009, issue 11, 111501, ISSN 188207784

[20] [Book] D. A. Neamen, "Semiconductor Physics and Devices, Basic Principles" R. D. Irwin, Inc., 2003, third edition

[21] [Webpage] organic semiconductor world
www.orgworld.de

[22] E. Hengge and G. Bauer, "Cyclopentasilane, the First Unsubstituted Cyclic Silicon Hydride", Angew. Chem. Internat. Edit. / Vol. 12, No. 4, 1973, page 316

[23] U. Zschieschang et al. "Dinaphto[2,3-b:2',3'-f]thieno[3,2-b]thiophene (DNTT) thin-film transistors with improved performance and stability", Organic Electronics 12, 2011, pp. 1370-1375

[24] T. Sekitani, U. Zschieschang, H. Klak and T. Someya, "Flexible organic transistors and circuits with extreme bending stability", Nature Materials, Vol. 9, 2010, pp. 1015-1022

[25] Organic Electronics, a future promise powerpoint presentation `www.phy.iitkgp.ernet.in/ptaccd2/ppt/ADhar.pdf`

[26] T. Someya, et al. "A large-area, flexible pressure sensor matrix with organic field-effect transistors for artificial skin applications", PNAS, July 6, 2004, vol. 101, no. 27, pp. 9966-9970

[27] Y. Noguchi, T. Sekitani, and T. Someya, "Organic-transistor-based flexible pressure sensors using ink-jet-printed electrodes and gate dielectric layers", Applied Physics Letters 89, 253507, 2006

[28] W. Chim, "A Flexible Electronic PAper with Integrated Display Driver using Single Grain TFT Technology", 2009, Msc. Thesis

[29] Ryoichi Ishihara, Tao Chen, Michiel van der Zwan, Ming He, H. Schellevis and Kees Beenakker, "Single-grain Si TFTs for high-speed flexible electronics", Proc. SPIE 7956, 795605 (2011); http://dx.doi.org/10.1117/12.876649

[30] L. Rosenberg, "Spray-on Silicon", Nature vol. 440, 6 April 2006, pp. 749, 750

[31] E. Hengge and G. Bauer, "Cyclopentasilane, the First Unsubstituted Cyclic Silicon Hydride", Angew. Chem. Internat. Edit. / Vol. 12, No. 4, 1973, page 316

[32] [Datasheet] Cyclopentasilan, 10149984-EN-GHS, Tri Chemical Laboratories Inc.

[33] V. S. Mastryukov et al. "Structure and Conformations of Cyclopentasilane, Si5H10", J. Phys. Chem. A, Vol. 103, No. 28, 1999, pp. 5581-5584

[34] Shimoda et al. "High order silane composition and method of manufacturing a film-coated substrate", US 2011/0318939 A1, Dec. 29, 2011

[35] R. Darby, "Chemical engineering fluid mechanics", Dekker, Chapter 3, "Fluid properties in perspective", 1996

[36] M. Żenkiewicz, "Methods for the calculation of surface free energy of solids", Journal of Achievements in Materials and Manufacturing Engineering, Vol. 24, Issue 1, Sept. 2007, pp. 137-145

[37] D. P. Subedi, "Contact Angle Measurement for The Surface Characterization of Solids", The Himalayan Physics, Vol. II, May 2011

[38] [Webpage] Interactive Learning Paradigm Incorporated `http://www.ilpi.com/inorganic/glassware/glovebox.html`

[39] [Manual] MBRAUN GmbH Operating Manual Glove Box Systems

[40] [Webpage] Geochemical Instrumentation and Analysis
http://serc.carleton.edu/research_education/geochemsheets/
techniques/SEM.html

[41] [Webpage] Princeton Instruments, Raman spectroscopy basics
http://www.princetoninstruments.com/cms/index.php/
library/37-application-a-tech-notes-sorted-by-product/
spectroscopy-cameras/spec-10-ccd

[42] T. Deschains et al. "Characterization of Amorphous and Microcrystalline
Silicon using Raman Spectroscopy", Thermo Fisher Scientific Inc., Appli-
cation Note 51735, 2009

[43] [Webpage] Dektak 150 Surface Profiler brochure
http://caat.engr.ucf.edu/aboutcaat/brochures/Dektak-150_
brochure.pdf

[44] N. Gorczak, "The role of hydrogen in the crystallisation process of hydro-
genated amorphous silicon films", PVMD, TU Delft report, 2009

[45] [Webpage] Thermo Nicolet, "Introduction to Fourier Transform Infrared
Spectrometry"
mmrc.caltech.edu/FTIR/FTIRintro.pdf

[46] T. Masuda, et al. "Spectral parameters and Hamaker constants of silicon
hydride compounds and organic solvents", Journal of Colloid and Interface
Science 340, 2009, pp. 298-305

[47] P. van der Wilt "Formation of Crystalline-Silicon Islands for Thin-Film
Transistors by Excimer-Laser-Induced Lateral Growth", PhD thesis, Delft
University of Technology, 2003, ISBN 90-6464-066-1

[48] M. He "Crystallographic Orientation- and Location-controlled Si Single
Grains on an Amorphous Substrate for Large Area Electronics", PhD the-
sis, Delft University of Technology, 2007, ISBN 978-90-8559-306-5

[49] V. Privitera et al. "Low-Temperature Annealing Combined with Laser
Crystallization for Polycrystalline Silicon TFTs on Polymeric Substrate",
Journal of The Electrochemical Society, 155 (10), H764-H770, 2008

[50] [Webpage] AccTecBV Material Analysis
www.acctec.nl

[51] [Webpage] Interface Science Western Research
www.uwo.ca/isw/facilities/Tandetron/ERD.htm

[52] [Webpage] Sciptopics
www.scitopics.com/Rutherford_Backscattering_Spectrometry_RBS.
html

[53] [Datasheet] Polyamic Acid Durimide 100, Technical Product Information, Fujifilm

[54] [Webpage] Polymer Science Learning Center
www.pslc.ws/macrog/imide.htm

[55] V. Gonda, "Excimer laser annealing for ultrashallow junctions and contacts", PhD thesis, 2008, ISBN 978-90-8559-475-8

[56] [Book] Harvard Business Essentials, "Managing Creativity and Innovation, Practical Strategies to Encourage Creativity", Harvard Business Press, 2003

[57] M. A. M. Leenen et al. "Printable electronics - flexibility for the future", Phys. Status Solidi A 206, No. 4, 588-597, 2009

[58] J. Noh, et al. "Scalability of Roll-to-Roll Gravure-Printed Electrodes on Plastic Foils", IEEE Transactions on Electronics Packaging Manufacturing, Vol. 33, No. 4, October 2010

[59] Anne Blayo and Bernard Pineaux, "Printing processes and their potential for RFID printing", sOc-EUSAI '05 Proceedings, ACM, New York, NY, USA, 27-30. DOI=10.1145/1107548.1107559 http://doi.acm.org/10.1145/1107548.1107559

[60] J.-W. Lee, et al. "A comparative study on roll-to-roll gravure printing on PET and BOPP webs with aqueous ink", Progress in Organic Coatings 64, 2009, pp. 98-108

[61] R. Kopola, et al. "Gravure printed organic light emitting diodes for lighting applications", Thin Solid Films 517, 2009, pp. 5757-5762

[62] M. Tuomikoski, et al. "Gravure printed optoelectronic thin films for flexible polymer LEDs and microsystems", Optical MEMS and Their Applications Conference, 2005, pp. 141-142

[63] H. Nakajima, et al, "Flexible OLEDs Poster with Gravure Printing Method, SID 05 Digest, 30.2, 2005, pp. 1196-1199

[64] K. E. Lilja, et al. "Gravure printed organic rectifying diodes operating at high frequencies", Organic Electronics 10, 2009, pp. 1011-1014

[65] D. Sung, et al. "Scaling and Optimization of Gravure-Printed Silver Nanoparticle Lines for Printed Electronics", IEEE Transactions on Components and Packaging Technologies, Vol. 33, No. 1, March 2010, pp. 105-114

[66] D. Deganello, et al. "Patterning of micro-scale conductive networks using reel-to-reel flexographic printing", Thin Solid Films 518 (2010), pp. 6113-6116

[67] J. Onohara, et al. "Development of Polymer Light-Emitting Diode (PLED) Displays using The Relief Printing Method", SID 11 Digest, 62.2, 2011, pp. 928-931

[68] G. E. Jabbour, et al. "Screen Printing for the Fabrication of Organic Light-Emitting Devices", IEEE Journal on Selected Topics in Quantum Electronics, Vol. 7, No. 5, Sept/Oct 2001

[69] D.-H. Lee, et al. "Single-layer organic-light-emitting devices fabricated by screen printing method", Korean J. Chem. Eng., Vol. 25, No. 1, 2008, pp. 176-180

[70] J. Bimstock et al. "Screen-printed passive matrix displays based on light-emitting polymers", Applied Physics Letters, Vol. 78, No. 24, 2001, pp. 3905-3907

[71] H. Minemawari, et al. "Inkjet printing of single-crystal films", Nature, vol. 475, 2011, pp. 364-367

[72] T. Sekitani, et al. "Organic transistors manufactured using inkjet technology with subfemtoliter accuracy", PNAS, April 1, 2008, vol. 105, no. 13, pp. 4976-4980

[73] S.-C. Chang, et al. "Multicolor Organic Light-Emitting Diodes Processed by Hybrid Inkjet Printing", Advanced Materials, Vol. 11, No. 9, 1999, pp. 734-737

[74] R. Parashkov, E. Becker, T. Riedl, H. H. Johannes, W. Kowalsky, "Large Area Electronics Using Printing Methods", Proceedings of the IEEE 93, 1321-1329 (2005).

[75] H. Sirringhaus, et al. "High-Resolution Inkjet Printing of All-Polymer Transistor Circuits", Science, Vol. 290, 2000, pp. 2123-2126

[76] [Webpage] American Printer
http://americanprinter.com/alt/your-turn/deprez-inkjet-72008/

List of Publications

M. Trifunovic, T. Yokota, Y. Kato, T. Tokuhara, I. Hirata, I. Osaka, K. Takimiya, T. Sekitani, T. Someya, R. Ishihara, "OTFT with PNDT3BT-20 dispersed solution by drop casting method", International Workshop on Active-Matrix Flat-panel Displays and Devices (AMFPD12), Kyoto, Japan, 2012

R. Ishihara, J. Zhang, M. Trifunovic, M. van der Zwan, H. Takagishi, R. Kawajiri, T. Shimoda and C.I.M. Beenakker, "Single-grain Si TFTs fabricated by liquid-Si and long-pulse excimer-laser", The Electrochemical Society's 222nd Meeting, Thin film transistor technologies 11 (ECS TFT-11), (Abstract Accepted)

To be submitted

"Single-Grain Si TFTs on plastic" IEEE International Electron Device Meeting (IEDM)